anal Ch

UNITED STATES DEPARTMENT OF COMMERCE

SEP 11 1936

Engineering Library

Journal of Research

of the

National Bureau of Standards

Vol. 17, No. 2 August 1936

CONTENTS

RP	TITLE AND AUTHOR	Page
907.	Experimental study of the scour of a sandy river bed by clear and by muddy water. Chilton A. Wright ..... [Price 5c]	193
908.	Joliet reference gas meter. Howard S. Bean, M. E. Benesh, and Frank C. Witting..... [Price 10c]	207
909.	Soluble decomposition products in aged vegetable-tanned leathers. Joseph R. Kanagy ..... [Price 5c]	247
910.	Distribution of compounds in portland cement. J. Arthur Swenson and E. P. Flint ..... [Price 5c]	261
911.	The System K_2O–PbO–SiO_2. R. F. Geller and E. N. Bunting ..... [Price 5c]	277
912.	Load distribution and strength of elevator cable equalizers. Ambrose H. Stang and Leroy R. Sweetman..... [Price 5c]	291

The articles listed above may be purchased separately (see cover page II) at the prices indicated in the table of contents

A monthly periodical of pure and applied science published by our National Government

Journal of Research

of the

National Bureau of Standards

The July 1936 issue of the Journal of Research of the National Bureau of Standards began the seventeenth semiannual volume of this periodical. Fundamental researches in progress in the Bureau's laboratories are reported in this JOURNAL. If you are interested in new developments in science and technology, you should receive the JOURNAL. If you are not already a subscriber you are invited to send in your subscription.

Technical News Bulletin

This is a monthly publication containing short articles reporting progress of work in the Bureau laboratories, abstracts of papers which appear in the Journal of Research, accounts of scientific and technical meetings in which the Bureau has taken part, a list of all publications by members of the staff, and other items within the Bureau's field. The BULLETIN is designed primarily to give a general and timely review of the activities of the Bureau in brief form. It is a prompt and reliable source of official information. If you have not already subscribed for the BULLETIN, you are invited to do so.

ANNUAL SUBSCRIPTION	Prices	
	United States Canada, Cuba, Mexico, Newfoundland, Republic of Panama	Other countries
Journal of Research of the National Bureau of Standards:		
12 monthly issues (2 volumes), paper covers	$2.50	$3.25
Bound volume (½ year, 1 volume), blue buckram	3.00	3.50
Technical News Bulletin, 12 monthly issues	.50	.70

Research Papers, reprinted individual articles appearing in the Journal of Research, are available from the Superintendent of Documents shortly after appearance of monthly issue of the JOURNAL.

Address orders only to
Superintendent of Documents, U. S. Government Printing Office,
Washington, D. C.

UNITED STATES DEPARTMENT OF COMMERCE
DANIEL C. ROPER, Secretary
NATIONAL BUREAU OF STANDARDS
LYMAN J. BRIGGS, Director

✦

Journal of Research

of the

National Bureau of Standards

✦

Volume 17, Number 2

August 1936

UNITED STATES
GOVERNMENT PRINTING OFFICE
WASHINGTON : 1936

For sale by the Superintendent of Documents, Washington, D. C. - - - - - Price 25 cents
$2.50 per year on subscription

The prices of the separate Research Papers appearing in this JOURNAL are given on the front cover page. If 100 or more copies of any separate are ordered, a discount of 25 percent is allowed. Those who desire copies of separate Research Papers should send their orders and remittances without delay to the Superintendent of Documents, U. S. Government Printing Office, Washington, D. C. This will aid him to determine the number of copies to be printed for sale. Research Papers are not printed from electrotypes, and usually no more reprints can be had when the first and only printing is exhausted.

U. S. Department of Commerce National Bureau of Standards

RESEARCH PAPER RP907

Part of Journal of Research of the National Bureau of Standards, Volume 17, August 1936

EXPERIMENTAL STUDY OF THE SCOUR OF A SANDY RIVER BED BY CLEAR AND BY MUDDY WATER[1]

By Chilton A. Wright

ABSTRACT

At the request of the U. S. Bureau of Reclamation, an experimental comparison was made of the scour produced in a bed of fine sand in a sloping flume by muddy water and by clear water, in attempted simulation of the conditions existing in the Colorado River at the Boulder Dam before and after construction.

Critical velocities of the water were determined for incipient movement of the sand bed in the form of riffles and were found to be greater for muddy water, that is, water containing an appreciable amount of clay in suspension, than for clear water. With the muddy water an increase of about 10 percent in mean velocity was necessary to scour out the same amount of Colorado sand as was scoured by clear water under otherwise similar conditions. For coarser sands this increase was greater.

It was concluded that when clear water is discharged at the Boulder Dam it will cause greater scouring away of the sand bed than did the muddy water under previous conditions.

CONTENTS

	Page
I. Introduction	193
1. Purpose of the investigation	193
2. Nature of the laboratory investigation	194
3. Materials used	194
II. Apparatus	196
III. Experiments	197
1. General procedure	197
2. Preliminary experiments	198
3. Final experiments	198
IV. Results	199
1. Roughness coefficient	199
2. Sand movement	200
3. Quantity of material scoured—scour	201
4. Effect of silt on the flow of water	204
5. Velocity distribution	205
V. Conclusions	205
VI. References examined	206

I. INTRODUCTION

1. PURPOSE OF THE INVESTIGATION

This investigation arose from the problems of the U. S. Bureau of Reclamation in connection with the design and construction of the Boulder Dam on the Colorado River. The Colorado River has

[1] Paper presented before the Section of Hydrology, at the 17th Annual Meeting of the American Geophysical Union, Washington, D. C., April 30, 1936.

always been heavily charged with fine silt, clay, and colloids up to a maximum of 10 percent by weight. It was expected that all of this material would be trapped in the new Boulder Reservoir, so that only clear water would be drawn off through the intake towers and discharged by the turbines into the river below. The Bureau of Reclamation wished to determine whether this clear water would cause a greater scour in the river bed than that caused by the original muddy water.

2. NATURE OF THE LABORATORY INVESTIGATION

Although it was not expected that this problem could be solved quantitatively in the laboratory, it was hoped that the experimental measurement of the difference in the scour produced in a bed of fine sand in a flume by clear water, and that produced by water containing clay in suspension, would throw some light on the problem. In this paper the clay suspension will be referred to as "muddy water" for brevity.

In establishing a criterion that would serve for both the clear- and muddy-water tests it was found necessary to distinguish between the ability of the water to *scour* its bed and its ability to *transport* bed load under constant conditions; that is, with the sand fed into the water upstream from the test bed at the same rate as that at which it is being carried away by the flowing water. In the actual river, prior to the construction of the dam, the conditions had to do with the transportation of sediment, whereas now the existing conditions have to do with the scour of the bed. Formerly the river not only carried suspended material, but also moved a considerable quantity of bed load; now it presumably carries neither suspended load nor bed load immediately below the dam. Strictly these same conditions should have been duplicated in the laboratory tests, but the difficulties involved in trying to determine and to feed into a stream of muddy water the same amount of sand that this stream is capable of transporting under given conditions appeared to be of such magnitude as to preclude the possibility of obtaining results on the particular comparison desired. It was therefore decided to restrict the problem still further and attempt merely to compare the scour that would result from passing a stream of muddy water over a sand bed with that which would be produced by a similar stream of clear water. Consequently no sand was fed into the flume during the investigation. This method of attack differs from that used by most investigators of sediment transportation, and accordingly the results obtained are not comparable with theirs.

3. MATERIALS USED

A quantity of typical Colorado River sand from Yuma, Ariz., was sent to the laboratory for the tests. As this sand appeared too fine to be used in developing the experimental procedure, a local commercial fine sand, referred to here as "asphalt sand", was obtained also. The asphalt sand was later divided into coarse and fine portions, as required by the experiments, by means of a large U. S. Standard no. 70 sieve (opening 210 microns).

The average size distribution of the particles of the suspended load or mud carried by the Colorado River was estimated from the

records of the U. S. Bureau of Reclamation and publications of the U. S. Geological Survey [4] [2]. After considerable search for a material for use in simulating this suspended load, a quantity of kaolin was obtained from Georgia. It was necessary for the kaolin to be finer than the actual suspended load in order to be maintained in suspension in the experimental flume. However, it was found later that a sufficient concentration of the undispersed kaolin could not be maintained in suspension until sodium carbonate was added as a dispersing agent. Particle-size distribution curves of the kaolin were determined by the pipette method [5], and are shown in figure 1.

For making the mechanical analyses of the materials, sieves 3 inches in diameter were constructed, and the weight of the samples was limited to 80 grams. At the beginning of the experiments the sieves were shaken by hand in accordance with ASTM practice [7],

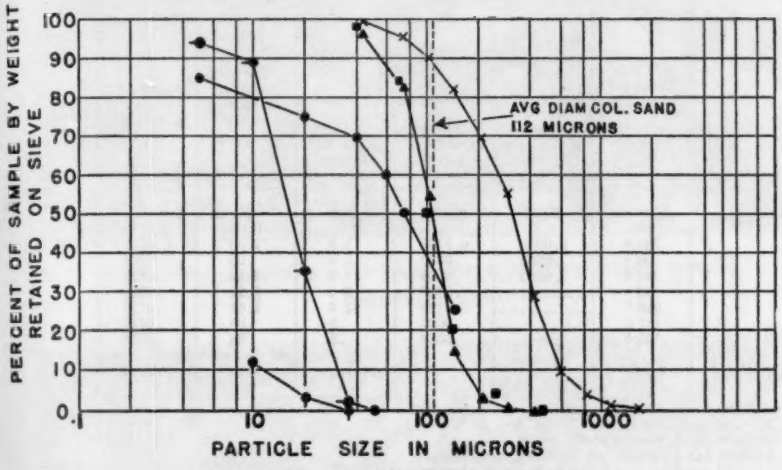

FIGURE 1.—*Particle size of materials.*

▲ Colorado River sand.
■ Typical Colorado River bed silt, analysis furnished by U. S. Bureau of Reclamation.
X Asphalt sand.
● Typical Colorado River suspended load.
◂ Kaolin, undispersed.
↑ Kaolin after dispersion.

and later a machine was developed which produced results agreeing within plus or minus 2 percent of those obtained by hand. Analyses of the bed sands are shown in figure 1.

Practically all of the Colorado sand was coarser than the openings in the U. S. Standard no. 325 sieve (44 microns), while practically all of the kaolin particles were finer. Consequently throughout the experiments the material coarser than the openings in this screen were classed with the sand or scoured material that moves as bed load, while all particles finer were classed with the clay or suspended load.

Photomicrographs of typical samples of asphalt and Colorado sand are shown in figures 2 and 3. Both sands are seen to have fairly sharp grains differing mainly in size. The kaolin was found to consist of flat particles with rounded edges. The particles of kaolin

[2] The figures given in brackets throughout the text correspond to the numbered references at the end of this paper.

coated and adhered to the sand grains in the test, as indicated in the photomicrographs.

A convenient average grain diameter for each sand was computed from curves similar to those in figure 1. The area to the left of the analysis curve bounded by the coordinate axes and the 100-percent line was computed. The size in microns indicated on the x-axis, which corresponded to the equivalent *rectangular* area bounded by these lines was called the "average diameter" of the material. Values for the materials used are summarized in table 1. This method of determining average diameter was found to correspond generally with that used by other investigators.

TABLE 1.—*Sand movement and roughness*

Average diameter	Sand movement			Roughness factor	
	No movement of sand	Critical movement of sand		Corresponding mean velocity (average)	Manning's n (average)
	Tractive force, upper limit	Critical tractive force	Critical mean velocity		
Microns (a)	lb /ft²	lb /ft²	fps	fps	
				0.98	0.0112
336 [b]	0.0032	0.0100	1.2	1.32	.0110
204 [c]	.0058	.0080	1.0	.96	.0167
384 [d]	.0060	.0088	1.0	1.12	.0128
342 [e]	----------	.0125	1.2	1.21	.0120
398 [f]	----------	.0125	1.4	1.41	.0127
107 [g]	----------	.0077	.8	.96	.0118
109 [h]	----------	.0087	.9	.98	.0115
			Average....	1.12	.0124

[a] No sand in flume.
[b] Asphalt sand, clear water.
[c] Asphalt sand passing no. 70 sieve, clear water.
[d] Asphalt sand retained on no. 70 sieve, clear water.
[e] Asphalt sand retained on no. 70 sieve with undispersed kaolin.
[f] Asphalt sand retained on no. 70 sieve with dispersed kaolin.
[g] Colorado sand, clear water.
[h] Colorado sand, with dispersed kaolin.

II. APPARATUS

The principal piece of apparatus used in this investigation was a wooden flume, adjustable in slope and supplied by an independent circulating system.

The flume itself, shown in figures 4 and 5, was 20 inches wide, 18 inches deep, and 40 feet long and was supported by adjustable steel jacks upon the lower steel return channel or forebay. The test sand bed was placed in the flume opposite a glass panel section 8 feet long. Water levels were controlled by means of the inclined tail gate at the end of the flume and were measured by means of a point gage traveling on the top of the flume. Most of the sand scoured from the bed was caught in the sand trap placed at the end of the flume, but any fine sand that passed the trap was caught in the forebay below leading to the measuring weir. Provision was made for draining and drying the material caught in these traps. For the muddy-water experiments, the kaolin was added to the supply basin and was thoroughly stirred into the water being pumped up to the sand bed.

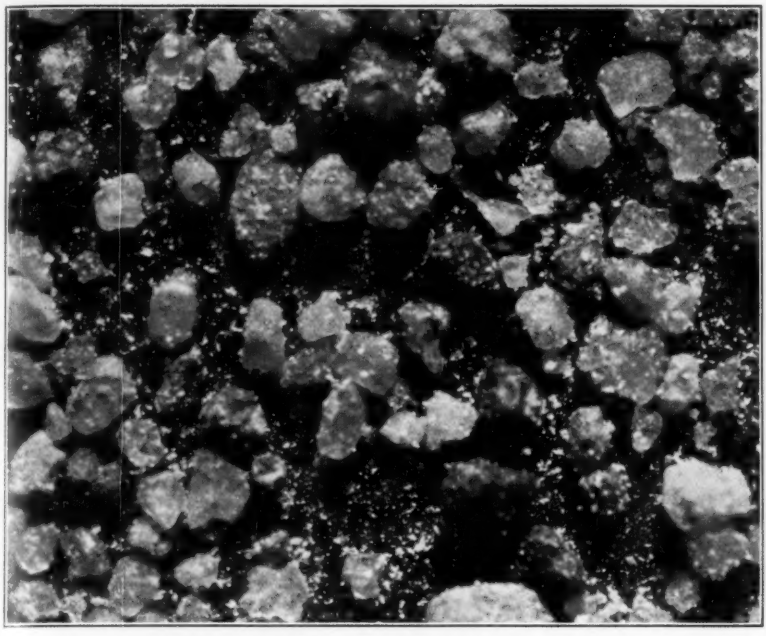

FIGURE 2.—*Asphalt sand with kaolin, typical sand-trap sample.*
Magnification ×25.

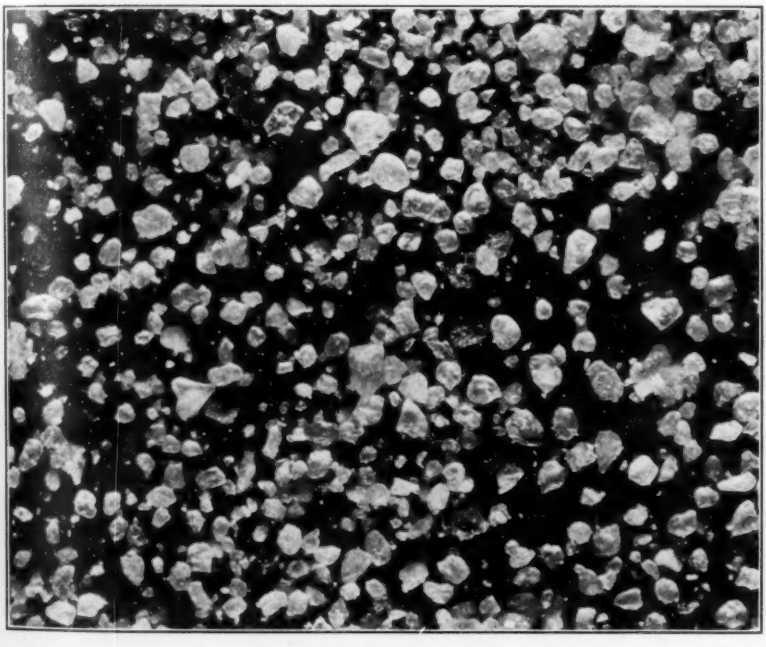

FIGURE 3.—*Colorado sand with kaolin, bed before experiment 103.*
Magnification ×25.

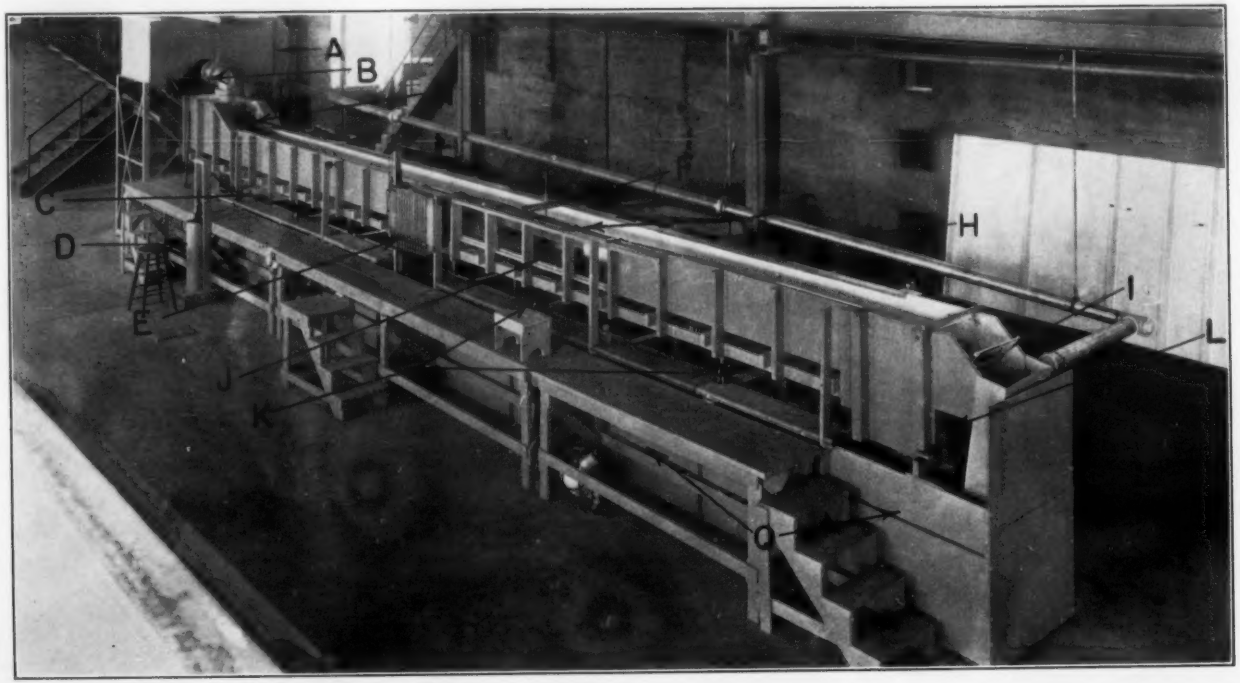

FIGURE 5.—*General view of apparatus.*

A.—Constant level tank.
B.—Supply valve.
C.—Weir.
D.—Weir gage.
E.—Gages.
F.—Point gage.
G.—Brass rails.
H.—By-pass pipe.
I.—Tail gate.
J.—Glass-panel section.
K.—Jacks.
L.—Coarse sand trap.
M.—Stone baffle.
N.—Radiator baffle.
O.—Sediment settling can.
P.—Raft.
Q.—Settling basin and weir forebay.
R.—Foot valve—pump.
S.—Supply basin.
T.—Supply pipe—pump to tank.
U.—Gage connections and drains.
V.—Sand bed.
W.—Approach floor.
X.—Overflow troughs leading to overflow pipe.

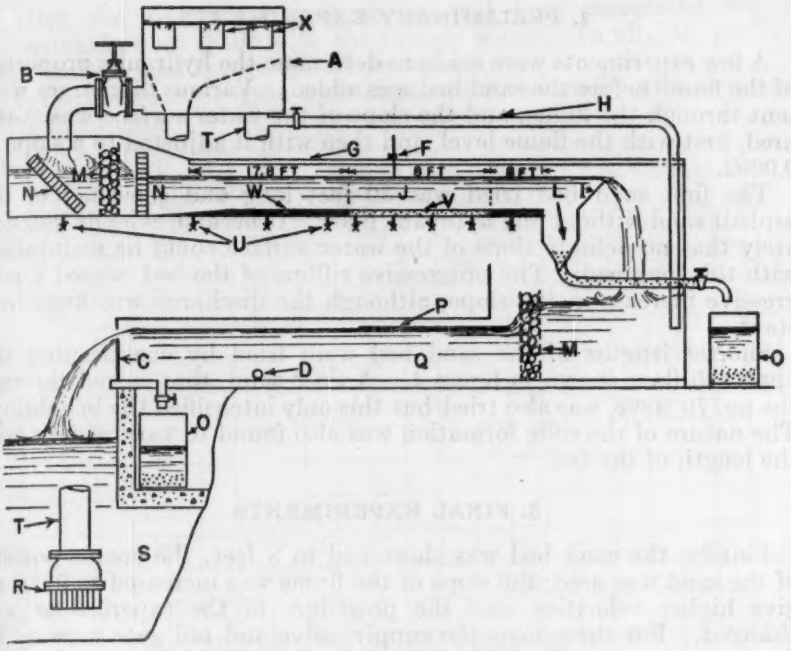

FIGURE 4.—*Sketch of sediment flume.*

A. Constant level tank.
B. Supply valve.
C. Weir.
D. Weir gage.
F. Point gage.
G. Brass rails.
H. By-pass pipe.
I. Tail gate.
J. Glass panel section.
L. Coarse sand trap.
M. Stone baffle.
N. Radiator baffle.
O. Sediment settling can.
P. Raft.
Q. Settling basin and weir forebay.
R. Foot valve—pump.
S. Supply basin.
T. Supply pipe—pump to tank.
U. Gage connections and drains.
V. Sand bed.
W. Approach floor.
X. Overflow troughs leading to overflow pipe.

III. EXPERIMENTS

1. GENERAL PROCEDURE

The general procedure was the same for most of the experiments. The sand bed was settled under water to eliminate air bubbles, and enough of the water was drained through the bed to allow the surface to be smoothed with a steel trowel. The tail gate was set, and the supply valve was adjusted until the slope of the water surface was approximately parallel to that of the bed. The scouring and riffling of the sand bed were studied through the glass panel. At the end of an hour the experiment was stopped, the flume slowly drained and the characteristics of the bed sketched and photographed. Samples of sand were taken from the bed, and the material in the traps was dried and sampled.

For the muddy-water experiments, the sand bed in the flume was settled in muddy water, and the clay in the supply basin was stirred thoroughly before each experiment. Four samples of the suspended load were taken during the experiment.

2. PRELIMINARY EXPERIMENTS

A few experiments were made to determine the hydraulic properties of the flume before the sand bed was added. Various discharges were sent through the flume, and the slope of the water surface was measured, first with the flume level, and then with it adjusted to a slope of 0.0002.

The first sand bed tried was 30 feet long and consisted of the asphalt sand without any approach floor. It became evident immediately that no definite slope of the water surface could be maintained with this long bed. The progressive riffling of the bed caused a progressive increase in the slope, although the discharge was kept constant.

Shorter lengths of the sand bed were tried by constructing the approach floor shown in figure 4. A finer sand, that sieved through the no. 70 sieve, was also tried but this only intensified the instability. The nature of the riffle formation was also found to vary widely over the length of the bed.

3. FINAL EXPERIMENTS

Finally, the sand bed was shortened to 8 feet, the coarse portion of the sand was used, the slope of the flume was increased to 0.001 to give higher velocities, and the procedure of the experiments was changed. For these tests the supply valve and tail gate were set in fixed positions at the beginning of each test and kept unchanged throughout its duration. The slope was measured with the point gage every 15 minutes during the test, which was allowed to run for an hour. Typical changes in the slope are shown in figure 6 for experiments 59, 70, 71, and 72.

Even with the short sand bed, as soon as scouring began at the upstream end of the bed and riffles began to form at its lower end, the slope of the water surface became steeper over the downstream end of the bed. In order to maintain this slope, the water backed upstream and consequently increased in depth. A typical development of the slope is shown in figure 6 for experiment 59. It is seen that the steep part of the slope tended to move down toward the end of the bed, the water surface finally becoming somewhat curved in profile. This tendency was less pronounced when the amount of scour was small and when the mean velocity of the water was low.

Since the computed values of the mean velocity and tractive force depend on both the slope of the water surface and the depth of the water, both of which changed during a test, the method used to select representative values for the slope and depth was of considerable importance. When the coarse asphalt sand was used, the changes in slope and depth during a given experiment were small enough to justify selection of their average values for use in analyzing the results. However, for similar experiments made with the fine Colorado sand, these changes were too great to allow the use of the average. Consequently the assumption was made that the initial conditions would determine the characteristic scouring of the sand bed, and values of the initial slope and depth were determined from curves similar to those shown in figure 6. These values were used in the computations.

After the clear-water experiments had been completed similar experiments were made with the muddy water. In all, 101 preliminary and 91 final experiments were made.

Vertical-velocity curves were measured occasionally with a simple glass Pitot tube.

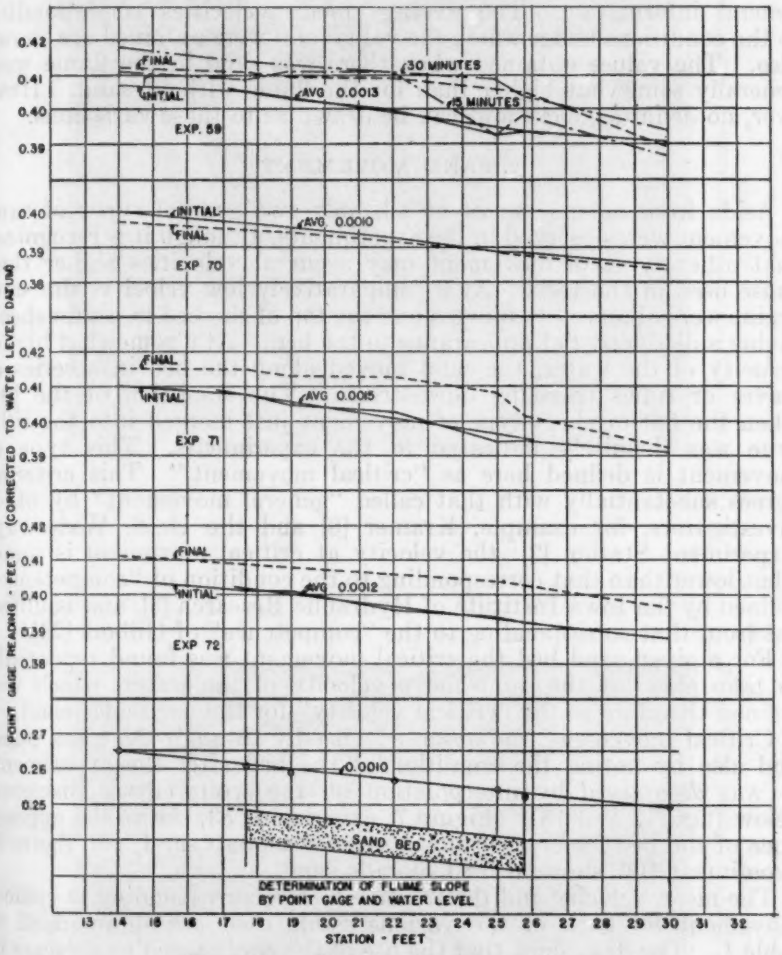

FIGURE 6.—*Typical water surface slopes.*

IV. RESULTS

The results were divided into (1) a study of the roughness coefficient (Manning's n); (2) types of sand movement as affected by the presence of clay in the water; (3) a quantitative study of the sand scoured; and (4) effect of silt on the flow of water.

1. ROUGHNESS COEFFICIENT

For each of the preliminary experiments the average slope of the energy line was determined, together with values of the depth and the hydraulic radius. By substitution in the Manning formula for flow in open channels, the corresponding roughness coefficient n was

determined. For each final experiment, values of the average *initial* slope were determined from diagrams similar to those given in figure 6, and the corresponding initial value of Manning's n determined. These values, which varied quite widely for the various sand beds, were averaged, and the results are shown in table 1 for general information. The average mean velocities corresponding to the conditions under which the values of n were obtained are shown also. The values obtained when there was sand in the flume were generally somewhat higher than for the flume without sand. However, no definite conclusions can be drawn as to these variations.

2. SAND MOVEMENT

Aside from no movement at all, only two general types of sand movement were observed in the experiments, although it is recognized that other types of movement may occur at velocities higher than those used in the tests. At a comparatively low velocity, the sand grains were observed to move along the top of the bed in a thin sheet, giving a distinctly flat appearance to the bed. At a somewhat higher velocity of the water, the sand moved along the bed in a series of waves or riffles traveling downstream. The condition of the bed when the flat or sheet type of movement just merged into the riffle type was definitely indicated in the experiments. This type of movement is defined here as "critical movement." This criterion agrees substantially with that called "general movement" by other investigators, for example, Kramer [8] and the U. S. Waterways Experiment Station [2]: the velocity at critical movement is somewhat lower than that corresponding to the condition of "competence" defined by the Iowa Institute of Hydraulic Research [3], and is different from that corresponding to the "competence" of Gilbert [25].

For a given sand bed the critical movement was found repeatedly to take place at the same mean velocity of the water, which was defined therefore as the "critical velocity" for the particular sand.

Critical movement was observed visually through the glass panel and also by noting the condition of the bed after the experiment. It was *determined* by interpolation on the scour curves discussed below (figs. 12 and 13). Figure 7, experiment 53, shows the appearance of the bed for critical movement for asphalt sand, and figure 8, experiment 106, shows it for Colorado sand.

The mean velocity and the tractive force [3] corresponding to critical movement for each of the various sands used are summarized in table 1. The data show that the use of the clay caused an increase in the value of critical mean velocity and critical tractive force.

At higher velocities a definite scour took place in the sand bed, usually with its maximum depth just downstream from the beginning of the bed, with the edges of the scoured area rounded. The scoured material traveled smoothly on a slight upgrade to the center of the bed, and thereafter in the form of riffles to the end of the bed. The scour for the muddy water differed somewhat in that the sand bed scoured away in small areas, leaving the edges sharp instead of rounded.

[3] Tractive force, F_t is defined as follows:

$$F_t = wds,$$

where F_t is the tractive force exerted by the flowing water on the bed, in pounds per square foot.
w is the specific weight of the water, in pounds per cubic foot.
d is the depth of the water, in feet, in uniform flow.
and s is the slope of the water surface.

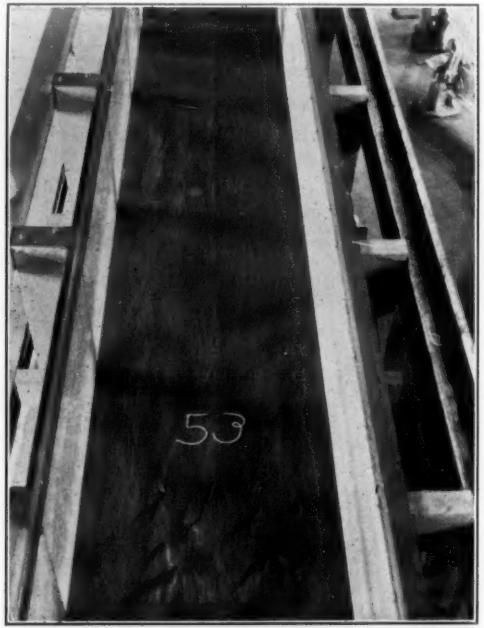

FIGURE 7.—*Bed after experiment 53, looking upstream.*

Asphalt sand, clear water, mean velocity 1.03 fps.

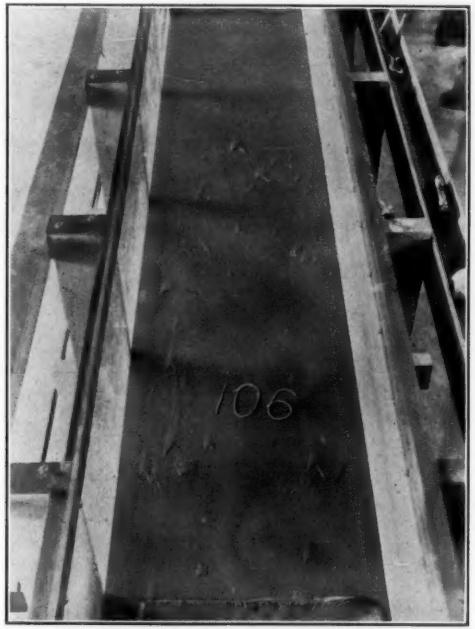

FIGURE 8.—*Bed after experiment 106, looking upstream.*

Colorado sand, clear water, mean velocity (initial) 0.81 fps.

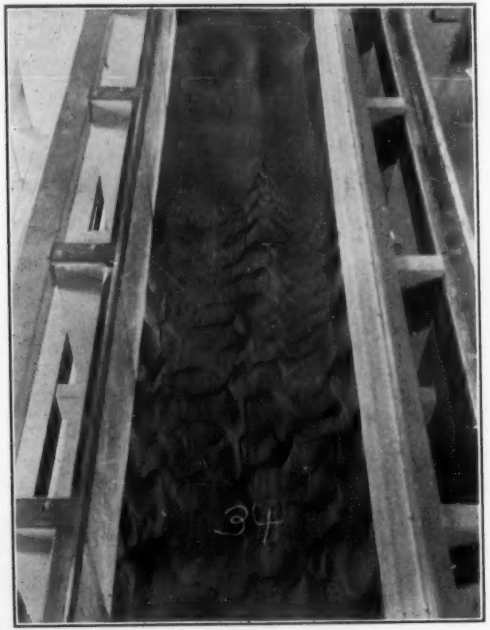

FIGURE 9.—*Bed after experiment 34, looking upstream.*

Asphalt sand, clear water, mean velocity 1.28 fps.

FIGURE 10.—*Bed after experiment 87, looking upstream.*

Asphalt sand, muddy water, mean velocity 1.28 fps.

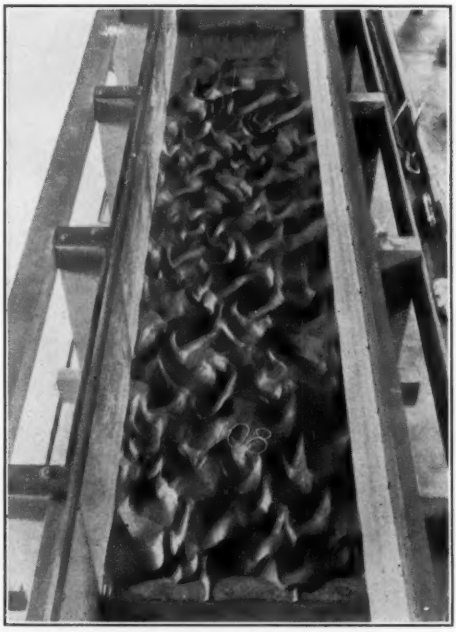

FIGURE 11.—*Bed after experiment 108, looking upstream.*
Colorado sand, clear water, mean velocity (initial) 1.04 fps.

UNIV. OF MICH.

Figures 9 and 10 show clearly the much greater scour produced by clear water than muddy water under otherwise similar conditions. In both of these experiments the bed was formed of asphalt sand and the mean velocity was 1.28 fps. However, in the experiment shown in figure 9, clear water flowed over the bed, while in that shown in figure 10, water containing dispersed kaolin flowed over the bed. The amount of material scoured in experiment 34 was about 26 times as great as that scoured in experiment 87. One reason for this large difference is to be found in the fact that the mean velocity in experiment 34 was above the critical velocity for asphalt sand and clear water, while in experiment 87, this same velocity was lower than the critical velocity for asphalt sand and water containing dispersed kaolin. (See table 2.)

TABLE 2.—*Comparison of scour with mean velocity*

Scour	Mean velocity		
	Clear water	Muddy water	Difference
lb/ft²/hr	fps	fps	fps
0.2	[a] 1.00	1.30	0.30
.5	1.10	[b] 1.40	.30
1.0	1.18	1.48	.30
1.5	1.23	1.53	.30
COLORADO SAND (SHALLOW WATER)			
.15	[a] .82	.90	.08
.2	.85	[b] .92	.07
.6	.90	.98	.08
1.5	1.05	1.10	.05

ASPHALT SAND

[a] Beginning of critical movement for clear water.
[b] Beginning of critical movement for muddy water.

A bed of Colorado sand is shown in figure 11, experiment 108, for clear water at an initial mean velocity of 1.04 fps. The excessive scouring and riffling shown are in great contrast to those of the corresponding muddy-water experiments. At this velocity the latter exhibit a flat bed, generally similar to that shown in figure 8, except for the small riffles.

3. QUANTITY OF MATERIAL SCOURED—SCOUR

The weight of material scoured out of the bed in 1 hour and caught in the traps divided by the area of the bed is defined as "scour." It is measured in pounds per square foot per hour.

Values of the scour for the asphalt-sand experiments with the clear water, and experiments with dispersed kaolin in the water are plotted logarithmically against the corresponding values of mean velocity in figure 12. This figure shows that, in order to cause the same scour with the muddy water as with the clear water, an increase of about 25 percent in the mean velocity is necessary. The scour tends to be proportional to the tenth, or greater, power of the mean velocity, and the steepness of the curves further shows that a great increase in the scour may occur for a small increase in the mean velocity.

The experiments in which the bed movement took place in the form of a flat sheet are indicated in figure 12 by F, while those not so marked are for movement in riffles. The critical velocity at which

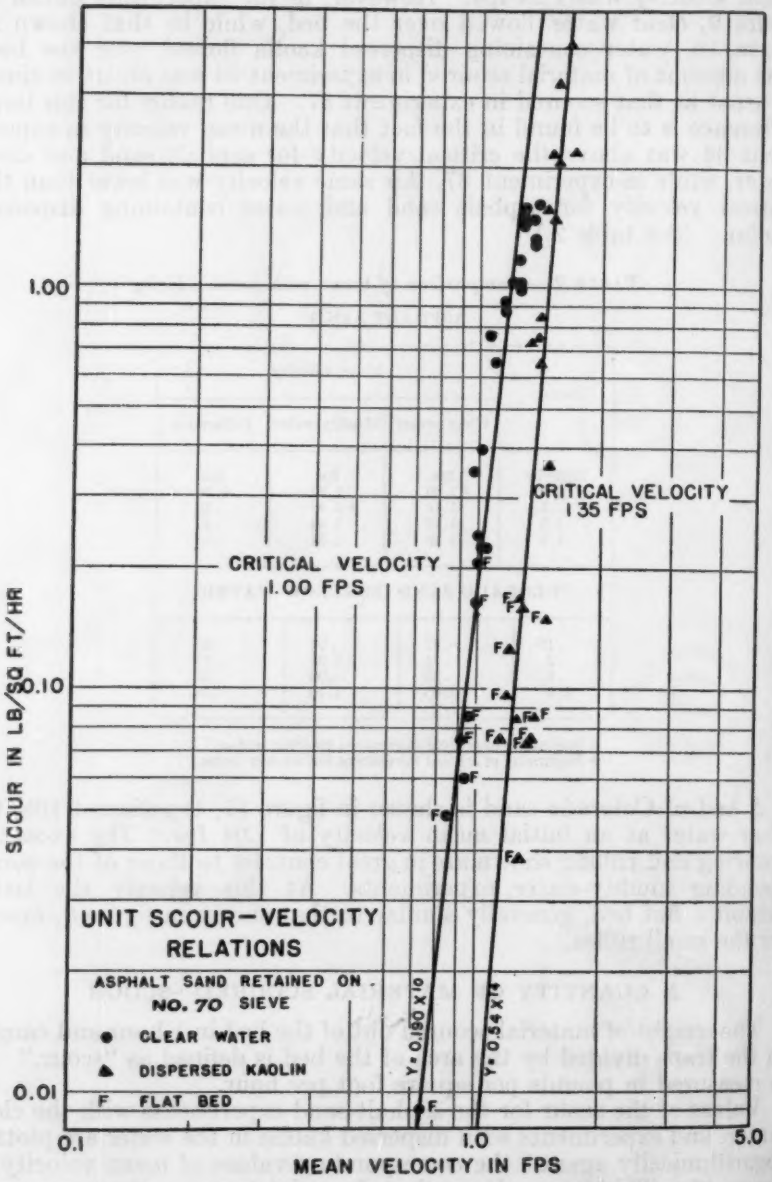

FIGURE 12.—*Scour-velocity relations, asphalt sand.*

the bed movement changes to the riffled form was determined from the figure and values of critical velocity are shown in table 1.

Figure 13 in which scour is plotted against *initial* mean velocity, shows the results for the Colorado sand. The initial mean velocity

was used here instead of the average mean velocity because of the unstable slope and depth due to excessive riffling of this fine sand as previously explained.

For those tests in which the depth of the water was small, a clear-cut contrast exists between the results for clear water and those for

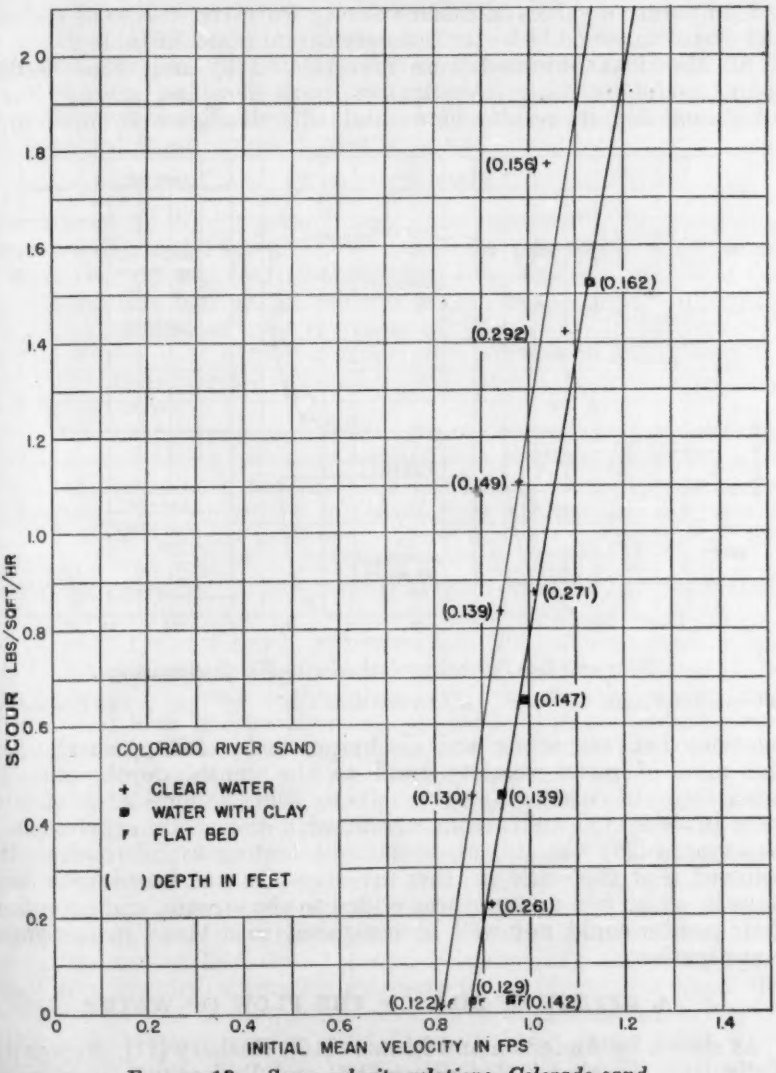

FIGURE 13.—*Scour-velocity relations, Colorado sand.*

muddy water. The results for the clear-water tests lie on a straight line to the left of a straight line that represents the results of the muddy water tests. It is seen that the scour increases with the mean velocity, and also that a 10 percent increase in the velocity of the muddy water is necessary to cause the same scour that occurred with the clear water. However, for depths about double those for which

the above-mentioned curves were obtained, the points for the tests with clear water tend to become superimposed on the curve representing values for the tests with muddy water. Comparative data for muddy water at these depths are unfortunately not available, since the experiments had to be stopped because of loss of clay through a leak in the supply basin.

Comparative values of mean velocity for given values of scour for the clear- and muddy-water tests are summarized in table 2.

All the data obtained were investigated by numerous methods found useful by other investigators, both here and abroad, but no additional definite results were obtained. Studies were made of the

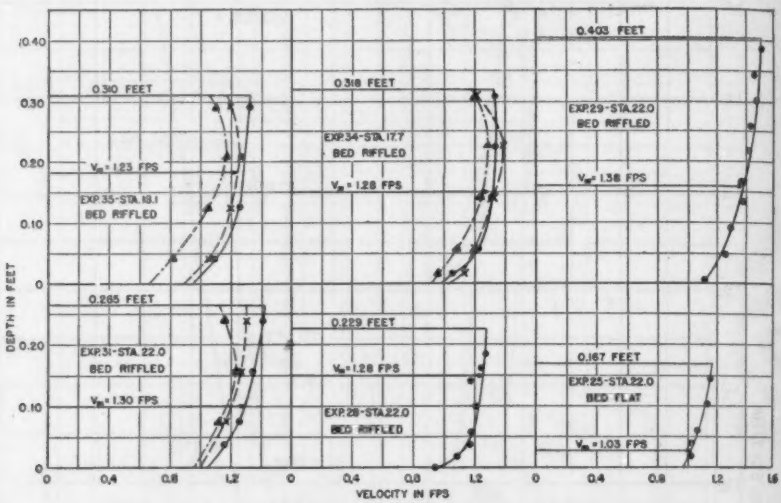

FIGURE 14.—*Typical vertical velocity-distribution curves.*

● Center line of flume. ▲ 0.2 ft from south wall. × 0.2 ft from north wall.

relations between scour and discharge, bed velocity, energy head, the ratio of mean velocity head to the depth, depth, etc. The possibilities of correlating the results by using dimensionless variables were investigated and a comparison with the scour experiments of Nakayama [28] was also made without finding useful results. It is believed that the work of other investigators was based upon conditions in which bed material was added to the stream, and accordingly their results could not well be compared with those in the present investigation.

4. EFFECT OF SILT ON THE FLOW OF WATER

As shown by Anderson and Matson [10], Rothery [11], Stevens [12], Kelly [16], Buckley [24], Gilbert [25], and Parker [27], opinions are very conflicting regarding the effect of adding silt in suspension on the flow of a clear stream under given conditions. However, it is believed that the resulting small increase in viscosity and density tends to increase the tractive force slightly and to cause a corresponding increase in the scouring power. On the other hand, a heavy load of suspended silt in the water lays down a protecting mat of cohesive particles which fill the interstices at the top of the bed and thus enable it to resist scour. However, in the experiments with the asphalt sand and the coarser undispersed kaolin, when this mat

was once broken through by the water, a greater scour resulted with the muddy water than with clear water. Nevertheless, in general, it was found that the clay tended to restrict the scour, as shown by the data in tables 1 and 2.

5. VELOCITY DISTRIBUTION

A few typical vertical velocity-distribution curves obtained by means of the Pitot tube are shown in figure 14. The shape of the curves indicates that the distribution of the velocity in the flume is similar to that usually found in a typical open channel. Data for the studies with bed velocity and velocity ratios mentioned above were obtained from curves similar to these.

V. CONCLUSIONS

The results of the laboratory tests show that, in order to scour a given amount of sand when the water contains fine clay in suspension, a greater velocity is necessary than when the water is clear. For the asphalt sand this increase in velocity amounted to 25 percent, while for the Colorado River sand it was much less, about 10 percent. It was also shown that a very considerable increase in scour resulted from a very small increase in mean velocity above the critical velocity for the given sand.

Admittedly the laboratory results cannot be applied quantitatively to the Colorado River for many reasons. In the first place, the laws by which the results of the small-scale tests can be converted to the corresponding values for the full-sized river are not known for the complicated phenomena involved. Prior to the construction of the dam, large floods, with their relatively great scouring of the river bed, occurred periodically; whereas now that the dam has been constructed, the flow downstream will be regulated. The velocities in the actual river (4 to 10 fps) are much higher than in the test flume, while the river bed is practically the same. Material which could only be transported as bed load in the laboratory tests may be transported partly as bed load and partly as suspended load in the actual river. However, the qualitative statement may be made that large volumes of clear water discharged onto a bed of Colorado River sand just below the Boulder Dam will tend to cause a greater scouring of the bed than did muddy water prior to the construction of the dam, first because the muddy water brought sand and silt with it to compensate somewhat for the material scoured and carried away, and second because, as the laboratory tests have shown, clear water scours the bed more easily than does muddy water. It may be mentioned also, as pointed out by Rothery [11] and Stevens [12], the clear-water stream may require a smaller gradient for a given flow than the muddy stream and consequently may have additional capacity for cutting and transporting the sand from its bed. Since there is no large tributary for 80 miles below the Boulder Dam to provide additional bed load, this scour will probably tend to progress gradually downstream.

A complete report on this investigation is available for loan.

Many valuable suggestions, together with editorial assistance, were furnished in this investigation by H. N. Eaton, Chief of the Hydraulic Laboratory Section. The apparatus for the mechanical analyses was

designed and the analyses were made by B. H. Monish. J. M. Buswell and C. W. Elliot of the laboratory staff were responsible for the design and construction of the sediment flume and drying apparatus.

VI. REFERENCES EXAMINED

[1] W. N. Weigel. Size and Character of Grains of Non-Metallic Mineral Fillers. Tech. Pap. 296, U. S. Bur. Mines, Washington, D. C. (1924).

[2] Studies of River Bed Materials and Their Movement, With Special Reference to the Lower Mississippi River. Pap. 17, U. S. Waterways Experiment Station, Vicksburg, Miss. (January 1935).

[3] F. T. Mavis, Chitty Ho, and Y. C. Tu. The Transportation of Detritus by Flowing Water. Pt. I, Studies in Engineering, University of Iowa, Iowa City, Iowa, [294] Bul. 5 (March 1, 1935).

[4] C. S. Howard. Sizes of Particles of Suspended Matter Carried by the Colorado River. Office Mem. U. S. Geol. Survey, Washington, D. C. (Aug. 12, 1932).

[5] C. E. Jackson and C. M. Saeger, Jr. *Use of the pipette method in the fineness test of molding sand.* J. Research NBS **14,** 59 (January 1935) RP757.

[6] C. S. Howard. Quality of Water in the Colorado River, 1928–1930. Water Supply Pap. 639–D, U. S. Geol. Survey, Washington, D. C.

[7] *Standard method of test for sieve analysis of aggregates for concrete.* Stand. C 41–33, Am. Soc. Testing Materials, Pt. II, 240 (1933).

[8] Hans Kramer. *Sand mixtures and sand movements in fluvial models.* Trans. Am. Soc. Civil Engrs. **100,** 798 (1935).

[9] M. P. O'Brien. *Review of the theory of turbulent flow and its relation to sediment transportation.* Trans. Am. Geophys. Union, Sec. Hydrol. 487 (1933).

[10] M. S. Anderson and S. Matson. Properties of the Colloidal Soil Material. Dept. Bul. 1452, U. S. Dept. Agr., Washington, D. C. (Nov. 1926).

[11] S. L. Rothery. *A problem of soil in transportation in the Colorado River* Trans. Am. Soc. Civil Engrs. **99,** 530 (1934).

[12] J. C. Stevens. *The silt problem.* Proc. Am. Soc. Civil Engrs. pt. I, **60,** 1206 (Oct. 1934).

[13] B. H. Hendrickson. *The choking of pore space in the soil and its relation to runoff and erosion.* Trans. Am. Geophys. Union, Sec. Hydrol. 500 (1934).

[14] C. E. Ramser. *Dynamics of erosion in controlled channels.* Trans. Am. Geophys. Union, Sec. Hydrol. 488 (1934).

[15] E. S. Bellasis. Hydraulics. p. 198 (Spon & Chamberlain 1924).

[16] *Prevention of silt deposits in conduits.* Report of Subcommittee of Hydraulic Power Committee. Pacific Coast Elec. Assn. Elec. West, **60,** 399 (May 15, 1928).

[17] William Kelly. *The Colorado River problem.* Discussion by J. C. Hill. Trans. Am. Soc. Civil Engrs. **88,** 415 (1925).

[18] R. G. Hemphill. *Silting and life of southwestern reservoirs.* Trans. Am. Soc. Civil Engrs. **95,** 1072 (1931).

[19] O. A. Faris. The Silt Load of Texas Streams. Tech. Bul. 382, U. S. Dept. Agr. (Sept. 1933).

[20] L. R. Fiock. *Records of silt carried by the Rio Grande and its accumulation in Elephant Butte Reservoir.* Trans. Am. Geophys. Union, pt. II, 472 (1934).

[21] A. H. Gibson. Hydraulics and its Applications, p. 339 (D. Van Nostrand Co. New York, N. Y., 1925).

[22] H. J. Casey. Über Geschiebebewegung. Dissertation. Technische Hochschule, Berlin, Germany (Mar. 11, 1935).

[23] J. C. Stevens. *The Silt Problem.* Discussion by E. W. Lane. Proc. Am. Soc. Civil Engrs. **61,** 409 (Mar. 1935).

[24] A. B. Buckley. *The influence of silt on the velocity of water flowing in open channels.* Min. Proc. Inst. Civil Engrs. **216,** pt. II, 183 (1922–1923).

[25] G. C. Gilbert. The transportation of Debris by Running Water. Prof. Pap. 86, U. S. Geol. Survey (1914).

[26] J. M. Lacey. *Some problems connected with the rivers and canals in southern India.* Min. Proc. Inst. Civil Engrs. **216,** pt. II, 150 (1922–1923).

[27] P. A. M. Parker. The Control of Water. (George Routledge & Sons, Ltd., London, Eng., 2nd ed. 1932).

[28] H. Nakayama. *Some model investigations about the motion of sand along a self-formed channel.* J. Tokyo Faculty Eng. **13,** (Mar. 1923).

WASHINGTON, May 25, 1936.

U. S. DEPARTMENT OF COMMERCE NATIONAL BUREAU OF STANDARDS

RESEARCH PAPER RP908

Part of Journal of Research of the National Bureau of Standards, Volume 17, August 1936

JOLIET REFERENCE GAS METER

By Howard S. Bean, M. E. Benesh, and Frank C. Witting

ABSTRACT

Upon invitation, the National Bureau of Standards, cooperated with the Peoples Gas Light and Coke Co., Chicago, Ill., in the design, construction, and testing of a reference gas meter capable of being used over a wide range of conditions and having a high maximum capacity. The meter is of the proportional type in which the main gas stream is divided into a large and a small stream in a known or determinable ratio. The rates of flow in the two streams may be varied and the actual ratio of the mass rates of flow is determined by a thermal method. Two heat exchangers, one in each gas stream, receive heat through the medium of hot water from a common source. The rates of flow of the hot water to the two heat exchangers are adjusted until the temperatures of the outlet water streams are the same. The outlet water streams are discharged into weighing tanks from which the ratio between their rates of flow is obtained.

The rates of flow of the gas in the two streams are then adjusted to bring together their temperatures on the outlet side of the heat exchangers. Hence, if the two gas streams are warmed through one temperature range, while the two water streams are cooled through another temperature range, the ratio of the mass rates of flow of the gas streams will be equal to the ratio of the mass rates of flow of the water streams.

The rate of flow in the small gas stream is measured with a large piston meter. The pressure and temperature of the gas in the piston meter are carefully measured, and the specific gravity of the gas, referred to air, is determined. With these data, and the displacement of the piston for the duration of the test, the density and total mass of gas that passed through the small passage are computed. Dividing this total mass flow by the duration of the test gives the mass rate of flow through the small branch.

The total mass rate of flow into the reference meter may now be computed by the formula

$$w = w_s(C_m + 1)$$

in which

w(lb/sec) = total mass rate of flow into reference meter.
w_s(lb/sec) = mass rate of flow through the small stream.
C_m = ratio of mass rate of flow in the large stream to that in the small stream,
= ratio of mass rates of flow of water into the two heat exchangers.

The operation of the piston meter is described, and the procedure of making a test with the reference meter is outlined.

The results of 15 tests of an orifice meter with the reference meter are presented and discussed. It is shown that excepting for the determination of the specific gravity of the gas, which is done with auxiliary equipment apart from the meter, the probable uncertainty in any item or factor will not affect the indicated rate of flow by more than about ± 0.05 percent.

CONTENTS

	Page
I. Introduction	208
II. General principle of operation	209
III. Some general characteristics of the Joliet reference meter	210
IV. Detailed description of the Joliet reference meter	210
1. Conditions to be fulfilled	210
2. General arrangement of parts	211

IV. Detailed description of the Joliet reference meter—Continued. Page
3. Proportioning chamber ... 212
4. Piston displacement meter ... 218
5. How the piston meter works ... 221
6. Capacity range of the reference meter ... 226
V. Operating the Joliet reference meter ... 227
1. Quantities observed when operating the reference meter ... 227
2. Instruments and methods of measurement ... 228
3. Procedure of operating the reference meter ... 230
VI. Tests made with the reference meter ... 232
1. General procedure ... 232
2. Observed quantities and computed results for the Joliet reference meter ... 232
3. Observed data for the orifice meter and comparison of the discharge coefficients ... 236
VII. Discussion of test results and possible sources of error ... 239
1. Discussion of test results ... 239
2. Heat losses ... 240
3. Conclusion ... 242
VIII. Appendix A.—Piston gages for measuring pressures ... 242
1. Piston gages used for measuring differential pressures ... 242
2. Piston gages for measuring static pressure ... 245
IX. Appendix B.—Discharge coefficients of orifices determined on the basis of the reference meter tests, compared with values calculated from equations in Report 2 of the Gas Measurement Committee, Natural Gas Department, American Gas Association ... 245

I. INTRODUCTION

Disputes have sometimes arisen over the correctness of registration of large-capacity gas meters, and on some of these occasions it would have been advantageous to have a reference meter available with which the meter in question could be compared over the range of its operating conditions. Similar occasions may arise in the future.

The reference meter to be used in such cases should have, among others, the following characteristics:

1. *Accuracy.*—The probable errors of indication should be low, certainly not over 0.5 percent and preferably not over 0.1 or 0.2 percent.

2. *Range.*—It should be possible to operate the meter under a wide range of conditions as regards mass rate of flow, pressure, temperature, and composition of the gas.

3. *Pulsations.*—The meter should be free from the effects of pulsations in the gas stream.

A meter which, it is believed, meets these requirements for a reference meter, has been constructed and installed at the Joliet Meter Station of the Chicago District Pipeline Co., near Joliet, Ill. For this reason the meter will be referred to here as the Joliet reference meter. It is connected in series with and on the downstream side of a 10-in. orifice check meter. This check meter can be connected in series with any one of 12 regular 10-in. orifice-meter runs. Six of these twelve runs are owned by the Chicago District Pipeline Co. and the other six by the Natural Gas Pipeline Co. of America. The discharge from the reference meter is connected into the outlet line from the station. These connections to the reference meter can readily be altered to permit connecting other meters in series with it.

The design and construction of the reference meter presented many problems. The solution of these problems and the final con-

struction of the meter were made possible by the interest and support of the Peoples Gas Light and Coke Co., Chicago, Ill.

One of the functions of the National Bureau of Standards is to develop improvements in making measurements for both laboratory and commercial purposes and to cooperate with others in similar undertakings. Therefore, when invited to cooperate in designing and constructing a reference meter which, it was hoped, would fulfill the above requirements the Bureau accepted. Its cooperation consisted in furnishing information and advice on some of the materials used and the design and testing of some of the meter parts, and in the loan of scientific laboratory instruments.

The essential features of design and operation of the reference meter were evolved [1] by one of the authors (Benesh), who also made the necessary arrangements incident to its construction. Another of the authors (Witting) designed many of the separate parts of the meter and supervised the assembling and testing of the meter. The remaining author (Bean) acted in a liaison capacity between his colleagues and the Bureau, and assisted in some of the tests of the meter and in the writing of this paper.

II. GENERAL PRINCIPLE OF OPERATION

The Joliet reference meter is essentially a large proportional meter. In conformance with the principle of this type of meter, the main gas stream is divided, upon entering the meter, into a large and a small stream. The rates of flow of gas in these two streams are controlled by adjustable restrictions in the outlet passages of the two streams. The ratio of the mass rate of flow in the smaller stream to that in the larger stream is determined by the following thermal method. Heat exchangers, located in the two gas stream passages, receive heat through the medium of hot water from a common source. By means of valves the ratio of the rates of flow of water through the two heat exchangers is adjusted until the water streams leaving the heat exchangers are at the same temperature. The rates of flow of water from the two heat exchangers are determined by weighing the discharge from each. In a somewhat similar manner the rates of flow of gas are so adjusted that the two streams issue from the heat exchangers at the same temperature. Thus, if the two gas streams are heated through the same temperature range, ΔT_g, while cooling the two water streams through a common temperature range, ΔT_w, the ratio between the mass rates of flow in the two gas streams will equal the ratio between the mass rates of flow in the two water streams, which latter has been determined by weighing.

Upon leaving the heat exchangers the smaller gas stream is directed through a piston meter. The temperature and pressure of the gas in the piston meter are carefully controlled and measured. These quantities, together with the displacement, or volume indications of the piston meter, enable one to compute the mass rate of flow of gas in the small stream (assuming of course that the necessary physical properties of the gas are known).

[1] United States patent 2015249 covering these features has been dedicated to the public.

The mass rate of flow of gas, w, entering the reference meter may be computed by the equation

$$w(\text{lb/sec}) = w_s(C_m + 1), \tag{1}$$

in which

C_m = the proportioning ratio,
$= \frac{\text{mass rate of flow in large stream}}{\text{mass rate of flow in small stream}}$.
$w_s(\text{lb/sec})$ = mass rate of flow in small stream.

III. SOME GENERAL CHARACTERISTICS OF THE JOLIET REFERENCE METER

The Joliet reference meter was designed and constructed to operate under gas pressures ranging from atmospheric to 600 lb/in^2. It can readily be operated with incoming gas temperatures ranging approximately from -20 to $+180°$ F. To operate at pressures or temperatures very much outside these limits would not change any of the basic principles of operation but would require many changes in the details of construction.

The meter is not affected by any pulsations there may be in the gas stream, provided there is no actual reversal in the direction of flow. Moreover, the meter will not introduce any pulsations. It will operate satisfactorily with any gas or vapor, but will not operate correctly if the fluid to be metered is a mixture of a liquid and vapor, i. e., a fog. In this case, either the liquid should be separated and the two fluids measured separately or the fluid mixture should be heated until it is all vapor, and then metered.

The proportioning ratio can conveniently be varied from about 5:1 to about 60:1. These proportioning limits are not imposed by the construction of the meter but are believed to be the limits of convenient operation. The temperature ranges through which both the water and gas are changed may be varied over rather wide limits. Thus, for any given rate of flow of the gas, the meter may be operated with various proportioning ratios and temperature ranges—a characteristic which may be utilized in checking the indications of the meter and in analyzing the possible sources of error.

As will be more fully discussed later, both the maximum and minimum capacities of the meter depend, in part, upon the relative heat-transferring capacities of the heat exchangers. The maximum capacity depends also upon the strength of some of the parts. As constructed, the meter has a maximum capacity of about 120,000 ft^3/hr of natural gas at 200 lb/in.^{2}, which is equivalent to about 1,633,000 ft^3/hr when the pressure is reduced to atmospheric. The minimum capacity as a proportional meter is about 2,400 ft.^{3}/hr at 200 lb/in^2. Very much lower rates of flow may be metered by blanking off the outlet of the large gas stream so as to divert all the gas through the piston meter.

IV. DETAILED DESCRIPTION OF THE JOLIET REFERENCE METER

1. CONDITIONS TO BE FULFILLED

In order to make use of the assumption that the ratio of the mass rates of flow of gas in the two gas streams is equal to the ratio of the

weights of water discharged from the two heat exchangers in a given interval of time, it is necessary that the following requirements should be fulfilled:

1. The temperature of the gas entering the small heat exchanger must be the same as that of the gas stream entering the large heat exchanger.
2. There should be no transfer of heat from one heat exchanger to the other or from one gas stream to the other; neither should there be any cross transfer of heat from either heat exchanger to the other gas stream.
3. There should be no transfer of heat between either the heat exchangers or the gas streams and the outside.
4. The temperature of the water entering the small heat exchanger must be the same as that of the water entering the large exchanger.
5. There should be no transfer of heat between the water connections of one heat exchanger and the gas stream passing over the other heat exchanger.
6. The temperature of the water leaving the large heat exchanger must be equal to that of the water leaving the small heat exchanger.
7. The temperature of the gas leaving the large heat exchanger must be equal to that of the gas leaving the small heat exchanger.

In endeavoring to fulfill these requirements particular attention was given to methods of heat insulation and temperature measurement. While provisions for fulfilling all of them are embodied in the construction of the meter, the final fulfillment of requirements 6 and 7 is a part of the procedure of operating the meter.

2. GENERAL ARRANGEMENT OF PARTS

The general arrangement of the meter is shown diagrammatically in figure 1. The gas enters the proportioning chamber at the left and flows through mixing baffles A. The division of the gas takes place at the upstream face of inlet radiation shield B, the small stream entering the central tube and the large stream flowing along the annular space outside it.

The heat exchangers, indicated by C, are located a few inches from the inlet radiation shield. After passing through the heat exchanger the large gas stream flows through the second series of mixing baffles A′, through the two outlet radiation shields B′, and out of the proportioning chamber.

The small gas stream is conducted from the proportioning chamber to relief bell chamber R of the piston meter. A slide valve, located in the base of R (but not shown in fig. 1) directs the gas to displacement piston chamber P, and back to the top of the relief bell chamber, whence it passes through adjusting valve K, and joins the large gas stream.

The other parts of the meter shown in figure 1 are as follows: D is the boiler, which is the primary source of heat supply. E is a steam-fed water heater where the water for the heat exchangers is heated. F is a valve for regulating the temperature of the water to the heat exchangers. G and H are, respectively, the large and small weighing tanks for determining the amounts of water discharged from the two heat exchangers. I is the storage tank from which the water is circulated to the heat exchangers and back by means of motor-driven pump J.

L is a large-area orifice placed in the outlet pipe of the large gas stream to provide a pressure drop slightly in excess of that occurring in the small gas stream due to friction in the passages of the piston meter. The size of this orifice may be changed and by this means

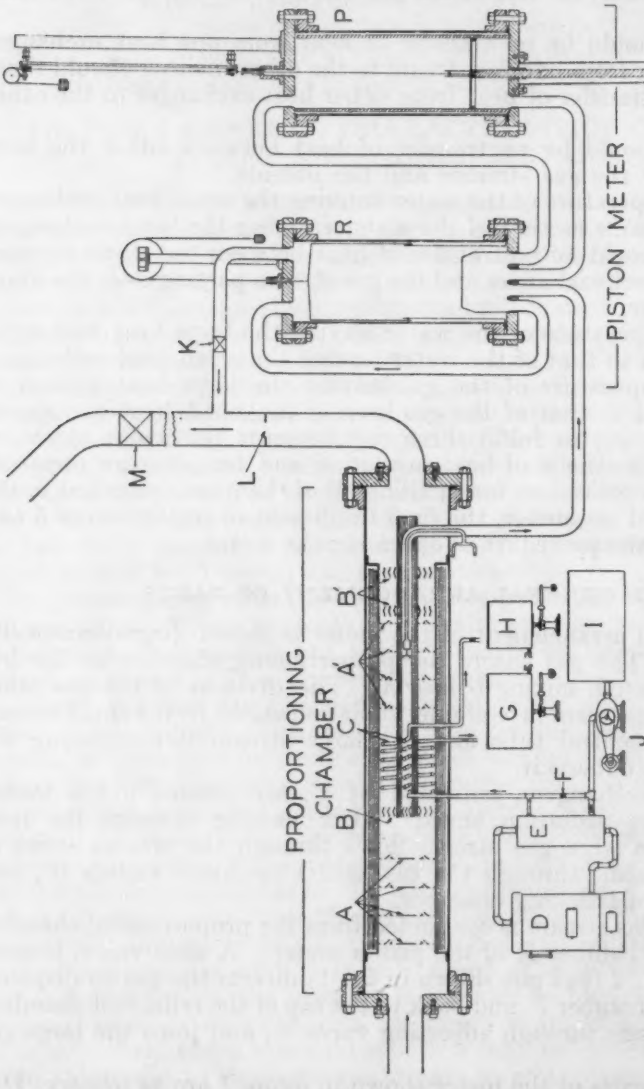

FIGURE 1.—*Schematic diagram of arrangement of the reference meter parts.*

the proportioning ratio may be varied over a wider range than would be possible with valve K alone. M is a large regulating valve by which the main rate of flow through the reference meter is controlled.

3. PROPORTIONING CHAMBER

Figure 2 shows a horizontal section through the proportioning chamber. The chamber is 12 ft. long, and the outer wall is a section

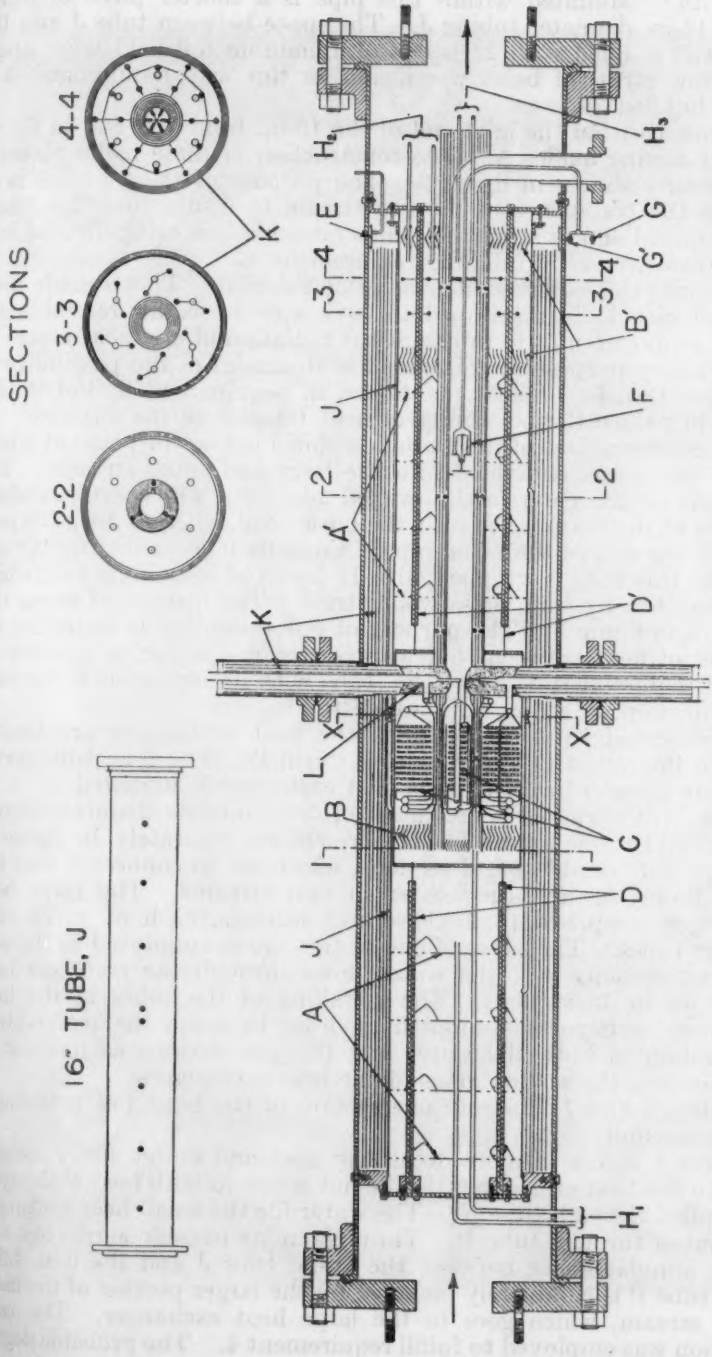

FIGURE 2.—*Horizontal section through proportioning chamber.*

of heavy walled, 24-in. pipe capable of withstanding a gas pressure of 600 lb./in.^{2} Mounted within this pipe is a shorter piece of light-walled 16-in. diameter tubing J. The space between tube J and the outer wall is filled with 22 layers of aluminum foil held ⅛ in. apart by narrow strips of balsa wood, and in this way requirement 3 is partly fulfilled.

Mounted within the inlet end of the 16-in. tube (left end in fig. 2) are four mixing baffles A. The construction of these baffle plates is more clearly shown in figure 3. The purpose of these baffles is to increase the turbulence of the gas stream to insure that it is thoroughly mixed and at a uniform temperature before being divided into two streams, thereby fulfilling requirement 1.

Following the baffles is inlet radiation shield B. This is made from strips of nickel silver stamped to have a cross section resembling a V, and so mounted as to intercept the radiation of any heat across it. The primary purpose of this shield is to minimize the possibility of the cross transfer of heat mentioned in requirement 2, but it also serves to reduce the possibility of heat transfer to the outside.

The upstream face of this radiation shield is also the plane at which the incoming gas is divided into the large and small streams. The small gas stream enters a thin-walled 3-in. tube which extends along the axis of the chamber to near the outlet end, where it turns to pass through the wall of the 24-in. pipe. From its inlet to slightly beyond the turn this tube is wrapped with 11 layers of aluminum foil, which are separated by ⅛-in. balsa-wood strips. The manner of doing this is shown in figure 4. The purpose of this insulation is to reduce the transfer of heat between the two gas streams as far as possible—a part of requirement 2. The 3-in. tube with its insulation is encased, for protection, in a 6-in. thin-walled tube.

As indicated by C in figure 2, the heat exchangers are located close to the outlet side of radiation shield B. The 6-in. tube serves as a core about which the large heat exchanger is mounted.

Both heat exchangers are made of ⅛-in. outside diameter copper tubing. The small heat exchanger, shown separately in figure 5, consists of 11 double-spiral sections, which are so connected that the water flows through the heater in two streams. The large heat exchanger comprises 13 double-spiral sections, each of which contains 28 tubes. The tubes of one section are so connected to those of adjacent sections that the water flows through the complete heat exchanger in 56 streams. The spiralling of the tubes in the heat exchanger sections was adopted in order to make the temperature distribution in both the water and the gas streams as uniform as possible over the section areas of the heat exchangers.

Figures 6 and 7 illustrate one section of the large heat exchanger before assembly.

Figure 8 shows in more detail the inlet and outlet water connections to the heat exchangers. The hot water to both heat exchangers is supplied through tube N. The water for the small heat exchanger is diverted through tube P. Throughout its passage across one side of the annular space between the 16-in. tube J and the 6-in. tube, small tube P is completely jacketed by the larger portion of the main water stream, which goes to the large heat exchanger. This construction was employed to fulfill requirement 4. The probable degree

Research Paper 908
Journal of Research of the National Bureau of Standards

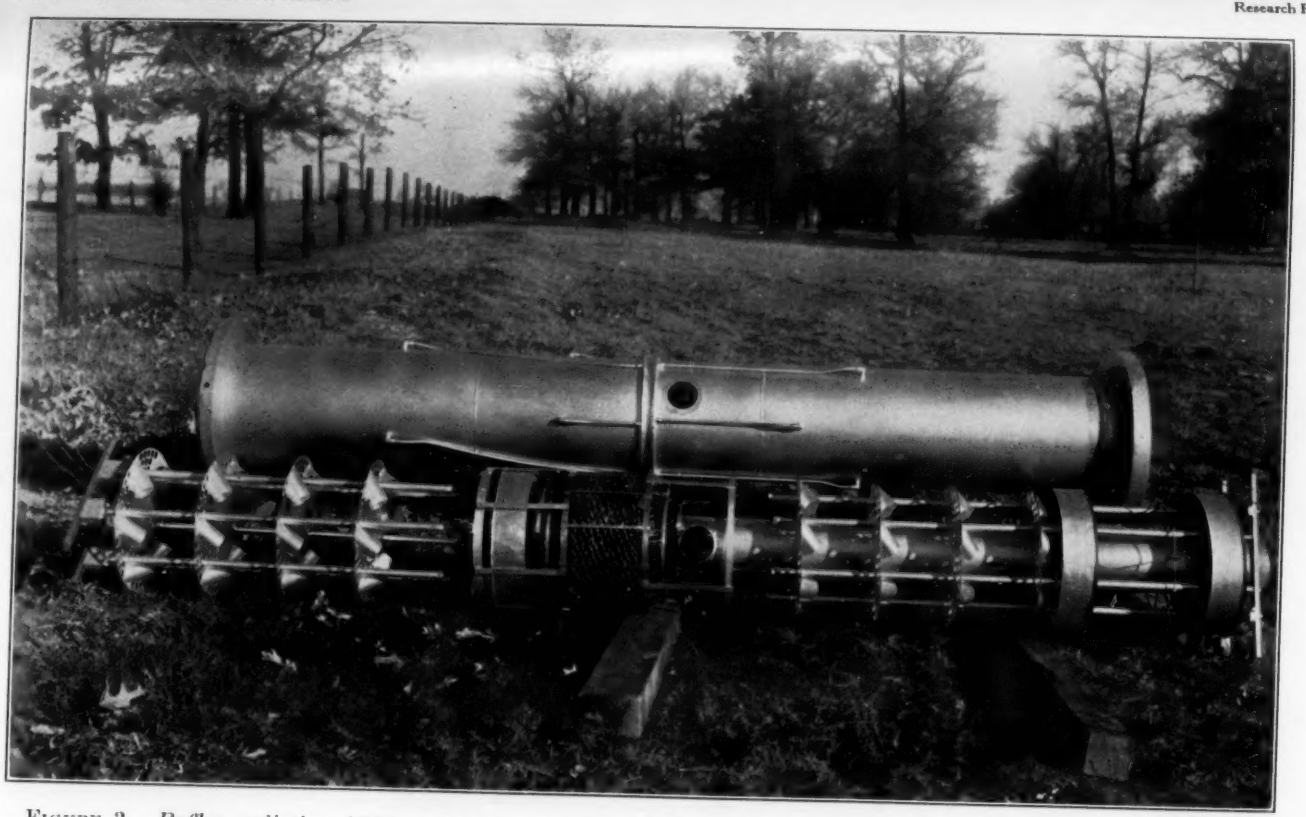

FIGURE 3.—*Baffles, radiation shields, and heat exchanger assembly (foreground) before being placed in 16-inch tube (rear).*

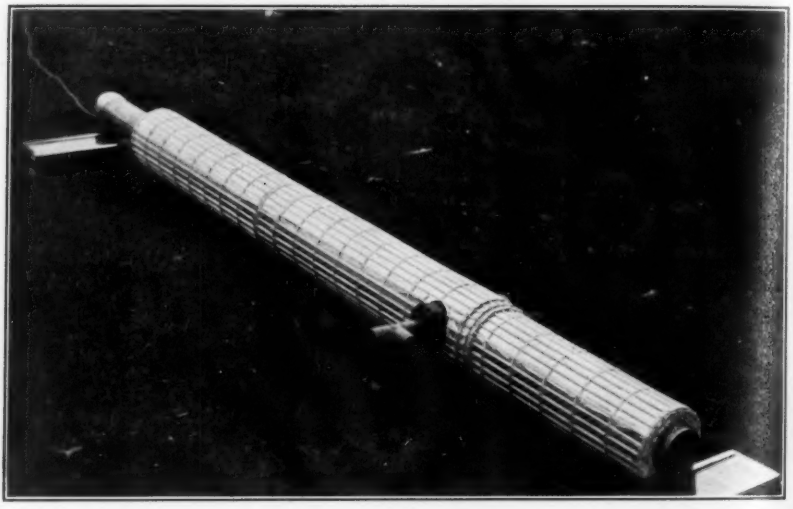

FIGURE 4.—*Application of aluminum-foil insulation to small gas stream passage.*

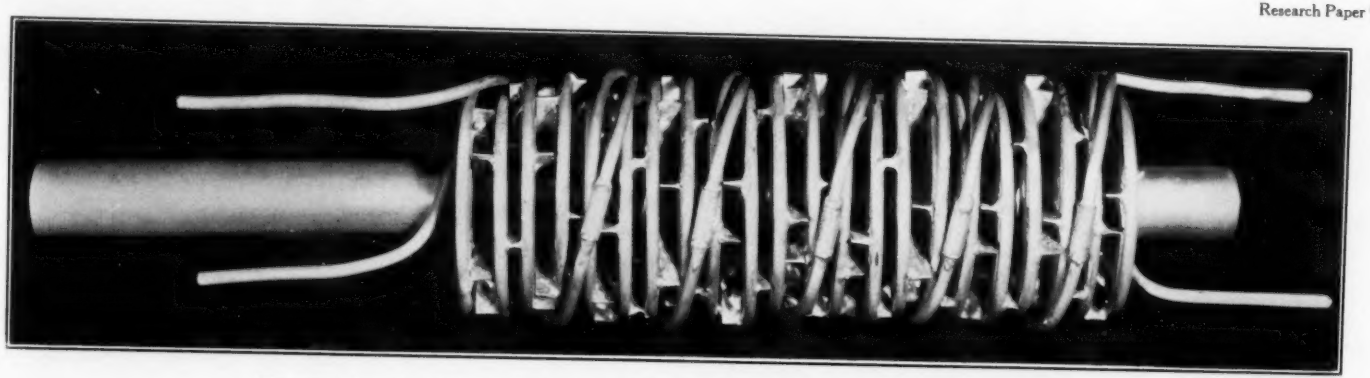

FIGURE 5.—*Small heat exchanger before being placed in the proportioning chamber.*

The upstream (left) end of the core, which is a thin-walled tube, is capped so that no gas flows through it.

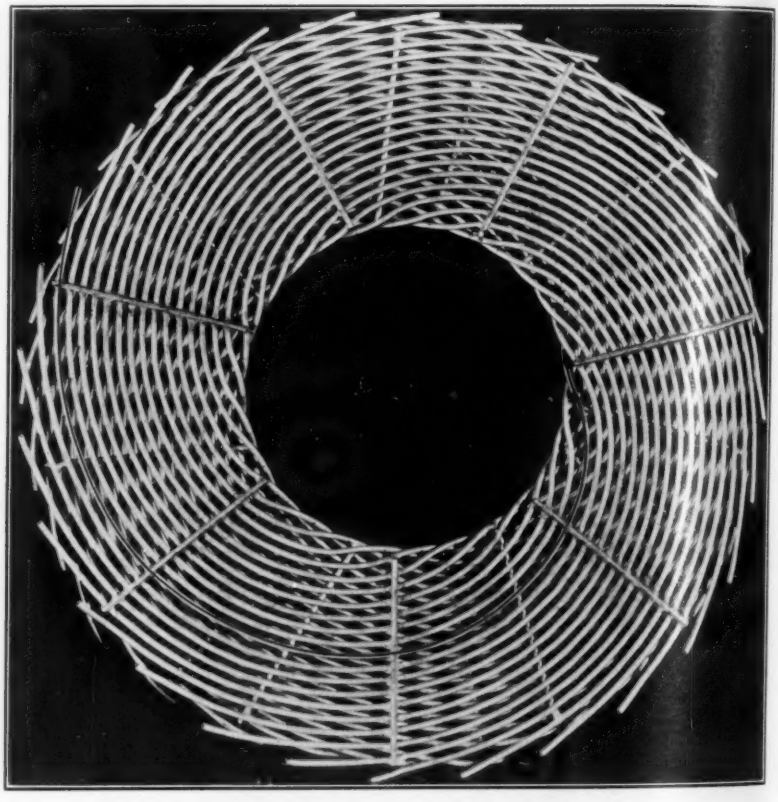

FIGURE 6.—*Section of the large heat exchanger.*
One tube has been marked to facilitate tracing the path.

FIGURE 7.—*Section of large heat exchanger.*

Side view. Arrows indicate the ends of one tube.

UNIV. OF MICH.

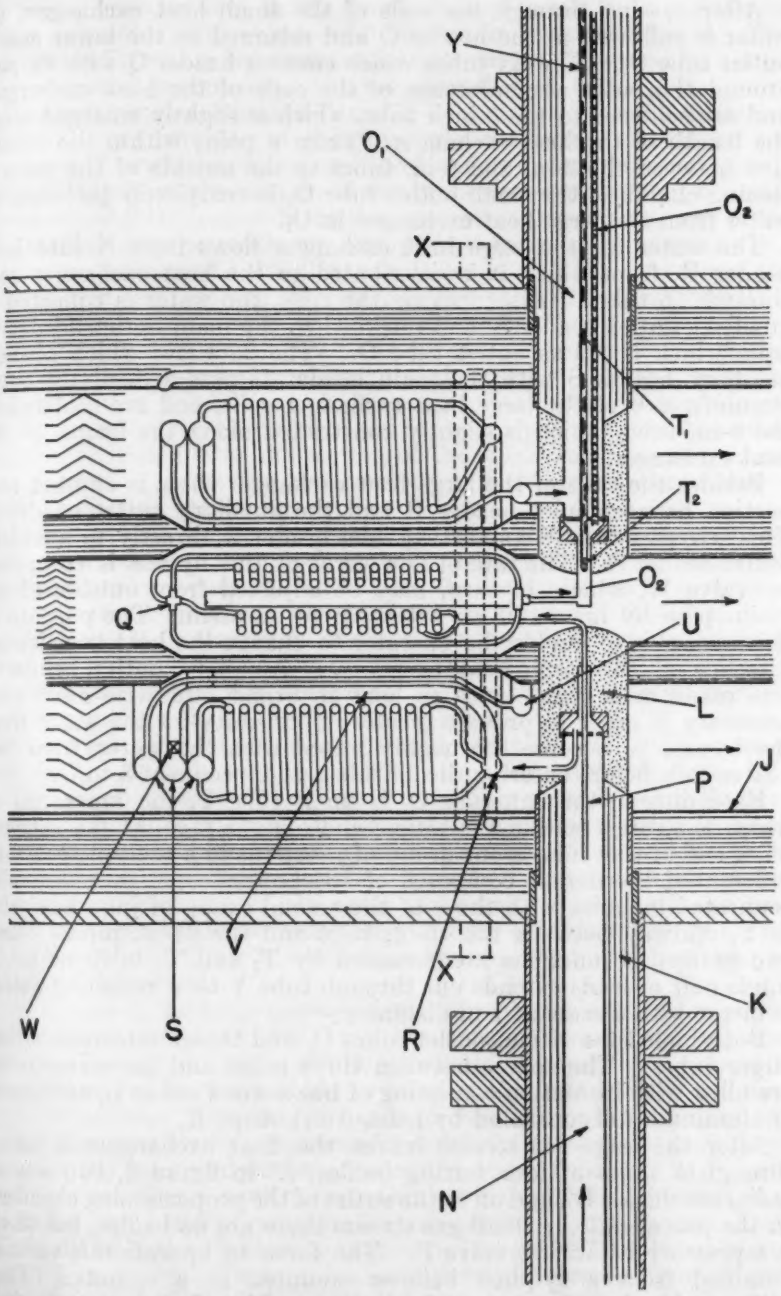

FIGURE 8.—*Diagrammatic representation of water connections to heat exchangers.*

to which the methods of insulation used reduce heat losses is discussed in a later section.

After passing through the coils of the small heat exchanger, the water is collected in the header Q and returned to the lower end of outlet tube O_2. The six tubes which connect header Q with O_2 pass around the outer circumference of the coils of the heat exchanger, and are soldered to the 3-inch tube, which is slightly enlarged along the length of the heat exchanger. From a point within the insulation between the 3-in. and 6-in. tubes to the outside of the proportioning chamber, the small outlet tube O_2 is completely jacketed by water from the large heat exchanger in O_1.

The water for the large heat exchanger flows from N into inlet header R, from which it is distributed to the heat exchanger coils through 56 tubes. After leaving the coils, the water is collected in auxiliary outlet header S, and returned to the main outlet header U, from which it enters outlet tube O_1. The 28 tubes which connect auxiliary header S with the main header U pass around the inner circumference of the large heat exchanger coils, and are soldered to the 6-in. tube, which is slightly constricted along the length of the heat exchanger.

Besides the coils of the large heat exchanger there is another connection between inlet header R and the auxiliary outlet header S. This is bypass tube V connecting inlet header R, directly to auxiliary outlet header S. The rate of flow through this bypass is controlled by valve W, which, in turn, may be adjusted from outside of the 24-in. pipe by means of an extension to its stem. The purpose of this bypass is to enable the operator to change the heat transferring capacity of the large heat exchanger. Auxiliary outlet header S was made more than twice as long as would otherwise have been necessary in order to provide greater opportunity for the water from the bypass to become thoroughly mixed with the water from the heater coils before entering the 28 tubes which connect S to U.

Extending in through tube O_1 is small tube Y, the inner end of which is entirely within the intake end of tube O_2. At the extreme inner end of this tube is one group of junctions of a multiple-junction differential thermopile composed of 18 chromel-copel thermocouples connected in series with those of the second group of junctions, also in Y, midway between the 16-in. tube and the 24-in. pipe. These two groups of junctions are indicated by T_2 and T_1 in figure 8. A single pair of leads extends out through tube Y to a reflecting galvanometer with a scale at 1 m distance.

Both inlet tube N and outlet tubes O_1 and O_2 are mounted within larger tubes. The spaces between these tubes and the water tubes are filled with insulation consisting of balsa-wood cubes L, and layers of aluminum foil separated by balsa-wood strips K.

After the large gas stream leaves the heat exchangers it passes through a series of four mixing baffles, A′ in figure 2, two sets of radiation shields B′, and on to the outlet of the proportioning chamber. In the passage of the small gas stream there are no baffles, but there is a pressure balancing valve F. The force to operate this valve is obtained from a sylphon bellows mounted in a chamber. This bellows chamber is connected to the outside of the proportioning chamber by a tube to which either pressure or suction for operating the valve may be applied through valves G and G′. The purpose of

valve F is to introduce additional pressure drop in the small gas stream so that the pressure drops in the two gas streams will be more nearly the same, since without it, the pressure drop in the large gas stream would be greater at most rates of flow, than in the small stream. The difference of pressure between the two streams is measured by a mercury manometer connected to pressure tubes H_2 and H_3.

Located across sections 2–2 and 3–3, figure 2, between radiation shields B′, are two sets of thermocouple junctions. At section 2–2 there are 12 single junctions, and the leads from each junction go to a junction block on the outside of the proportioning chamber housing. By means of this junction block it is possible to connect any one of the 12 junctions in series with any one of the remaining 11 junctions in a galvanometer circuit. In this way it is possible to determine the difference in temperature between any two of the 12 junctions within about 0.02° F.

Distributed over section 3–3 there are in all 36 junctions comprising a second multiple-junction differential thermopile. As shown by the view of section 3–3 in figure 2, 18 of these junctions are spaced uniformly over the cross section of the large gas passage, and the other 18 are distributed over the section of the small gas passage. These two groups of junctions are connected in a circuit containing a second reflecting galvanometer.

At several sections along the chamber single thermocouple junctions have been attached to the inner and outer walls of the small gas stream passage. Section 2–2, figure 2, illustrates such a section. Other junctions have been placed along the surface of the 16-in. tube J. In figure 2 the locations of the thermocouple junctions are indicated by the solid dots. The purpose of the junctions is to make it possible to measure the differences in temperatures between these various points in the proportioning chamber.

At the inlet end of the proportioning chamber, the annular space between the 24-in. pipe and the 16-in. tube is completely closed by a solid supporting ring. At the outlet end this space is normally open so that the entire space is subjected to the outlet pressure. Thus, regardless of the pipe-line pressure, the 16-in. tube will never be subjected to a greater pressure difference than that due to the friction drop along the chamber. In order to be able to test for leaks, provision has been made for completely sealing off this space by means of rubber tube E, figure 2, which may be inflated at any time through a tube to the outside.

As the gas in the large passage flows through the heat exchanger its temperature rises, and ordinarily the temperature of the adjacent section of the 16-in. tube would follow this temperature change to some extent. This would tend to increase the heat loss by radiation and conduction. An attempt has been made to reduce these effects as much as possible by arranging for most of the temperature change between the inlet and outlet ends of the 16-in. tube and 24-in. pipe to take place over a very narrow band, which, for convenience, may be called the band of temperature change. At the section X–X, figures 2 and 8, the 16-in. tube is encircled by two 0.5-in. tubes placed about 1 in. apart. These tubes are clearly shown in figure 3, just to the left of the large hole in the 16-in. tube. Each encircling tube is connected to the 16-in. tube by several pairs of longitudinal tubes, as also shown in figure 3. Consider first the upstream (left in fig. 3)

encircling tube and its connecting tube. Because of the baffles and radiation shield within the 16-in. tube, the static pressure of the gas at the openings of the long longitudinal tubes will be slightly higher than at the openings of the short longitudinal tubes. Some gas will therefore enter the longer tubes, flow to and around the encircling tube and back into the large gas stream through the short tubes. This circulation of the inlet gas will tend to keep the 16-in. tube at the inlet gas temperature as far downstream as the encircling tube.

Opposite the two encircling tubes the 24-in. pipe is encircled by two sheet metal disks 2 in. apart, which form a hollow partition between two sets of water sprays. The water sprayed onto the inlet portion of the casing is maintained at the inlet gas temperature, as nearly as possible, while that sprayed onto the outlet section is maintained at the outlet gas temperature.

4. PISTON DISPLACEMENT METER

The tally meter used to measure the small gas stream is a piston meter of the positive displacement type. As is shown in figure 1, this meter has two main parts or chambers, the first being the relief bell and valve chamber R, and the second, measuring chamber P. The side wall of each chamber is a 5-ft length of 24-in. heavy-walled steel pipe. One series 60 and three series 40 blind flanges form the tops and bases of the chambers, the heavier flange serving as the base of the measuring chamber. This heavy construction of these chambers was adopted so that the meter might be safely operated under line pressures as high as 600 lb/in^2.

The measuring cylinder is made of cast iron about 1 in. thick and about 5 ft. long. It was machined on the outside and carefully ground on the inside to an average diameter of 20.522 in. With this cylinder in a vertical position, measurements of four diameters in each of five sections agreed within $\pm$ 0.001 in. The sections at which these measurements were made were spaced uniformly along the length of the cylinder. The cylinder stands on a thin paper gasket in a groove cut in the series 60 blind flange. It is entirely free of the chamber walls and top, so that variations in the gas pressure should not affect its volume. The annular space between the cylinder and chamber wall is partly filled with oil so as to prevent gas leaking through the joint between the cylinder and base.

The piston, also of cast iron, has three grooves. The two outside gro ves hold cast-iron piston rings, while the middle groove acts as an oil distributing header. Each piston ring is backed with 24 coil springs that give it bearing pressures equal to those used on steam engines. The oil distributing header is connected to a small oil reservoir located on the top of the piston at its center. The level of the oil in this reservoir is kept high enough that the pressure of the oil in the oil groove is greater than that of the gas on either side of the piston. Thus, oil will continually seep out between the piston and cylinder and prevent gas leakage past the piston.

A 2-in. piston rod, fastened to the under side of the piston, extends through a lapped bronze bushing in the cylinder housing base into the oil-power cylinder. As will be more fully explained, oil pressure against the end of this rod operates the piston. In addition, the rod serves as a guide to keep the piston from tilting.

In order to compute the piston displacement, the stroke of the piston must be known. This is measured as follows: A phosphor-bronze wire extends from the top of the piston, through a lapped gland on top of the cylinder housing and is attached to a steel contact button. At the top of a 6-ft post mounted on the cylinder housing there is a pulley over which a steel ribbon passes. One end of the ribbon is attached to the contact button and the other to a counterweight, which keeps the ribbon and wire taut as the piston moves up and down. As the piston nears either end of its stroke, the contact button passes through a guide sleeve and comes to rest against the arm of a dial micrometer or indicator. The piston remains at the end of the stroke long enough for a reading of the micrometer to be made. The micrometers are mounted on the ends of a rod so that they may be turned simultaneously to bring the ends of the contact arms onto the ends of a steel reference bar, and a second reading of the micrometer taken. By comparing the two sets of micrometer readings, which may be made to 0.001 in., with the known length of the steel bar, the stroke of the piston is determined. Two of these steel bars were made and their lengths compared; then one was taken to the National Bureau of Standards to be calibrated and kept for reference, while the other remains in use at Joliet.

The gland through which the bronze wire passes is in the top of a steel forging mounted on top of the cylinder housing. Just below the gland there is a duct through which oil is fed to the center of the forging, so that the oil may flow down the wire into the oil reservoir on top of the piston. Near the base of the forging there are two small glass windows, diametrically opposed, through which the oil level in the piston reservoir may be observed, the top of this reservoir being a glass tube.

Within the relief bell housing there is a sheet-metal inner wall attached at the base to the housing wall and extending up about half the height of the chamber. The annular tank thus formed is about an inch wide. It is filled with mineral seal oil in which the relief bell is suspended, as shown in figure 9. The relief bell is made of sheet zinc 0.01 in. thick, and is guided by six wires so that it cannot touch either wall of the annular tank. A phosphor-bronze wire fastened to the top of the bell extends up through a lapped gland in the top of the bell housing. The upper end of this wire is fastened to a chain which, in turn, wraps around and is fastened to an aluminum pulley of about 1 ft. diameter. The bell is balanced by a weight suspended by a second chain also wrapped around and fastened to the aluminum pulley. The two chains are of such size that as they wind and unwind from opposite sides of the pulley they balance the buoyancy effect of the oil on the bell. The reason for fastening the chains to the pulley, so that any movement of the bell rotates the pulley without slippage, will be explained later.

In the space under the relief bell there are located the D-slide valve which directs the gas flow to and from the measuring cylinder; the small oil cylinder and piston for operating the D-valve, G, figure 11; the 4-way cock H, which controls the movement of this piston; the two 2-way cocks I, which control the direction of oil flow to the main oil cylinder below the measuring cylinder; and an oil sump or reservoir.

The D-valve and seat are made of cast iron and the sliding surfaces ground to fit. Two oil sprays, one above and the other below the

valve, and controlled from outside, permit positive lubrication of the sliding surfaces while the meter is in operation. In this way the possibility of gas leakage between these surfaces is minimized.

Although, for convenience of illustration, it is not so represented in figure 11, the 4-way cock is actually located in the bottom of the oil sump, with its core vertical. An extension attached to the core passes through the base of the bell housing so that, by means of a lever attached to the extension, the cock may be operated from the outside. In one position oil from the pump is delivered to one end of small cylinder G, forcing the piston therein to the opposite end. The movement of this piston moves the gas D-valve from one end position

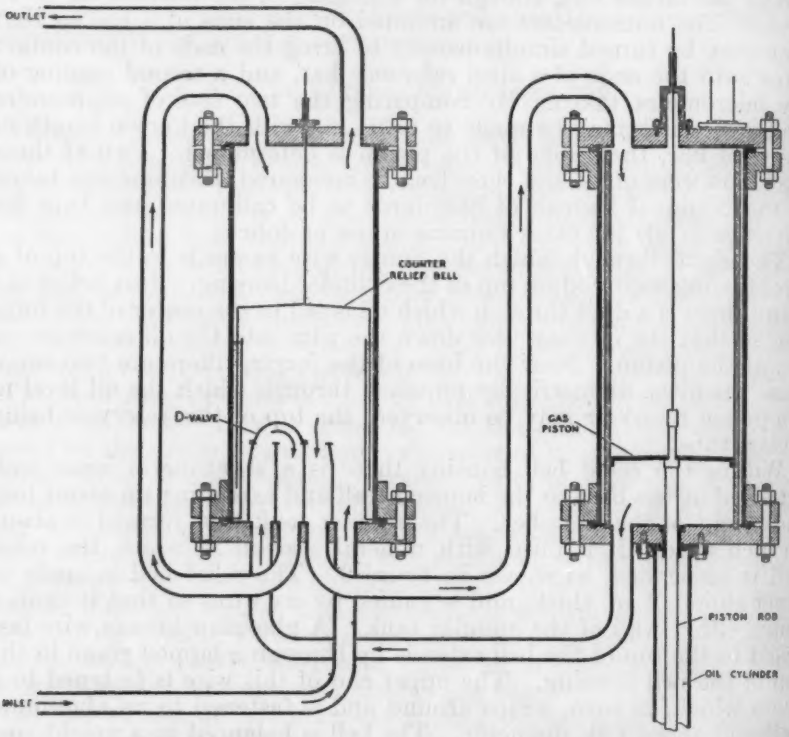

FIGURE 9.—*Gas passages through the piston meter.*

to the other by a simple yoke connection. By means of lugs on this yoke the movement of the small piston also closes one of the 2-way cocks I, and opens the other. These lugs are so placed that the D-valve moves about two-thirds of its travel before the 2-way cocks are moved. Turning the 4-way cock through 90° admits oil to the other end of the small cylinder causing the piston to move the D-valve to its other position and to reverse the open and closed relation of the 2-way cocks.

The oil sump is open to the gas pressure and therefore the oil pump supplies only the additional pressure required to operate the large gas piston. This also makes it unnecessary to change the adjustment of the relief valve for different gas pressures.

The outside of the two pressure vessels and all of the gas and oil piping of the piston meter are sprayed with water from a constant-temperature tank. The rate of circulation of the spray water is about 80 gallons per minute. This water may be maintained at any desired temperature by a sensitive thermostat which operates on a temperature differential of about 0.1° F. Both the support for the stroke-measurement mechanism and the calibrated bar are kept at this same temperature by jacketing with water from the constant-temperature tank.

5. HOW THE PISTON METER WORKS

Some of the details of the displacement meter and the functions of some parts already described, can be best explained by describing a cycle of operation. The connections by which the small gas stream is conducted to, through, and from the piston meter are shown diagrammatically in figures 1 and 9.

As the small gas stream leaves the proportioning chamber it passes through a heat exchanger (not shown on any of the sketches) where it is brought to the piston-meter temperature, and it then enters the relief bell chamber on the under side of the bell. With the D-valve at the left end of the stroke, as shown in figure 9, gas will pass from under the bell to the top of the piston. At the same time gas escaping from under the gas piston passes through the D-valve to the top of the bell chamber, whence it is piped back to the main stream. When the gas piston has reached the end of its stroke it remains stationary for a few seconds, during which interval the gas entering the system causes the relief bell to rise, displacing gas from the space above the bell into the outlet connection. Because of the careful counterbalancing and the light construction it requires so little gas pressure to move the bell up or down, that differential pressure across this bell is entirely negligible, regardless of its position, rate of movement, or direction of movement.

As the gas piston nears the end of its stroke (within less than 0.1 in.) the contact button of the stroke measuring mechanism causes an extension attached to the indicator arm to close small snap switch A, figure 10. When the piston has come to rest, the inflow of gas is taken up by the relief bell, which rises and thereby rotates the aluminum wheel. As this wheel rotates, adjustable striker U mounted on the rim closes the second snap switch B. This completes an electrical circuit to supply current from dry-cell batteries to one of the solenoids S. The energized solenoid pulls a trigger that releases a water-filled bucket, which in falling pulls the 4-way cock lever through an arc of 90°. As one water bucket falls, it pulls the other, which is empty, up into place to be filled and ready for the next reversal. Heavy lighting circuit toggle switches T are connected in each solenoid circuit and are operated by the 4-way cock lever in such a way that as soon as the lever has swung a few degrees the toggle switch in the closed circuit is opened, and the other toggle switch is closed. This manner of opening the solenoid circuits protects the small snap switches, which would otherwise be burned out quickly.

As the gas piston moves downward, the piston rod displaces oil from the cylinder, and the oil flows back to the oil sump through the lower 2-way cock, as shown by the solid arrows in figure 11. Near

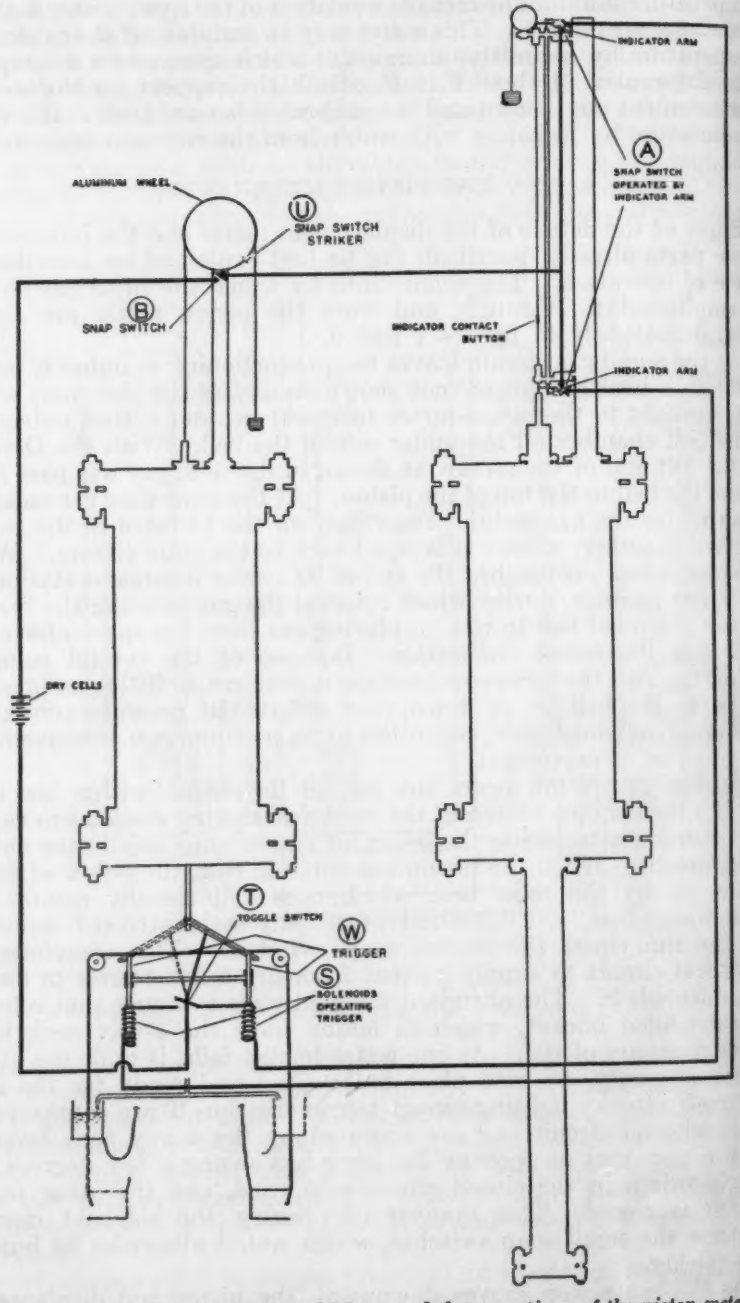

FIGURE 10.—*Electric circuits which control the operations of the piston meter.*

the end of its stroke the piston rod automatically operates one of two sleeve valves, D in figure 11, which gradually shuts off the oil flow, thus bringing the piston to rest gently. The rate of acceleration or deceleration of the piston may be varied by adjustments of the sleeve valves. The length of time that the gas piston remains stationary at the end of its stroke is regulated by the position of the striker on the rim of the large aluminum pulley.

As previously described, turning the 4-way cock through 90° results in shifting the D-valve and reversing the open and closed positions of the 2-way cocks. With these cocks reversed, oil under pressure from the oil pump starts to flow back into the large oil cylinder and to raise the piston rod and gas piston. As the shifting of the D-valve is completed before the 2-way cocks are fully reversed there is no chance for the gas piston to move before the D-valve is in place.

There are three other valves in the oil line which remain to be described and their functions explained. These are: Valve E, figure 11, for regulating the rate of flow of the oil; valve F for directing the flow of the oil through the proper sleeve valve; and relief valve C.

The connections between valves E and F and sleeve valves D and D′ in the base of the oil cylinder are shown diagrammatically in figure 12. This figure also indicates the essential features of construction of these valves. Starting with the gas piston descending, as in figure 9, oil is leaving the oil cylinder through valves D and F, as indicated by the solid arrows, in Figure 12. When the gas piston has come to rest, the relief bell rises, thereby rotating the large aluminum pulley, figure 11. This pulley is mounted on and rigidly fastened to the core of valve E, and the raising of the bell rotates the core in the direction to open the valve. After the D-valve and the 4- and 2-way cocks have been reversed, as previously explained, oil starts to flow back into the oil cylinder through the same passages, as shown by the solid arrows but in the opposite direction. The inflow of oil into the oil cylinder causes the piston rod and gas piston to rise, thereby releasing valve D, which is opened wide by a spring. With both valves D and E wide open, oil enters the cylinder fast enough to cause the rate of displacement of the gas piston to exceed the rate of inflow of gas under the relief bell, so that the bell falls. As the bell nears the bottom of its travel it nearly closes valve E. This sets up a differential pressure across the valve, which is communicated to the ends of valve F, and as the pressure at end 1 is greater than at end 2, the piston in valve F moves to the right to position 2 shown in dotted outline. This causes the oil to enter the oil cylinder through valve D′, which is also wide open, as indicated by the dotted arrows. The rate of flow of the oil continues to be controlled through valve E by the position of the relief bell, so that the displacement rate of the gas piston exactly equals the volume rate of flow of the gas. It was expected that in order to secure this balance there would be a small amount of "hunting" by the bell, but there has appeared to be almost none.

As the gas piston nears the end of its travel the piston rod engages a link which gradually closes valve D′, bringing the gas piston to rest gently. After the D-valve and 4- and 2-way cocks are reversed oil

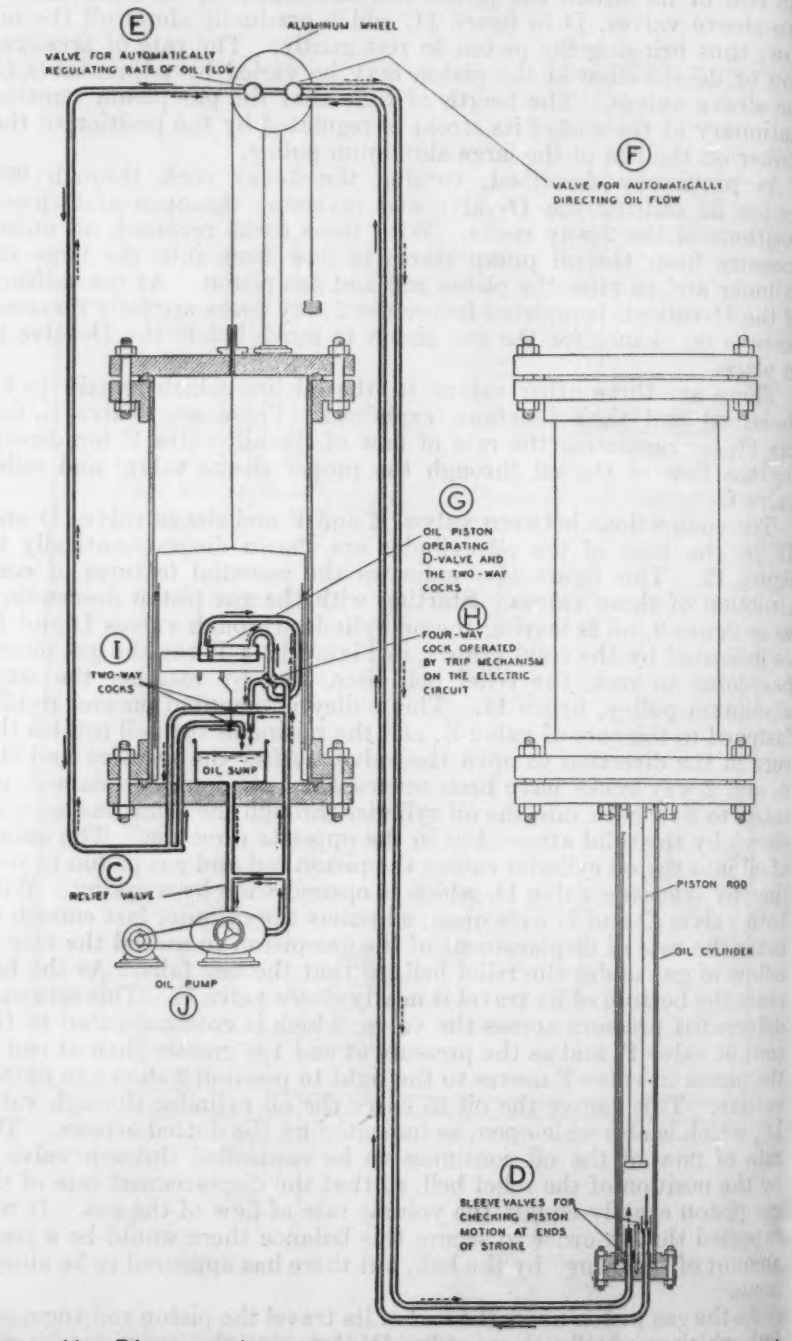

FIGURE 11.—*Diagrammatic representation of the oil circuit by which the power to operate the piston meter is transmitted.*

starts to leave the oil cylinder along the path of the dotted arrows, but in the opposite direction. Again, as the displacement rate of the gas piston overtakes the rate of gas flow the relief bell closes valve E. This time, however, the difference of pressure across valve E is in the

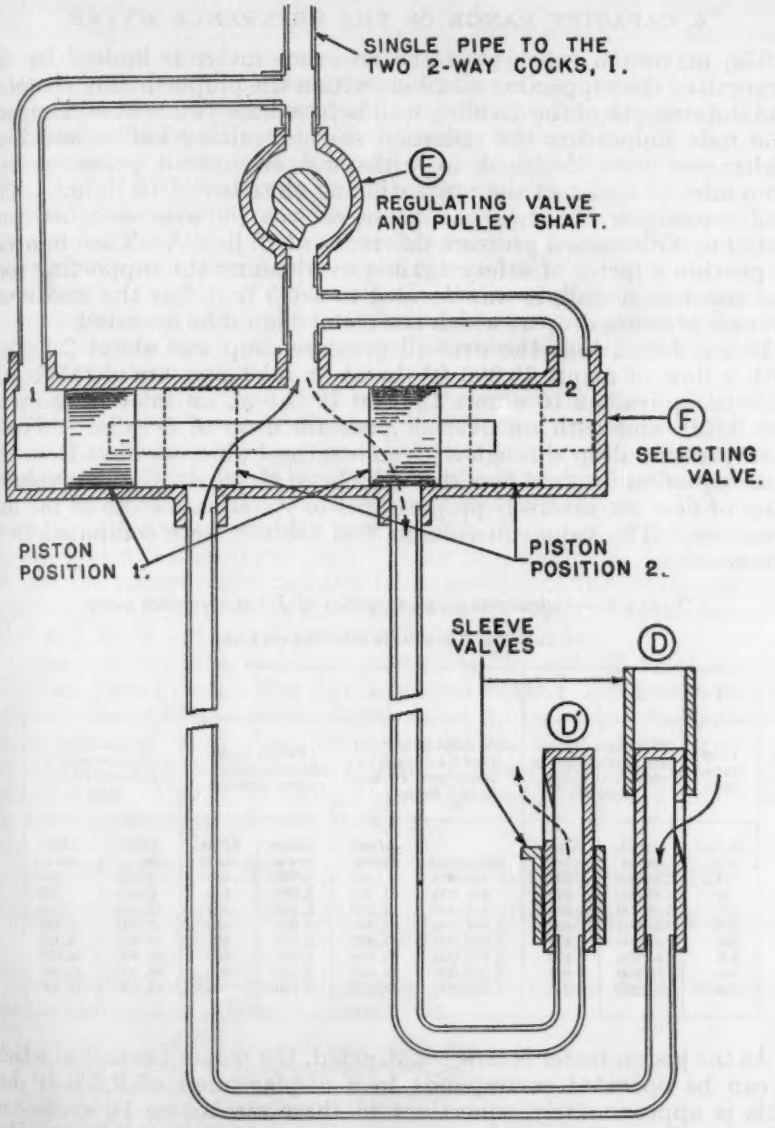

FIGURE 12.—*Diagram of connections between valves* D, D', E, *and* F.

opposite direction, so that the pressure at end 2 of valve F is greater than at end 1, and the piston in valve F is forced back to position 1. Oil now leaves the oil cylinder along the path of the solid arrows, and a cycle of changes is completed.

Relief valve or unloading valve C, figure 11, is located in a by-pass line connecting the oil-pump discharge to the oil sump. When the

gas piston and piston rod are descending and the upper 2-way cock is closed, this relief valve permits the discharge from the pump to return to the oil sump without subjecting the pump and piping to excessive pressures.

6. CAPACITY RANGE OF THE REFERENCE METER

The maximum capacity of the reference meter is limited by the strength of the supporting members within the proportioning chamber and the strength of the dividing wall between the two heat exchangers. The rods supporting the radiation shields, mixing baffles and heat exchangers were designed to withstand an overall pressure drop from inlet to outlet of the proportioning chamber of 10 lb/in.^{2}. The wall separating the two gas passages was likewise designed and tested to withstand a pressure difference of 10 lb/in.^{2}. Then in order to provide a factor of safety against overloading the supporting rods and separation wall, it was decided to set 5 lb/in.^{2} as the maximum over-all pressure drop at which the meter should be operated.

It was found that the over-all pressure drop was about 2 lb/in.^{2}, with a flow of about 73,200 ft^3 /hr at an inlet pressure of 215 lb/in.^{2}. This is equivalent to about 120,000 ft^3 /hr at an inlet pressure of 200 lb/in.^{2} and with an over-all pressure drop of 5 lb/in.^{2}. For a fixed pressure drop through a given length of pipe, we have from the usual equation for fluid flow through closed channels, that the volume rates of flow are inversely proportional to the square roots of the line pressures. The values in column 2 of table 1 were computed from this relation.

TABLE 1.—*Calculated safe capacities of Joliet reference meter*

[All rates of flow are in cubic feet per hour]

1	2	3	4	5	6	7	8	9
Line pressure	Safe rates of flow into proportioning chamber, at line pressure		Safe rates of flow into proportioning chamber, reduced to 14.7 lb/in.^{2}		Piston meter displacements at line pressure		Piston meter displacements reduced to 14.7 lb/in.^{2}	
lb/in.^{2} abs.	*Maximum*	*Minimum*	*Maximum*	*Minimum*	*Maximum*	*Minimum*	*Maximum*	*Minimum*
14.7	120,000	400	120,000	400	2,000	400	2,000	400
50	120,000	400	408,000	1,360	2,000	400	6,800	1,360
100	120,000	400	816,000	2,720	2,000	400	13,600	2,720
200	120,000	400	1,633,000	5,440	2,000	400	27,200	5,440
300	98,000	400	2,000,000	8,160	2,000	400	40,800	8,160
400	84,900	400	2,310,000	10,880	2,000	400	54,400	10,880
500	75,900	400	2,580,000	13,600	2,000	400	68,000	13,600
600	69,200	400	2,823,000	16,320	2,000	400	81,600	16,320

As the piston meter is now constructed, the maximum rate at which it can be operated corresponds to a displacement of 2,000 ft^3 /hr. This is approximately equivalent to three strokes or 1½ cycles per minute. In order to make it operate at a higher rate, it would be necessary to increase the weight of the gas piston in order to provide an increased pressure for driving the oil out of the oil cylinder on the downward stroke; and a higher oil pressure would then be required to raise the gas piston. Moreover, when the piston is moving at a displacement rate of 2,000 ft^3/hr, there is a difference of about 4 in. of water between the gas pressures on the two sides of the piston.

The oil seal, provided by the reservoir and middle piston groove, is adequate to this pressure difference, but it would not be if the pressure difference were increased very much, as would be the case at a higher displacement rate.

Theoretically, the displacement rate of the piston meter may decrease almost to the vanishing point, but practically a minimum rate of displacement is reached when the movement of the gas piston becomes irregular. This irregular operation is apparently due to gas dissolved in the oil escaping from solution and forming gas pockets in the oil piping. In some preliminary trials this difficulty was encountered at a displacement rate of about 400 ft^3/hr or one stroke in 2 minutes. At that time the difficulty was overcome by removing the gas bubbles through vents. There has been no occasion to see how much farther the displacement rate could be decreased in practice, but it is believed that a displacement rate of 100 ft^3/hr or one stroke in 8 minutes might possibly be reached. In preparing table 1 a minimum displacement rate of 400 ft^3/hr is given as a conservative value (column 7), this being the lowest rate at which the meter has actually been operated.

The proportioning ratio at which the meter can be operated depends upon the relative areas of the heat transferring surfaces of the two heat exchangers, and upon the regulation of the water flow, which can be obtained by the by-pass around the large heat exchanger and the valves on the outlets of the two heat exchangers. The range over which this proportioning ratio may be thus varied conveniently is from about 5:1 to about 60:1. Since the maximum displacement rate for the piston meter is 2,000 ft^3/hr this limits the maximum rate of flow into the proportioning chamber to 120,000 ft^3/hr, as shown in column 2, table 1, for line pressures below 200 lb/$in.^2$

If the outlet to the large gas passage is blanked off all of the gas will then pass through the displacement meter. This converts the reference meter from a proportional meter into a simple displacement meter. In this way, also, the minimum capacity of the reference meter becomes the same as the minimum rate of displacement of the piston meter. Hence, in table 1, the figures in column 3 and 5 are the same as those in columns 7 and 9.

V. OPERATING THE JOLIET REFERENCE METER

1. QUANTITIES OBSERVED WHEN OPERATING THE REFERENCE METER

Observations of the following quantities are made and recorded when operating the reference meter:

1. Weight of water from small heat exchanger.
2. Weight of water from large heat exchanger.
3. Gage pressure of the gas in the piston meter.
4. Temperature of the gas in the piston meter.
5. Length of piston strokes.
6. Number of piston strokes or cycles.
7. Duration of run (i. e., length of test period).
8. Specific gravity of the gas.
9. Barometric pressure during the period of the test.
10. Difference between the pressures of the gas in the large and small gas streams at the gas differential thermometer (section 4–4, figure 2).
11. Temperature of the gas entering the proportioning chamber.
12. Temperature of large gas stream at proportioning chamber outlet.

13. Difference in temperatures of water streams leaving the two heat exchangers.
14. Difference in temperatures of the large and small gas streams leaving proportioning chamber.
15. Temperature of the water entering the heat exchangers.
16. Pressures of water at inlet and outlet to heat exchangers.
17. Temperatures of the inlet and outlet sections of the proportioning chamber case (i. e., temperatures of the bath waters with which these sections are sprayed).
18. Temperature of the piston meter bath water.
19. Differential pressure across relief bell.

Items 1 to 9, inclusive, are necessary for computing the rate of flow through the reference meter. Since any error in measuring or recording these quantities will affect the final result in greater or lesser degree, it is necessary to study the effects of errors in each quantity upon the final result, so that each quantity may be measured with the necessary degree of precision.

Items 10, 11, and 12 are not needed in computing the rate of gas flow unless the pressure adjusting valve in the small gas stream F, figure 2, is not used, or is inoperative. In such a case these items are used for computing a small correction for the Joule-Thompson effect.

Items 13 and 14 never enter directly into computation of the flow, but since the determination of the proportioning ratio assumes that these differences are sensibly zero it is necessary that they be indicated and observed very carefully.

The remaining five items are used only as guides in the operation of the meter.

2. INSTRUMENTS AND METHODS OF MEASUREMENT

The weight of the water flowing from the small heat exchanger is determined with an equal arm over-and-under scale. The balance has a capacity of 30 lb, and the value of the smallest weight used with it is 0.1 lb. In addition, the balance is equipped with a scale and pointer with which readings may be made to the nearest 0.001 lb. The general procedure followed when operating the meter is to weigh about 20 lb of water at a time. Two pails of equal capacity are used alternately for collecting and weighing the water.

The weight of water flowing from the large heat exchanger is determined with two beam scales of 300-lb capacity. The beams of these scales have a range of 3 lb divided to ¼ oz. Ordinarily, about 250 pounds of water are weighed at a time and the scale beam setting read to the nearest ounce. Each scale is equipped with a weigh tank, and while one tankful is being weighed and emptied the other tank is filling.

Both of the scales and also the balance were calibrated for commercial accuracy by the Bureau at its track-scale depot in Clearing, near Chicago. In addition, intercomparisons have been made between the indications of these scales and master scales maintained by the Chicago Department of Weights and Measures. The results of these comparisons are utilized in calculating the results of a test.

The gage pressure of the gas in the piston meter, item 3, is measured with a dead-weight gage tester modified as so to be conveniently used as a piston gage. Special weights were made for use with this piston gage, which permitted the measurement of pressures to 0.01 lb./in.^{2}, although it is not always necessary to measure pressures closer than to the nearest 0.1 lb/in.^{2}. During a test, readings of the gas pressure

in the piston meter are made at 4-minute intervals. (A more detailed description of this piston gage is given in Appendix B.)

The temperature of the gas in the piston meter, item 4, is not measured directly but is assumed to be the same as that of the constant-temperature bath water. The temperature of the bath water, item 18, is measured with a mercury-in-glass thermometer graduated to 1° F, which has been compared with a thermometer calibrated by the Bureau. The indications of the thermometer in the water bath are estimated to the nearest 0.1° F, and these readings are made at 2-minute intervals.

The length of each piston stroke, item 5, is obtained by readings of the dial micrometers (described in section IV–4) at the end of each stroke. Although it is not necessary to know the stroke of the gas piston to less than 0.01 in., indications of the dial micrometers may be read easily to the nearest 0.001 in.

The number of piston strokes during a test, item 6, is recorded by the observer taking the micrometer readings. Each stroke of the piston is also recorded on a chronograph by means of an electrical connection.

The length of a test period, item 7, is determined by means of a clock with a mercury-compensated seconds pendulum. This clock is equipped with a sweep second hand, and may be regulated so that its variations will be less than 5 seconds a day.

In order to reduce the errors of observing the time at the start and end of a test, and to obtain a permanent record against time of several of the meter functions, a multiple-pen chronograph is used. By means of a photoelectric-cell system, one of the pens records the time in seconds, as measured by the clock pendulum. Other pens are connected to record each stroke of the gas piston, and the starting and stopping of the water flow into each weighing tank.

The specific gravity of the gas, item 8, is determined with a gravity balance. During a test this determination is made at about half-hour intervals.

The barometric pressure, item 9, is determined with a mercurial barometer located in a building about 100 yd from the meter, and at the same elevation. One reading is taken during each test period.

The differential pressures between the gas streams at the section of the differential thermometers, item 10, and across the relief bell, item 19, are obtained with liquid manometers designed to withstand safely the line pressures. Mercury is used in the manometer for item 10, and mineral seal oil in the manometer for item 19. During a test these manometers are read at 2-minute intervals.

The temperature of the gas entering the proportioning chamber, item 11, and the temperature of the large gas stream leaving the proportioning chamber, item 12, are determined with mercurial thermometers similar to that used for item 4. These thermometers are inserted in stainless steel wells partially filled with mercury. The wells are located in the 10-in. pipe conveniently close to the inlet and outlet of the proportioning chamber. Readings of these thermometers are taken at 2-minute intervals.

The multiple-junction thermopiles used to determine the differences in temperatures of the water streams and gas streams leaving the heat exchangers, items 13 and 14, have been described in section IV–3. As there are 18 pairs of chromel-copel junctions in each differ-

ential thermometer and the resulting electromotive forces are measured with high quality reflecting galvanometers equipped with scales at 1 meter distance, it is possible to detect temperature differences of about 0.001° F. Item 5 is determined with a mercurial thermometer which is read to the nearest degree Fahrenheit every 2 minutes.

The water pressures at the inlet and outlet to the heat exchangers, item 16, are measured with bourdon-tube type pressure gages, which are read at 2 minute intervals.

The temperature of the water sprayed on the upstream section of the proportioning chamber case, item 17, is obtained with a mercurial thermometer read to the nearest degree Fahrenheit every 2 minutes. The temperature of the downstream section of the case is presumably the same as that of the piston meter because the spray water for both is drawn from a common sump. Each section of the case is sprayed with water at the rate of about 30 gallons per minute.

3. PROCEDURE OF OPERATING THE REFERENCE METER

Before starting a test with the reference meter it is necessary to bring all parts to a state of thermal equilibrium. To do this requires the following operations, which are carried out in close succession or simultaneously by the several members of the crew. All of the pumps supplying water for the sprays are started and the spray-water temperatures brought to the desired values as soon as possible. After these temperatures are obtained, that of the water spraying the inlet section of the proportioning chamber case is maintained by manual control, while that of the water to the outlet section and the piston meter is maintained by a thermostat.

The gas flow through the meter is started and adjusted to the desired rate. The steam boiler is started and also the pump for circulating water through the heat exchangers. The water valves at the outlets of the two main heat exchangers are adjusted to give the desired rate of water flow through each. After steam is up and hot water is being circulated through the heat exchangers, the circuits of the differential thermocouple thermometers in the gas and water streams are closed and the relative rates of flow of the two gas and water streams adjusted until their corresponding temperature differences are approximately zero. Most of this regulation is made by means of the valve in the large heat exchanger by-pass W, figure 8, and the gas valve in the piston-meter outlet K, figure 1. When a stable condition of temperatures has been obtained observation of the differential thermometer galvanometers is discontinued and the circuits are opened to avoid possible injury to the galvanometers, while the reference meter is operated under these adjustments for a period of 1 to 2 hours.

During this stabilizing period the gas flow is kept constant. Since the temperature of the incoming gas is not constant it is necessary continually to adjust the valve in the by-pass of the steam to water heater F, figure 1, so that the temperature of the gas leaving the proportioning chamber shall be approximately equal that of the piston-meter bath water. As the piston of the piston meter is not operated during this period, the relief bell rises out of the sealing oil and permits the gas to flow in and out of the relief chamber without entering the measuring cylinder.

At the end of the stablizing period, oil-pump J, figure 11, is started and the piston of the piston meter thereby set in motion. This

automatically causes the relief bell to fall into the sealing oil. The circuits of the differential thermocouple thermometers are again closed, and any necessary adjustments made to the water and gas streams to bring the temperature differences between the two gas streams and between the two water streams substantially to zero. This temperature balance is continually observed and maintained throughout the test, thus fulfilling the conditions 6 and 7, stated in section IV–1.

After the piston meter has been in operation from 15 to 30 minutes, and all conditions about the reference meter have become stabilized, the meter is ready for a test, and the chronograph is started. The start of a test is made when the piston is at one end of its stroke, and the exact instant of starting is when one of the triggers releases the lever of the 4-way cock. The approach of the starting instant is indicated by the aluminum wheel, figure 10, starting to revolve. At the instant the lever starts to move the water streams from the two heat exchangers are diverted into empty weighing tanks. Not only is the shifting of the valves and the diversion of the water streams recorded by the chronograph, but at the instant of starting, the clock is also observed and the time recorded.[2]

Subsequent diversions of the water streams to empty weighing tanks are always made as the valves reverse in exactly the same part of the piston-meter cycle, as indicated by the position of the 4-way cock lever. The procedure for ending a test is similar to that of starting. The most important reason for starting and stopping the test the instant the 4-way cock lever starts to move from one and the same side of its swing is to have the volume of gas under the relief bell at the end of the test equal to that at the start. In order that there might be no lost motion between the movements of the relief bell and the striker on the aluminum wheel the chains supporting the relief bell and its counterweight were fastened to the wheel. In this connection it may be pointed out that it would not be satisfactory to start and stop the run at the instant the large gas piston comes to rest because, due to the deceleration of the gas piston by sleeve valves D, figure 11, the relief bell starts to rise before the gas piston comes to rest.

Throughout a test it is necessary to maintain the total mass rate of flow of the gas as nearly constant as possible. To accomplish this an orifice is located about 30 ft. upstream from the proportioning chamber inlet, and a sensitive differential pressure gage (described in Appendix B) is connected across the orifice. An observer stationed by this gage can keep the differential pressure within very close limits by operating the valve at reference-meter outlet M, figure 1, through a system of pulleys and cable connections. The static pressure in the line is normally maintained constant within a commercial limit of 2 or 3 lb./in.^{2}, by automatic pressure regulators located about 3 miles upstream. If closer regulation than this should be required, an operator could be sent to the regulator station to control the pressure manually.

[2] This was accomplished by the use of an auxiliary signal to the observer at the clock, since the clock is in a separate building from that housing the reference meter.

VI. TESTS MADE WITH THE REFERENCE METER

1. GENERAL PROCEDURE

To study the performance of the reference meter a series of tests were made of an orifice meter. As already stated, an orifice is used in connection with the regulation of the rate of flow; and the determination of the discharge coefficient of the orifice offered a convenient method of making such a study. For computing the discharge coefficients, the rates of flow calculated from the reference-meter readings were taken as correct. This of course means that any variations found between the values of the discharge coefficient computed from different tests reflect the possible errors of observation and operation of *both* the orifice meter and the reference meter. In making these tests, not only was the rate of flow varied, but the proportioning ratio and the temperature rise of the gas were also varied over such ranges as could be covered conveniently in the time then available.

The data required for the orifice in addition to those for the reference meter were the static and differential pressures at the orifice, and the temperature of the gas passing through the orifice. To obtain more data on the orifice, two pairs of pressure taps were used in connection with the orifice; with one of these pairs, the flange taps, the pressure holes were located 1 in. from the orifice plate; with the other pair, the pipe taps, the taps were 2½ pipe diameters upstream and 8 pipe diameters downstream from the orifice plate.

During these tests a 6-in. square-edged orifice was used in the 10-in. check meter mentioned in the introduction.

The static pressures, taken from the upstream tap in each case, were measured with the same piston gage as used for measuring the static pressure of the piston meter. These pressures were read to the nearest 0.10 lb. every 4 minutes, in rotation with that of the piston meter.

The differential pressures were measured with special piston-type, differential pressure gages. (See Appendix A for detailed description.) These gages were read to the equivalent of 0.002 in. of water once a minute.

The gas temperature was taken to be the same at the orifice as at the inlet to the proportioning chamber, the same thermometer reading being used for both.

2. OBSERVED QUANTITIES AND COMPUTED RESULTS FOR THE JOLIET REFERENCE METER

The observed data from the operation of the reference meter for the 15 tests are presented in table 2. The data in columns 11, 12, and 13, were necessarily obtained from auxiliary apparatus entirely apart from the meter, but are essential to computing the rate of flow through the meter. The data in columns 14 to 19, inclusive, are not needed for computing the rate of flow but are of interest and assistance in operating the meter.

TABLE 2.—*Quantities observed when operating the Joliet reference meter*

1	2	3	4	5	6	7	8	9	10
Run	Duration of test t	Proportioning chamber data					Piston meter data		
		Inlet gas temperature	Outlet gas temperature	Difference gas stream pressures, section 4-4 $(p_4)_S-(p_4)_L$	Water through large exchanger M_L	Water through small exchanger M_S	Gas temperature T'	Absolute pressure of gas p	Number of cycles n
	sec.	°F	°F	In Hg	lb	lb	°F	lb/in.²	
1	5,133	62.3	74.8	+0.34	3,048.51	79.453	74.6	220.35	51
2	5,198	64.0	75.2	+.34	2,949.06	77.564	74.3	220.43	52
3	5,572	60.8	73.9	−1.15	2,313.50	156.972	74.2	220.94	138
4	5,604	59.4	74.2	−1.14	2,322.43	158.844	74.1	221.40	140
5	5,610	61.4	67.3	+.39	2,226.62	52.937	67.8	219.03	50
6	5,929	61.9	67.4	+.41	2,171.95	52,756	67.5	217.08	54
7	5,458	60.1	66.8	−1.15	1,590.91	110.234	67.1	219.07	135
8	5,288	58.1	66.7	−1.18	1,601.67	112.730	67.1	220.19	133
9	5,513	60.9	69.0	.0	3,313.13	126.167	69.0	216.28	136
10	4,942	60.5	68.8	+.01	2,828.04	107.554	68.9	215.02	122
11	4,860	61.3	69.9	+1.01	2,867.76	84.218	70.2	215.81	121
12	6,091	57.4	69.0	+1.16	4,246.59	118.044	69.9	214.25	145
13	5,330	56.8	68.8	+1.11	3,530.15	100.670	69.8	212.59	131
14	5,711	59.6	68.3	+1.05	3,522.28	101.941	68.2	212.52	141
15	5,550	57.8	67.9	+1.00	3,476.54	100.514	68.2	213.85	137

11	12	13	14	15	16	17	18	19
Run	General			Auxiliary operating data				
					Water pressures, gage		Spray temperatures proportioning chamber	
	Barometric pressure p_a	Specific gravity of gas G	Supercompressibility factor of gas y	Water temperature at exchanger inlets	Heat exchanger inlets	Outlet, large exchanger	Outlet, small exchanger	Inlet section	Outlet section and piston meter
	lb/in.²			° F	lb/in.²	lb/in.²	lb/in.²	° F	° F
1	14.43	0.6673	1.0318	136	45	0	16	70.9	74.6
2	14.42	.6697	1.0318	133	41	0	15	71.1	74.3
3	14.39	.6723	1.0318	160	53	25	0	71.0	74.2
4	14.42	.6690	1.0318	179	53	25	0	70.4	74.1
5	14.50	.6687	1.0331	109	48	0	10	61.8	67.8
6	14.50	.6703	1.0327	107	46	0	9	62.3	67.5
7	14.50	.6723	1.0331	129	52	15	0	59.8	67.1
8	14.49	.6747	1.0331	149	52	17	0	60.5	67.1
9	14.44	.6730	1.0318	138	44	0	0	64.2	69.0
10	14.44	.6740	1.0318	141	43	0	0	63.8	68.9
11	14.43	.6723	1.0318	164	42	0	13	64.8	70.2
12	14.29	.6703	1.0316	177	54	0	20	58.1	69.9
13	14.29	.6700	1.0314	186	51	0	17	57.0	69.8
14	14.36	.6740	1.0316	158	45	0	14	64.8	68.2
15	14.29	.6707	1.0314	172	47	0	15	65.0	68.2

Table 3 gives the computed rates of flow of gas through the reference meter, and also the values for the more important intermediate steps.

TABLE 3.—*Computation of rate of flow of gas through Joliet reference meter*

1	2	3	4	5	6	7	8	9	10
Run	Temperature rise of gas in proportioning chamber ΔT_g	Observed ratio of water flows C'_m	Correction factor	Proportioning ratio C_m	Gas density at piston meter conditions ρ_p	Total displacement of piston meter V_p	Mass of gas through piston meter W_s	Rate of flow of gas	
								Through piston meter only w_g	Through reference meter $w_g\ (C_m+1)$ w
	° F				lb/ft³	ft³	lb	lb/sec	lb/sec
1	12.5	38.369	0.99918	38.338	0.76414	1,096.19	837.64	0.16319	6.420
2	11.2	38.021	.99909	37.986	.76760	1,117.69	857.94	.16505	6.435
3	13.1	14.738	1.00264	14.777	.77250	2,966.17	2,291.37	.41116	6.487
4	14.8	14.622	1.00231	14.656	.77046	3,009.16	2,318.15	.41366	6.476
5	5.9	42.062	.99802	41.979	.77193	1,074.70	829.61	.14798	6.356
6	5.5	41.170	.99778	41.079	.76703	1,160.68	890.28	.15016	6.319
7	6.7	14.432	1.00516	14.506	.77726	2,901.69	2,255.34	.41322	6.407
8	8.6	14.208	1.00415	14.267	.78402	2,858.70	2,241.31	.42385	6.471
9	8.1	26.260	1.00000	26.260	.76444	2,923.18	2,234.61	.40533	11.049
10	8.3	26.294	.99996	26.293	.76126	2,622.27	1,996.23	.40393	11.024
11	8.6	34.052	.99647	33.932	.76026	2,600.77	1,977.26	.40684	14.212
12	11.6	35.975	.99700	35.867	.75280	3,116.63	2,346.20	.38519	14.201
13	12.0	35.067	.99722	34.970	.74663	2,815.71	2,102.27	.39442	14.187
14	8.7	34.552	.99638	34.427	.75326	3,039.65	2,282.87	.39973	14.161
15	10.1	34.588	.99702	34.485	.75412	2,944.68	2,220.61	.40011	14.198

During these tests gas-pressure balancing valve F, figure 2, was inoperative, so that the pressure of the gas at the plane of the gas differential thermocouple thermometer, section 4–4, figure 2, was seldom the same in the large gas stream as in the small stream, due to the difference in the frictional resistance in the two gas passages. With the gas then being metered, this means that had there been no heat added by the heat exchangers the temperature of the stream at the lower pressure would have been lower than the temperature of the other stream by the amount of the Joule-Thompson effect. But since the meter was so operated that the temperature difference between the two gas streams was sensibly zero, the ratio of heat quantities added to the two gas streams was slightly greater or less than C_m, the ratio of mass flows of gas in the two streams, depending on the direction of the pressure difference. But the fundamental concept underlying the operation of the proportioning chamber involves the assumption that the ratio of the quantities of heat received by the gas streams from the water streams is equal to C'_m, the ratio of the weights of water passed through the heat exchangers. Hence, to obtain the true gas proportioning ratio, C_m, a correction computed from the Joule-Thompson coefficient for methane has been applied to the ratio of the observed water flows C'_m.

The method of computing C_m and the total mass rate of flow was as follows:

Let

C_m=the gas proportioning ratio, i. e., the ratio of the mass of gas passing through the large passage to the mass of gas passing through the small passage in a given time interval.

C'_m=ratio of weights of water passing through the heat exchangers in the same interval.
c_g(Btu/lb/°F)=specific heat of the gas at constant pressure.
c_w(Btu/lb/°F)=specific heat of water.
G=Specific gravity of the gas referred to dry air as unity.
M(lb)=total mass of water to either heat exchanger.
N=supercompressibility factor for the gas to correct for the departure from a linear relationship between pressure and density.
n=number of cycles of piston meter during test interval.
p(lb/in.^{2})=absolute static pressure of the gas.
Q(Btu)=quantity of heat transferred from the water to the gas.
T(°F)=observed temperature of the gas.
t(sec)=time interval or duration of test.
W(lb)=total mass of gas through reference meter.
w(lb/sec)=total mass rate of flow of gas.
ΔT_g(°F)=temperature change of gas.
ΔT_w(°F)=temperature change of water.
μ'(°F/in. Hg)=Joule-Thompson coefficient for the gas under the average conditions in proportioning chamber.
ρ(lb/ft^3)=density of the gas.

Subscript L refers to the large gas stream or large heat exchanger.
Subscript S refers to the small gas stream or small heat exchanger.
Subscript 1 refers to the conditions in the proportioning chamber at section 1–1, figure 2.
Subscript 4 refers to the conditions at section 4–4.

If we assume there is no heat loss by radiation or conduction, then the ratio of the total quantities of heat received by the two gas streams is given by

$$\frac{Q_L}{Q_S}=\frac{M_L c_w \Delta T_w}{M_S c_w \Delta T_w}=\frac{W_L c_p \Delta T_g - W_L \mu' c_p (p_1-p_4)_L}{W_S c_p \Delta T_g - W_S \mu' c_p (p_1-p_4)_S}, \tag{2}$$

or

$$C'_m = C_m \left[\frac{1-\mu' \dfrac{(p_1-p_4)_L}{\Delta T_g}}{1-\mu' \dfrac{(p_1-p_4)_S}{\Delta T_g}} \right]. \tag{3}$$

Since $C'_m=\dfrac{M_L}{M_S}$ and is known, equation 3 is rewritten to give

$$C_m = C'_m \left[\frac{1-\mu' \dfrac{(p_1-p_4)_S}{\Delta T_g}}{1-\mu' \dfrac{(p_1-p_4)_L}{\Delta T_g}} \right]. \tag{4}$$

From figure 2 it is evident that we may let $(p_1)_L \equiv (p_1)_S$; and if the meter were so operated that $(p_4)_S=(p_4)_L$, the term in brackets in equation 4 would reduce to 1, and we should have $C_m=C'_m$. But when $(p_4)_S \neq (p_4)_L$ the term in the brackets represents the correction factor to allow for the Joule-Thompson effect.

The composition of the gas passing through the meter was about 85 percent of methane, the remainder being higher hydrocarbons and

nitrogen. The most recent data at hand [3] indicate that for methane at about 220 lb/in.², absolute, and 60° F, $\mu' = -0.026°$ F/in. Hg. The ethane will tend to raise this more than the trace of nitrogen will lower it. Hence, for the present purpose, we have used the even value

$$\mu' = -0.03° \text{ F/in. Hg.}$$

In the tests here reported neither $(p_1)_S$ nor $(p_4)_S$ was measured, but only the difference $(p_4)_S - (p_4)_L$. Hence, equation 4 cannot be solved exactly, but by the use of $(p_4)_S - (p_4)_L$ we may get a very close approximate solution. It was stated in section IV–6 that the over-all pressure drop along the proportioning chamber is restricted to 5 lb/in.², or about 10 in. Hg. Therefore, $p_1 - p_4$ will not exceed 10 in. Hg and will usually be much less. Furthermore, the lowest value of ΔT_g observed was over 5° F. Thus, the maximum value of $\frac{\mu'(p_1 - p_4)}{\Delta T_g}$ in either numerator or denominator of equation 4 will not exceed 0.06, and their difference will be less than 0.01. Under these conditions a close approximation to equation 4 may be obtained by setting

$$C_m = C'_m\left(1 - \frac{\mu'}{\Delta T_g}[(p_1 - p_4)_S - (p_1 - p_4)_L]\right), \tag{5}$$

and since $(p_1)_S = (p_1)_L$, this reduces to

$$C_m = C'_m\left(1 + \frac{\mu'}{\Delta T_g}[(p_4)_S - (p_4)_L]\right). \tag{6}$$

It may be noted that the sign of μ' is negative, so that when $(p_4)_L < (p_4)_S$, $C_m < C'_m$.

The values of $(p_4)_S - (p_4)_L$ are given in column 5 of table 2. The values of ΔT_g and the correction term are given in columns 2 and 4 of table 3.

The density of the gas leaving the piston meter was computed by the equation

$$\rho_p = 2.6926\frac{p_p NG}{(460 + T)}, \tag{7}$$

and these values are given in column 6 of table 3.

The quantities in the remaining four columns of table 3 were computed by the equations

$$V_p = 21.494n. \tag{8}$$

$$W_S = \rho_p V_p. \tag{9}$$

$$w_S = W_S/t. \tag{10}$$

$$w = w_S(C_m + 1). \tag{11}$$

3: OBSERVED DATA FOR THE ORIFICE METER AND COMPARISON OF THE DISCHARGE COEFFICIENTS

For presenting the observed data from the orifice meter, and for computing and reducing the discharge coefficients, the following additional symbols will be used:

D (in.) = orifice diameter.

[3] J. H. Perry and C. V. Herrmann. *Joule-Thompson effect of* CH_4, N_2, *and mixtures of these gases.* J. Phys. Chem. **39**, 1189 (Dec. 1935).

K=discharge coefficient with velocity of approach factor included.

k=ratio of specific heats of the gas assumed to be 1.28.

w_t(lb/sec)=theoretical mass rate of flow of gas through the orifice.

x=ratio of differential to upstream static pressure.

Y=expansion factor for a gaseous fluid flowing through a square-edged orifice.

β=ratio of orifice to pipe diameter.

Δp(lb/in.^{2})=differential pressure.

μ(lb(mass)/ft-sec)=viscosity of the gas; it is assumed to be 0.000 0069.[4]

Subscript 1, in connection with the orifice data, refers to the conditions at the upstream pressure tap.

The discharge coefficient of the orifice may be defined by the equation

$$K=w/w_t, \tag{12}$$

in which w is taken from the reference-meter computations as given in table 3. The theoretical mass rate of flow is computed from the equation

$$w_t=0.5249D^2\sqrt{\Delta p\rho_1}. \tag{13}$$

Equation 7 is used for computing ρ_1, values of p' being used in place of p_p. The Reynolds number, column 11, Table 4, was computed by

$$R_d=\frac{48w}{\pi D\mu}. \tag{14}$$

TABLE 4.—*Orifice meter data and calculated coefficients*

[Orifice diam.=6.000 in.; diam. ratio, β=0.5889]

1	2	3	4	5	6	7	8	9	10	11
Run	Gas temp.	Flange taps		Pipe taps		Theoretical rates of flow		Discharge coefficients		Reynolds no.
		Static pressure	Differential pressure	Static pressure	Differential pressure	Flange taps	Pipe taps	Flange taps	Pipe taps	
		p_1	Δp	p_1	Δp	w_t	w_t	K	K	$R_d\times10^{-3}$
	° F.	lb./in.^{2}	lb./in.^{2}	lb./in.^{2}	lb./in.^{2}	lb./sec.	lb./sec.			
1	62.2	220.91	0.3540	220.90	0.2254	9.9645	7.9507	0.6443	0.8075	2379
2	64.0	220.95	.3547	220.94	.2252	9.9754	7.9495	.6451	.8095	2370
3	60.8	222.30	.3542	222.29	.2249	10.0527	8.0111	.6453	.8098	2395
4	59.4	222.74	.3543	222.73	.2255	10.0533	8.0202	.6442	.8075	2392
5	61.4	219.56	.3506	219.55	.2218	9.9062	7.8798	.6416	.8066	2358
6	61.9	217.53	.3499	217.52	.2218	9.8556	7.8462	.6412	.8054	2345
7	60.1	220.41	.3510	220.40	.2220	9.9686	7.9293	.6427	.8080	2360
8	58.1	221.54	.3526	221.53	.2231	10.0585	8.0005	.6433	.8068	2348
9	60.9	218.37	1.0571	218.35	.6701	17.2165	13.7067	.6418	.8061	4090
10	60.5	217.14	1.0576	217.12	.6706	17.1912	13.6882	.6413	.8054	4080
11	61.3	218.61	1.7645	218.58	1.1196	22.2350	17.7099	.6392	.8025	5285
12	57.4	216.96	1.7649	216.93	1.1197	22.2105	17.6899	.6394	.8028	5270
13	56.8	215.21	1.7641	215.18	1.1191	22.1194	17.6162	.6414	.8053	5265
14	59.6	215.28	1.7609	215.25	1.1173	22.1022	17.6050	.6407	.8044	5260
15	57.8	216.58	1.7619	216.55	1.1180	22.1683	17.6572	.6402	.8041	5275

[4] See Viscosity of Natural Gas. U. S. Bur. Mines. Tech. Pap. 555; also Appendix A, Report 2, Gas Measurement Committee, Natural Gas Dept., Am. Gas Assn.

The values of K given in columns 9 and 10, table 4, correspond to the particular conditions at the orifice under which the tests were made. In order to compare these values of K on a more nearly common basis, it was necessary to correct for the effects of expansion and viscosity (Reynolds number). This has been done, and the resulting values are presented in table 5. The expansion factors for the two pairs of pressure taps used were computed by the equations[5]

$$\text{For flange taps } Y_1=1-(0.41+0.35\,\beta^4)\frac{x}{k} \tag{15}$$

$$\text{For pipe taps } Y_1=1-[0.333+1.145(\beta^2+0.7\beta^5+12\beta^{13})]\frac{x}{k} \tag{16}$$

and are given in columns 2 and 3 of table 5. To compute the values of K which might have been obtained had there been no expansion of the gas, the observed values of K are multiplied by $1/Y_1$, and these values are given in columns 4 and 5 of table 5.

TABLE 5.—*Results of the orifice tests compared*

1	2	3	4	5	6	7	8	9	10	11
Run	Expansion factor		Coefficients for no expansion		Adjustment to K for $R_d=\infty$		Coefficients adjusted to $Y_1=1$ and $R_d=\infty$		Departures	
	Flange taps Y_1	Pipe taps Y_1	Flange taps	Pipe taps	Flange taps	Pipe taps	Flange taps K_0	Pipe taps K_0	Flange taps $0.6427-K_0$	Pipe taps $0.8070-K_0$
1	0.9994	0.9994	0.6447	0.8080	−0.0005	−0.0007	0.6442	0.8073	−0.0015	−0.0003
2	.9994	.9994	.6455	.8100	−.0005	−.0007	.6450	.8093	−.0023	−.0023
3	.9994	.9994	.6457	.8103	−.0005	−.0007	.6452	.8096	−.0025	−.0026
4	.9994	.9994	.6446	.8080	−.0005	−.0007	.6441	.8073	−.0014	−.0003
5	.9994	.9994	.6420	.8071	−.0005	−.0007	.6415	.8064	+.0012	+.0006
6	.9994	.9994	.6416	.8059	−.0005	−.0007	.6411	.8052	+.0016	+.0018
7	.9994	.9994	.6431	.8085	−.0005	−.0007	.6426	.8078	+.0001	−.0008
8	.9994	.9994	.6433	.8093	−.0005	−.0007	.6428	.8086	−.0001	−.0016
9	.9983	.9982	.6429	.8075	−.0003	−.0004	.6426	.8072	+.0001	−.0002
10	.9983	.9982	.6424	.8069	−.0003	−.0004	.6421	.8065	+.0006	+.0005
11	.9972	.9970	.6410	.8049	−.0002	−.0002	.6408	.8047	+.0019	+.0023
12	.9972	.9970	.6412	.8052	−.0002	−.0002	.6410	.8052	+.0017	+.0018
13	.9972	.9970	.6432	.8077	−.0002	−.0002	.6430	.8075	−.0003	−.0005
14	.9972	.9970	.6425	.8068	−.0002	−.0002	.6423	.8066	+.0004	+.0004
15	.9972	.9970	.6420	.8065	−.0002	−.0002	.6418	.8063	+.0009	+.0007
Averages							.6427	.8070	±.0010 ±0.16%	±.0011 ±0.14%

On the basis of a series of tests made at Ohio State University for a joint committee of the American Gas Association and the American Society of Mechanical Engineers,[6] it has been found that the discharge coefficients of orifices continue to decrease slightly even after rather high Reynolds number values are reached. By plotting values of K against $10^6/R_d$ it was possible to obtain an expression for

[5] For an explanation of these equations see National Bureau of Standards Research Papers RP335 and RP459; also Report 2, Gas Measurement Committee, Natural Gas Dept., American Gas Association.

[6] See Report of Joint AGA–ASME Committee on Orifice Coefficients; also Prof. S. R. Beitler, *The flow of water through orifices*, Ohio State Univ. Studies, Eng. series IV, no. 3 (May 1935).

the value which K approaches as a limit, for any value of β, as R_d increases without limit. By using these relations, as derived from the Ohio State University tests, the adjustments to refer the values of K to the limiting condition were computed, as given in columns 6 and 7 of table 5. The values of K thus adjusted for expansion and viscosity effects and designated K_0 are given in columns 8 and 9. In columns 10 and 11 are given the differences between the individual values of K_0 and the average value for each pair of pressure taps.

VII. DISCUSSION OF TEST RESULTS AND POSSIBLE SOURCES OF ERROR

1. DISCUSSION OF TEST RESULTS

It should be noted that the variations of the individual values of the coefficients from the average, columns 8 and 9 of table 5, were obtained in the operation of the whole system and not of either one of the two meters individually.

During the first eight tests the rate of flow of the gas through the reference meter and orifice was practically constant, while the proportioning ratio was changed from 14.2:1 to 42.6:1, and the gas temperature rise changed from 5.5 to 14.7° F. Even with these changes in operating conditions, the variations in the orifice coefficients for these tests were only slightly higher than the average for the entire group of 15. Slightly greater variations were to be expected because at the lower rate of flow the orifice measurements are less reliable.

There appears to be no relation between the variations of the results and the changes in the operating conditions of the reference meter.

In studying the results of such tests it is often instructive to make an estimate of the uncertainties in the individual quantities observed. Estimates of this kind have been made for the reference- and orifice-meter system, which indicated that the departure of a test from the average might amount to 0.25 percent, which is about the maximum shown in table 5. Without giving these estimates in detail, we may state that with the exception of the specific gravity of the gas, the estimated uncertainty did not exceed 0.05 percent in any item. With the specific gravity, the best that could be expected was ± 0.2 percent, and it is doubtful whether even this accuracy was attained, although a high-grade instrument was used for its determination. One reason for this uncertainty in the gravity is that it was impossible to make more than three determinations during a test. Another and more important reason is that there were actual changes in the gravity of the gas during the duration of a test amounting in some cases to about 1 percent. That these were genuine changes, and not errors of determination, is confirmed by the fact that the routine operators of the Joliet Measurement Station obtained similar changes during approximately the same intervals, and have frequently observed such changes at other times. Since these tests were made, there has been constructed at the Joliet Measurement Station, a specific gravity apparatus with which it is believed that readings may be made at 10-minute intervals to better than 1 part in 500.

2. HEAT LOSSES

To aid in designing the meter a test was made to determine the thermal conductivity of the aluminum-foil insulation with different widths of spacing between the layers of foil. It was found that there was no advantage in having the layers of foil closer than ⅛ in. With this spacing and for the estimated temperature differences and gas pressures to be encountered, the conductivity of this type of insulation was found to be 0.31 Btu per hour per square foot per inch thickness per degree Fahrenheit difference in temperature.

For the purpose of calculating the possible heat losses two rates of flow are used. The low rate is taken as 1/50th of the listed capacity. At a line pressure of 200 lb/in^2 this will be 2,400 ft^3/hr, or 32,660 ft^3/hr when the pressure is reduced to 1 atmosphere. For the high rate the full listed rate of flow will be used.

As a basis for estimating the heat loss from the gas streams to the outside, or from one gas stream to the other, it will be assumed either that no attempt had been made, when constructing the meter, to localize the temperature change in the 16-in. shell to the band of the two encircling tubes (section X–X, figure 8), or that the upstream encircling tube is clogged. It may then be assumed that at least half of the temperature change along the 16-in. tube takes place gradually over the part surrounding the heat exchangers—a band about 11 in. wide. If the temperature of the gas rises 10° F, this will mean that at least a 5° F rise in the shell temperature is spread over this 11-in. band. To simplify the calculations, this band is divided into 1-in. bands and the heat loss from each calculated. In this way it is found that the heat loss to the outside may amount to about 0.009 percent of the total heat input to the meter.

We next consider the heat loss from the water streams entering and leaving the heat exchangers. This loss is due to the fact that the temperature of the incoming water is very much higher than the temperature of the warmed gas, and that of the outlet water is several degrees higher. From figure 8 it will be seen that the large gas stream will receive some heat from those portions of the inlet and outlet water tubes that extend across the large gas stream passage. Even here, the heat which the large gas stream receives from that portion of the total water flow supplied to the large heat exchanger is not "lost" heat. But such a transfer of heat will lower the heat content of the small water streams in tubes P and O_2, and this will be a heat loss. The amount of this loss will be proportional to the amount of water flowing in the two streams. In addition, there may be a small loss of heat from the inner ends of tubes P and O_2 to the large gas stream. As a basis for calculating the possible effect of these losses, it is again assumed the meter is operating at 1/50th its listed capacity and that the difference between the inlet water and outlet gas temperatures is 17.5° F, while that between the outlet water and outlet gas is 13.5° F. For these conditions the possible loss may amount to 0.034 percent of the heat transferred from the small water stream. This would affect the proportioning ratio by the same percentage.

Finally, the possibility of heat transfer between the large and small gas streams through the insulation between the 3- and 6-in. tubes remains to be considered. For such a flow of heat to take place there must be a temperature difference between the two streams.

In normal operation the pressures as well as the temperatures at section 4–4, figure 2, are balanced, but upstream of the pressure balancing valve F, the pressures of the two streams will not be the same at very low or very high rates of flow. Therefore, for these conditions, the temperatures of the two gas streams, upstream of valve F, will differ by the amount of the Joule-Thompson effect corresponding to the pressure difference. From the data of run 10 it is estimated that at 1/50th capacity and a 5:1 ratio the pressure difference might amount to 0.18 in. of Hg. The corresponding temperature difference would be about 0.0054° F. Taking 7 ft^2 as the area of the insulating partition between the two gas streams (which is probably high), the heat transferred between the gas streams might amount to 0.0004 percent of the heat input to the small gas stream.

Similar calculations have been made for a high rate of flow such as 120,000 ft^3/hr at a line pressure of 200 lb and using a 60:1 proportioning ratio. The results of these calculations are shown in column 3 of table 6.

TABLE 6.—*Calculated possible effects of heat losses*

1	2	3
Location of heat loss	Effect of—	
	Low rate of flow of gas	High rate of flow of gas
	%	%
Through outer insulating jacket	0.009	0.0002
From inlet and outlet water tubes	.034	.0022
Between the two gas streams	.0004	.003

If it is assumed that the effects of all of these heat losses are in the same direction, and additive, the total effects for the two rates of flow will be about 0.044 and 0.005 percent, respectively. As pointed out above, these heat-loss effects would appear as errors in the proportioning ratio.

It appears from this analysis, that if it is desired to limit the possible errors due to heat losses to ± 0.05 percent, the reference meter should not be operated as a proportional meter at rates below about 32,000 ft^3/hr, referred to a pressure of 1 atmosphere. By reference to table 1 it will be seen that placing such a limitation upon the operation of the meter will result in a gap between the maximum capacity of the piston meter alone and this arbitrary minimum value for the entire meter. This gap will vary in magnitude from about 30,000 ft^3/hr at a line pressure of 14.7 lb/$in.^2$ to about 5,000 ft^3/hr at a line pressure of 200 lb/$in.^2$ and will vanish when the line pressure is above about 240 lb/$in.^2$ At the present time a line pressure of 300 lb/$in.^2$ is always available at the Joliet Measurement Station, so that by proper adjustment of line valves it is possible to operate the meter over the entire range from 400 to 2,000,000 ft^3/hr, referred to a pressure of 1 atmosphere.

3. CONCLUSION

The results of the 15 tests and the above discussion suggest that the probable uncertainties of indication of the reference meter may be numerically less than those of almost any other meter of comparable capacity and range of operating conditions. Further experience with the meter may quite possibly suggest refinements in operation that will lead to a higher precision of metering than is shown by the few tests reported here. It is hoped, therefore, that in time the meter will prove to be of considerable value to the gas industry as a reference meter of medium and large capacity.

VIII. APPENDIX A—PISTON GAGES FOR MEASURING PRESSURES

1. PISTON GAGES USED FOR MEASURING DIFFERENTIAL PRESSURES

General views of one of the two piston gages used for measuring the differential pressures across the orifice are shown in figure 13. An equal-arm balance is used for measuring the force produced by the differential pressure upon the piston. Upon one pan of the balance are placed the calibrated weights. Suspended from the other pan is a sling from which, in turn, is suspended the piston across which

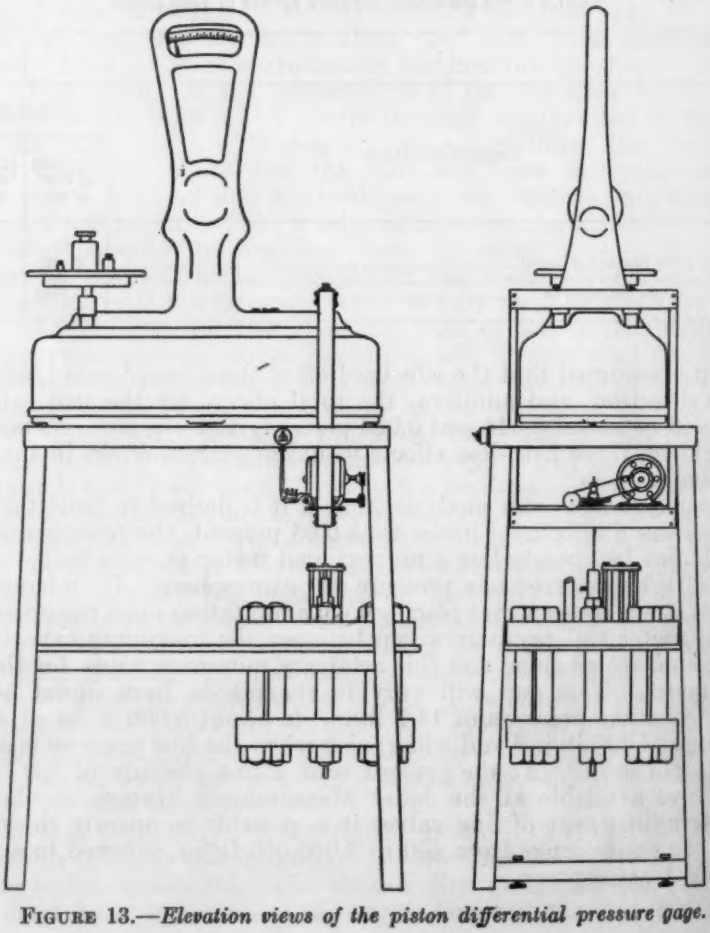

FIGURE 13.—*Elevation views of the piston differential pressure gage.*

the differential pressure is applied. The sling also carries a small motor and reduction gear for rotating the piston.

Figure 14 shows a section through the pressure chambers in which the piston and its cylinder are mounted. The chamber is firmly attached to the stand on which the balance is mounted. It is formed by a short steel cylinder 6, clamped between two carefully faced heavy flanges. This pressure chamber is capable of withstanding static pressures up to 600 lb/in^2.

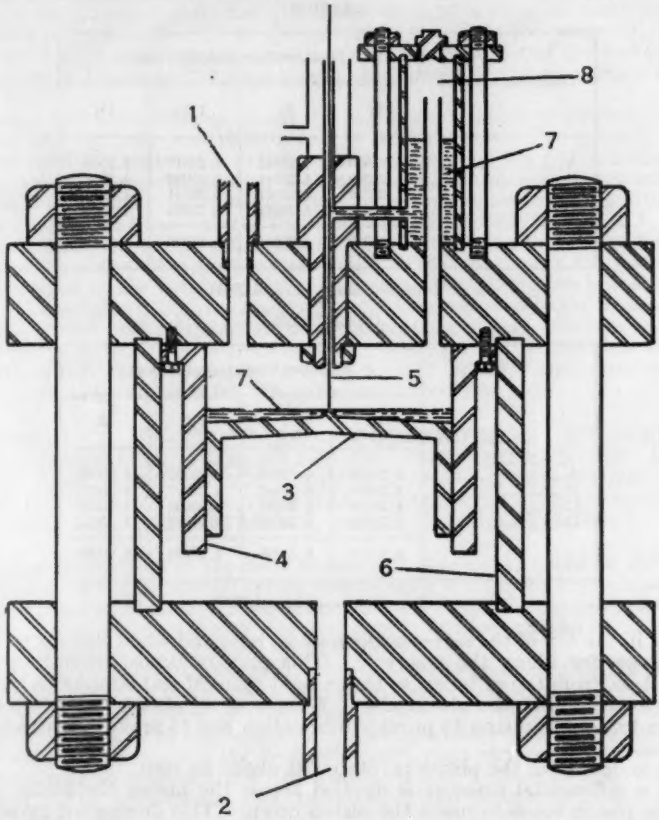

FIGURE 14.—*Section through pressure chamber of differential pressure gage.*

1. High-pressure connection.
2. Low-pressure connection.
3. Rotating piston.
4. Cylinder.
5. Piston drive shaft.
6. Pressure vessel.
7. Lubricating oil.
8. Oil reservoir.

Inner measuring cylinder 4 is attached to the upper flange, the two surfaces being ground to provide a gas-tight joint. This measuring cylinder is shorter than the outer cylinder, so that the annular space between the two cylinders is open to the downstream or low pressure, which is applied to the under side of the piston through the connection 2. The upstream or high pressure is communicated to the space above the piston through connection 1.

Piston 3 and the cylinder are carefully turned and ground to a very close fit. The results of measurements of the diameters of a cylinder and piston, as made with Johannsen gage blocks and indicator, are given in table 7. The piston and cylinder are made of case-hardened steel forgings.

Rod 5, by which the piston is suspended and rotated, is about 0.067 in. in diameter. It enters the pressure chamber through a lubricated sleeve or gland. Oil is supplied to this sleeve from reservoir 8. As shown by figure 14, the pressure

above the piston is also applied to the surface of the oil in the reservoir. The pressure of the oil supplied to the sleeve exceeds that of the gas by the amount the surface of the oil in the reservoir is above the top of the sleeve. This slight excess of pressure is sufficient to cause a slight seepage of oil down the rod and effectively prevent any leakage of gas.

TABLE 7.—*Diameters of cylinder and piston used in one of the differential gages*

PISTON

Diameter symbol	Distance from base (inches)			
	¼	¾	1¼	1¾
A	4.25040	4.25041	4.25041	4.25039
B	4.25040	4.25041	4.25042	4.25042
C	4.25039	4.25041	4.25041	4.25040
D	4.25040	4.25041	4.25042	4.25041
	4.25040	4.25041	4.25042	4.25041

Total average.....4.25041

CYLINDER

	Distance from base (inches)			
	½	1	1½	2
A	4.25100	4.25098	4.25097	4.25098
B	4.25099	4.25099	4.25097	4.25098
C	4.25100	4.25099	4.25098	4.25099
D	4.25099	4.25098	4.25098	4.250.7
	4.25100	4.25099	4.25098	4.25098

Total average.....4.25099

A plug in the top of the oil reservoir may be removed when there is no pressure on the gage, for filling the reservoir. This plug is almost directly above the pressure tube from the cylinder, so that a light mineral seal oil may be introduced directly to the top of the piston also. A layer of oil about ½ in. deep is maintained on top of the piston to provide lubrication and to prevent gas leakage past the piston.

When in operation the piston is rotated at about 15 rpm.

When a differential pressure is applied across the piston the higher pressure above the piston tends to move the piston down. This downward movement of the piston is transmitted by the supporting wire and sling to the balance, deflecting the pointer from its zero position. The magnitude of the weights required to restore the balance to zero position measures the force produced by the differential pressure upon the piston. Knowing this force and the mean area of the piston and cylinder, the differential pressure is readily computed. It was found that these differential-pressure gages responded to changes of differential pressures of as low as 1/500 in. of water.

It is necessary to take zero readings of these differential-pressure balances at the start and finish of a test, because these readings are influenced by changes in the static pressure and seepage of oil past the piston. In calculating the differential pressures observed during a test the zero reading used is obtained by correcting both observed zero readings to the average static pressure encountered during the test and then taking the mean of these corrected readings. At no time while making the tests reported in this paper did the difference between the first and second zero reading exceed 0.01 lb, which is equivalent to a differential pressure of about 0.02 in. of water.

These differential pressure balances as at present constructed can measure differential pressures up to about 50 in. of water. This range may, of course, be varied by changing the capacity of the balance, or, preferably, by changing the size of the piston and cylinder, parts 3 and 4.

When connecting pressure openings 1 and 2 to the two sides of an orifice flange, the usual 3-valve by-pass between the high and low pressure leads is, of course, included.

2. PISTON GAGES FOR MEASURING STATIC PRESSURE

For measuring static pressures a suitable piston gage was obtained by slightly modifying a high-grade dead-weight gage tester. The modifications included a restriction to the stroke of the piston so that it could not accidently be forced out of the cylinder during a test, and the installation of a large oil reservoir. The gas pressure is applied directly to the surface of the oil in the reservoir. The oil reservoir is of such size that the movements of the piston, and the leakage of oil past it during a 2-hour test, do not change the height of the oil surface by more than 0.1 in.

The piston had a diameter of about 0.5 in., but the mean effective diameter of the piston and cylinder was determined by experiment. The diameter of the piston was carefully measured, and the clearance between the piston and cylinder was determined by recording, with a chronograph, the rotational retardation of the piston when loaded with weights having known moments of inertia. The clearance could then be calculated from the known viscosity of the oil.[7]

The correction due to the difference in elevations of the bottom of the piston and the surface of the oil in the reservoir, minus the buoyancy of the piston in the oil, was included in the weight of the piston and table, giving the lowest pressure reading. The weights used were made specially to correspond to the mean effective area of the piston and cylinder, so that the reading of any pressure within the range of the gage would be correct within ± 0.005 lb. While weights were provided with which pressures could be read to 0.01 lb/in.^{2}, measurements to 0.1 lb/in.^{2} were usually sufficient for the purposes of the test.

IX. APPENDIX B—DISCHARGE COEFFICIENTS OF ORIFICES DETERMINED ON THE BASIS OF THE REFERENCE METER TESTS, COMPARED WITH VALUES CALCULATED FROM EQUATIONS IN REPORT 2 OF THE GAS MEASUREMENT COMMITTEE, NATURAL GAS DEPARTMENT, AMERICAN GAS ASSOCIATION

The orifice meter used in the tests reported in this paper could be operated in series with any one of six similar orifice meters used in the regular operation of the Joliet Measurement Station. These six orifice meters and the seventh, or comparison meter, are as nearly alike in size and details of construction as it was commercially possible to make them.

Each of these six operating meters has been carefully compared with the seventh or comparison meter. On the basis of this intercomparison, the discharge coefficient of an orifice used successively in each of the six operating meter lines, has been determined from the coefficients of the comparison run orifice [8] based on the tests reported in this paper. Following these intercomparisons a 5-in. orifice was used successively in each of the six operating meters, and coefficients for it were determined. The coefficients determined by these comparisons are given in columns 5 and 7 of table 8.

Coefficients for these orifice plates in these meter runs may be computed by the equations given in report 2 of the Gas Measurement Committee, Natural Gas Department, American Gas Association. The values so computed are given in columns 6 and 8 of table 8.

In connection with such a comparison it may be noted that the equations in report 2 were based on weighed water tests, with the factors for expansion effects based on many tests with different gases. Moreover, for the sizes reported here, the report places a tolerance of $\pm$ 0.5 percent on the values of the coefficients computed from the equations. In other words, the computed coefficient for a given orifice might differ by this amount from the value obtained by a test. It will be seen that the differences between the computed coefficients and those determined by the intercomparison are well within this tolerance.

In preparing table 8 an adjustment was made to the values determined by comparison, for the effects of expansion, so that the coefficient values in all four columns represent those for an incompressible fluid.

---

[7] C. H. Meyers and R. S. Jessup. *A multiple manometer and piston gages for precision measurements.* BS J. Research 6, 1061 (1931) RP 324.

[8] The orifice plate used in the comparison meter in these intercomparison tests was not the identical orifice used in the 15 tests with the reference meter, but the only known difference between the two was that of 0.0012 in diameter, which has been allowed for.

TABLE 8.—*Coefficients for the Joliet Measurement Station meters determined from the reference meter by a method of intercomparison and also by calculation*

1	2	3	4	5	6	7	8
Meter run	Pipe diameter D_1	Orifice plate no.	Orifice diameter D_2	Flange taps		Pipe taps	
				By comparison	By calculation	By comparison	By calculation
				Values of K at $R_d=4\times10^6$			
	Inch		*Inch*				
1	10.188	7	5.9995	0.6437	0.6439	0.8094	0.8101
2	10.197	7	5.9995	.6438	.6435	.8097	.8094
3	10.192	7	5.9995	.6435	.6438	.8102	.8098
4	10.181	7	5.9995	.6442	.6440	.8100	.8105
5	10.179	7	5.9995	.6440	.6441	.8136	.8106
6	10.193	7	5.9995	.6440	.6438	.8107	.8097
7	10.186	6	5.9988	.6430	.6437	.8074	.8100
				Values of K at $R_d=2.9\times10^6$			
1	10.188	8	4.9984	0.6197	0.6207	0.7217	0.7240
2	10.197	8	4.9984	.6196	.6206	.7225	.7238
3	10.192	8	4.9984	.6198	.6209	.7224	.7239
4	10.181	8	4.9984	.6209	.6206	.7233	.7243
5	10.179	8	4.9984	.6210	.6206	.7248	.7244
6	10.186	8	4.9984	.6201	.6207	.7225	.7240

WASHINGTON, May 27, 1936.

U. S. Department of Commerce National Bureau of Standards

RESEARCH PAPER RP909

Part of Journal of Reseach of the National Bureau of Standards, Volume 17, August 1936

SOLUBLE DECOMPOSITION PRODUCTS IN AGED VEGETABLE-TANNED LEATHERS

By Joseph R. Kanagy

ABSTRACT

Vegetable-tanned leathers, containing 0, 1, 2, 3, and 4 percent of sulphuric acid and aged for 2 to 10 years were examined for soluble nitrogen compounds. The soluble decomposition products were extracted with water and with 0.1 *N* sodium carbonate. Ammonia, amino nitrogen, and nitrogen precipitated with phosphotungstic acid were determined in the extracts.

A comparison is made between the results obtained from acid-treated leathers which had been aged, and those obtained from the direct hydrolysis of leather and hide substance in acid solutions.

The data indicate that most of the physical deterioration results from hydrolytic reactions.

CONTENTS

	Page
I. Introduction	247
II. Materials and methods	248
1. Water extractions	248
2. Sodium carbonate extractions	249
III. Experimental	250
1. Extractions	252
2. Ammonia	253
3. Amino nitrogen	253
4. Nitrogen precipitated by tannins and phosphotungstic acid	255
IV. Discussion	256
V. Summary	259
VI. References	259

I. INTRODUCTION

For the past few years a study of the effect of acids on leather [1] [1] has been carried on at the National Bureau of Standards. Leathers of different tannages, containing various leather-making materials and varying amounts of acid were aged under different conditions. It was shown that the governing factor of deterioration was the pH, as determined by making a water extract of the leather. Leathers finished and aged below pH 3 were almost certain to show a loss in tensile strength, while those finished above pH 3 and aged showed practically no deterioration in 2 years. It was also found that the deterioration of leather produced soluble nitrogen compounds.

It has been known for a long time that soluble nitrogen compounds can be extracted from deteriorated leathers. This has been especially noticeable in the case of old bookbinding leathers which have absorbed

[1] Numbers in brackets refer to references at the end of this paper.

large amounts of sulphur dioxide from the atmosphere. Veitch, Frey, and Leinback [2] studied a large number of bookbinding leathers and found that approximately one-third of the total nitrogen was extractable with water. Fifty percent of this nitrogen was in the form of ammonia. Innes [3, 4, 5] used the amount of soluble nitrogen as a criterion in making an extensive study of the various factors influencing deterioration. He analyzed the total soluble nitrogen for ammonia and amino nitrogen. Frey and Beebe [6] determined soluble nitrogen and ammonia in leathers exposed to sulphur dioxide in a gas chamber. They used as the figure for total nitrogen extracted the sum of that extracted with water and then with 0.1 *N* sodium carbonate.

In this investigation a more detailed study has been made of the soluble nitrogen compounds in aged vegetable tanned leathers with the purpose of obtaining some fundamental information for an accelerated aging test, and also, to study the cause of deterioration. The work reported in this paper deals only with the chemical changes produced in collagen.

II. MATERIALS AND METHODS

The leathers used were from the same lots and had undergone the same treatments as those which were used in the study of the effect of acids on the tensile strength of leather. The initial pH values of these leathers ranged from 1.7 to 5.0. After tensile-strength measurements were made the leathers were stored. The storage period varied from 2 to 10 years. Each sample of leather, containing approximately 0, 1, 2, 3, or 4 percent of acid, was ground and mixed to form a uniform sample.

1. WATER EXTRACTIONS

A 10-g sample of leather was extracted with 200 ml of water at 25° C by shaking in a bottle for 3 hours. The mixture was filtered and the total nitrogen extracted was determined by the kjeldahl method on an aliquot of the clear filtrate. The amounts of ammonia, amino nitrogen, and nitrogen precipitated by phosphotungstic acid were then determined in other aliquots of the clear filtrate.

The ammonia was determined as follows: 50 ml of the clear filtrate was placed in a kjeldahl flask and diluted to 200 ml. 25 ml of a 2-percent suspension of magnesium oxide was added and the ammonia distilled over into standard acid as in a kjeldahl distillation.

The amino nitrogen was determined on the residue remaining in the kjeldahl flask after the removal of the ammonia. The residue was made acid to litmus with acetic acid. It was diluted to 200 ml in a volumetric flask and the amino nitrogen determined on an aliquot of this solution by the Van Slyke method [7], which is based on the measurement of the volume of nitrogen evolved by the action of nitrous acid on primary amino groups.

Ten ml of a 5-percent solution of phosphotungstic acid in 2.5-percent solution of hydrochloric acid was added to a third aliquot of the water extract. After standing for 2 hours the mixture was filtered and the total nitrogen determined in the precipitate by the kjeldahl method.

2. SODIUM CARBONATE EXTRACTIONS

Frey and Beebe [6] pointed out that tannins form insoluble substances with gelatin and other partially hydrolyzed proteins, and therefore a complete extraction of the soluble nitrogen compounds in leather cannot be made with water. It is necessary to use a solvent which will dissolve the tannin as well as the protein. Since tannins and proteins are both soluble in alkaline solutions, a few preliminary experiments were made by the adopted procedure using 0.2 *N* sodium bicarbonate, 0.3 *N* disodium phosphate, 0.1 *N* sodium carbonate, and 0.1 *N* sodium hydroxide as solvents. The most nitrogen was extracted from the leather with the 0.1 *N* sodium hydroxide solutions, but subsequent experiments in which standard hide powder instead of leather was extracted, showed that it caused a breakdown in the protein molecule. The results are given in tables 1 and 2, and indicate that 0.1 *N* sodium carbonate solution is the most suitable solvent for this work because it extracts practically no more nitrogen from hide substance than does water.

TABLE 1.—*Nitrogen extracted from quebracho leather (lot 1) containing 4 percent of acid*

Solvent	Nitrogen extracted
	mg
0.2 *N* $NaHCO_3$	12.4
.3 *N* Na_2HPO_4	12.1
.1 *N* Na_2CO_3	60.8
.1 *N* NaOH	103.2

TABLE 2.—*Nitrogen extracted from standard hide powder*

Solvent	Nitrogen extracted
	mg
Water	4.5
0.2 *N* $NaHCO_3$	4.6
.3 *N* Na_2HPO_4	4.5
.1 *N* Na_2CO_3	4.8
.1 *N* NaOH	13.8

With 0.1 *N* sodium carbonate as the solvent, the same procedure was adopted in making the extraction as that which was used with water, except that 2 g of leather instead of 10 g was used.

The amount of nitrogen present as ammonia was determined. This was compared with that in the water extract so as to make a correction in the total amount of extracted nitrogen for that lost as ammonia by the alkaline carbonate treatment. An aliquot of the extracted solution was neutralized with hydrochloric acid and the amount of nitrogen precipitated by the excess tannins was determined. Phosphotungstic acid was then added to the filtrate from the tannin precipitate in order to remove all the incompletely hydrolyzed proteins. The sum of these two figures was recorded as the total nitrogen precipitated.

III. EXPERIMENTAL

To determine the effect of tannins on the hydrolysis and on the determination of soluble nitrogen compounds as outlined above, 1-g samples of hide substance and samples of chestnut- and quebracho-tanned hide substance, equivalent to 1 g of hide substance, were hydrolyzed at 60° C in 0.05 *N* solutions of sulphuric acid. At various intervals the solutions were tested for total nitrogen, amino nitrogen, ammonia, and nitrogen precipitated by phosphotungstic acid. The results given in figure 1 and table 3 show that the percentage of total nitrogen in solution as ammonia and amino nitrogen is nearly the same in each of the three cases for each interval, even though the amount of total nitrogen in solution is less for the tanned hide substances. This indicates that the tannins do not prevent the hydrolysis of the protein but retard the rate at which it goes into solution. Experiments have shown that tannins present in protein solutions cause high values for amino nitrogen. The error increases as the amount of tannin is increased. The amount of tannin present in the above experiments was not enough to cause an appreciable error.

TABLE 3.—*Soluble nitrogen compounds from hide substance and tanned hide substance hydrolyzed in 0.05 N sulfuric acid at 60° C for different periods of time*

[Results are given in percentage of total nitrogen in solution]

Material	pH	Time	Total nitrogen in solution	Phosphotungstic acid precipitate	Ammonia	Amino nitrogen
		Hours	mg	%	%	%
Hide substance	1.55	18	173.4	99.7	0.30	4.4
Quebracho	1.59	18	16.9	98.8	.25	0
Chestnut	1.59	18	57.0	97.8	0	5.8
		Days				
Hide substance	1.59	2	174.1	97.1	1.0	5.6
Quebracho	1.60	2	32.9	96.0	1.4	8.2
Chestnut	1.57	2	60.3	95.8	1.1	6.8
Hide substance	1.60	4	174.6	92.5	2.5	7.5
Quebracho	1.59	4	66.4	92.0	1.8	8.3
Chestnut	1.57	4	92.9	90.6	1.8	7.4
Hide substance	1.57	7	174.3	89.6	1.5	10.3
Quebracho	1.60	7	80.2	89.2	2.0	9.6
Chestnut	1.60	7	118.4	85.0	2.2	11.1
Hide substance	1.79	14	176.1	80.2	1.8	16.1
Quebracho	1.72	14	90.0	82.2	2.2	13.3
Chestnut	1.77	14	135.4	79.2	2.6	16.6
Hide substance	1.84	21	175.5	79.1	2.0	16.4
Quebracho	1.84	21	116.9	76.0	2.6	18.8
Chestnut	1.86	21	142.3	71.5	2.6	17.8
Hide substance	1.84	28	178.6	72.0	2.2	20.7
Quebracho	1.83	28	126.8	72.2	2.3	23.8
Chestnut	1.84	28	148.8	68.3	2.2	21.8

As a control experiment to determine the effect of pH on the formation of soluble nitrogen compounds, 2-g samples of standard hide substance were placed in sulphuric acid solutions of various concentrations ranging from 1.0 to 0.005 *N* and heated in an oven at 60° C for 4 weeks. At the end of this time the soluble nitrogen compounds in the solutions were determined using the methods described above. The results shown in figure 2 and table 4 indicate that at first the

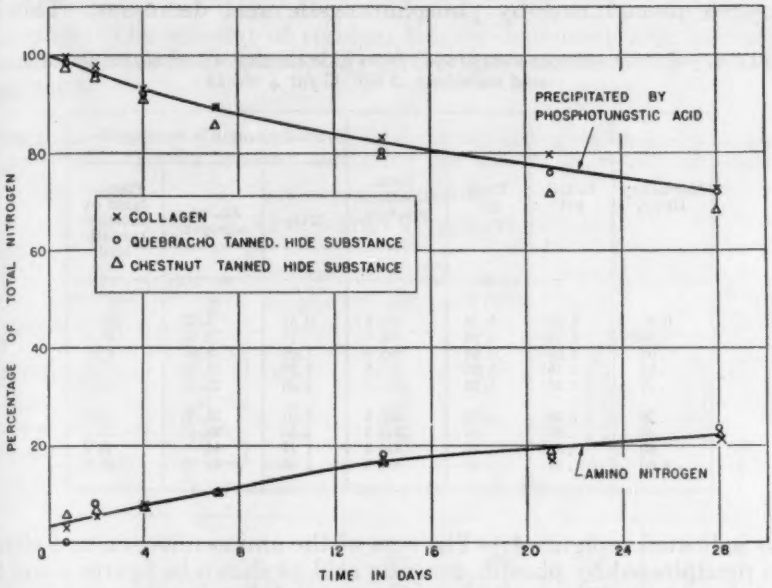

FIGURE 1.—*Rate of change of the total soluble nitrogen as amino nitrogen and as nitrogen precipitated by phosphotungstic acid for hide substance and tanned hide substances hydrolyzed in 0.05 N sulphuric acid.*

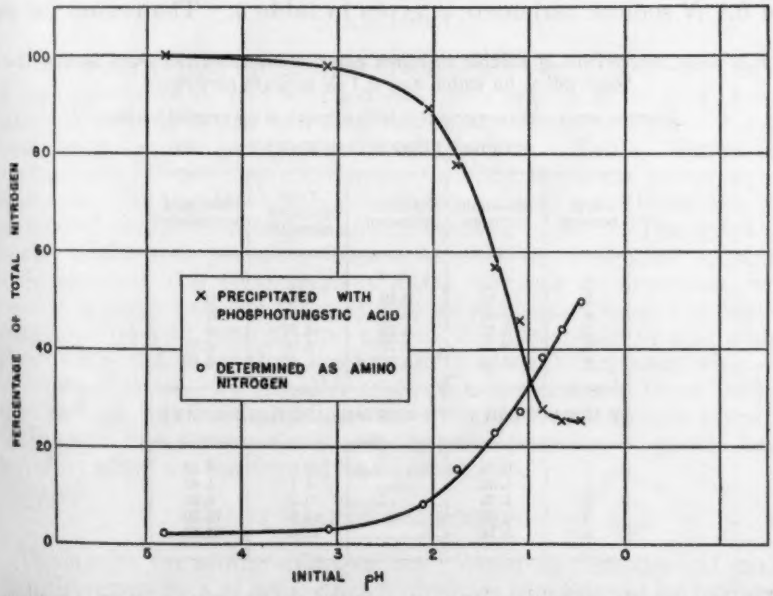

FIGURE 2.—*Change with* pH *of the amino nitrogen and the nitrogen precipitated with phosphotungstic acid for hide substance hydrolyzed in sulphuric acid solutions.*

amino nitrogen increases to approximately the same extent as the nitrogen precipitated by phosphotungstic acid decreases. This is

TABLE 4.—*Soluble nitrogen compounds from hide substance hydrolyzed in sulphuric acid solutions at 60° C for 4 weeks*

Normality H_2SO_4	Initial pH	Final pH	Total nitrogen in solution	Total nitrogen in solution as—		
				NH_3	Amino nitrogen	Precipitated by phosphotungstic acid
			mg	%	%	%
0.0	4.81	5.24	295.4	0.37	2.37	100.7
.005	3.10	3.96	295.9	.78	2.98	98.2
.02	2.09	2.49	295.4	1.99	8.60	89.7
.05	1.75	1.86	305.5	2.32	15.20	77.8
.10	1.36	1.50	308.6	2.30	22.80	56.7
.20	1.09	1.16	307.3	2.31	26.90	45.6
.40	.85	.85	300.2	2.36	38.40	27.7
.60	.66	.68	304.3	2.17	44.00	25.5
1.00	.45	.46	305.0	2.33	49.90	25.6

also indicated in figure 1. The sum of the amino nitrogen and nitrogen precipitated by phosphotungstic acid as shown in figures 1 and 2, slightly exceeds 100 percent because a part of the nitrogen precipitated is free amino nitrogen.

1. EXTRACTIONS

A comparison of the soluble nitrogen compounds extracted by water and 0.1 *N* sodium carbonate is given in table 5. The reason for the

TABLE 5.—*Comparison of soluble nitrogen compounds extracted from leather (lot 1 Quebracho) by water and 0.1 N sodium carbonate*

[Results are given in percentage of total nitrogen in the original leather]

Acid content	Ammonia nitrogen	Amino nitrogen	Total nitrogen extracted	Nitrogen precipitated
EXTRACTING WITH WATER				
%	%	%	%	%
0	0.35	0.40	0.65	0
1	1.83	0.51	2.08	0
2	3.12	0.22	3.37	0
3	5.10	0.27	6.00	0.97
4	5.22	0.57	7.22	1.69
EXTRACTING WITH 0.1 *N* SODIUM CARBONATE				
0	0.39	----------	2.1	0.58
1	1.32	----------	4.4	1.67
2	2.25	----------	10.3	6.05
3	4.01	----------	19.3	13.30
4	3.14	----------	41.6	34.50

differences in the soluble nitrogen extracted is obvious on an examination of table 6. Water extracts chiefly ammonia and amino acids. On the other hand the sodium carbonate extracts more tannin and a larger amount of soluble nitrogen because it dissolves the otherwise

insoluble tannin-protein compound. In both cases the residual leathers contained larger percentages of nitrogen than the original samples. The amount of residual leather decreased with increasing acid content, but the percentage of nitrogen remained approximately constant.

TABLE 6.—*Ratio of nitrogen to solids in the extract and in the residue of quebracho leather (lot 1) when extracted with water and with 0.1 N sodium carbonate* [1]

[Results for 1 g of leather]

Acid (approx.)	Tannins extracted	Non-tannins extracted [2]	Total solids extracted	Nitrogen in solids	Nitrogen in residual leather	Nitrogen in original leather
	EXTRACTING WITH WATER					
%	g	g	g	%	%	%
0	0.046	0.017	0.064	0.83	8.9	8.2
1	.040	.024	.064	2.5	8.9	8.4
2	.041	.028	.069	3.9	9.5	8.9
3	.049	.038	.088	5.6	9.2	8.9
4	.051	.043	.095	5.7	8.9	8.5
	EXTRACTING WITH SODIUM CARBONATE					
0	----------	----------	[3] 0.396	0.41	14.2	8.2
1	----------	----------	.402	.80	14.5	8.4
2	----------	----------	.392	1.76	13.9	8.9
3	----------	----------	.446	3.72	14.0	8.9
4	----------	----------	.584	5.31	13.0	8.5

[1] Determination of total solids, tannins, and non-tannins made by ALCA methods.
[2] Non-protein, non-tannins.
[3] These values are corrected for the sodium carbonate present in the solution.

2. AMMONIA

Table 4 shows that the amount of ammonia formed in the hydrolysis of hide substance in acid solution reaches a maximum of 2.32 percent in 0.05 *N* sulphuric acid and does not change appreciably beyond this figure in the more concentrated acid solutions. Table 3 shows that the tanned hide powders gave approximately the same percentage of ammonia. In the leathers aged under natural conditions the percentage of the total nitrogen as ammonia is higher. The oxidation in the leathers is probably caused in part by molecular sulphuric acid, therefore the percentage of total nitrogen as ammonia, after making a correction for the nitrogen as ammonia present in leather containing no acid, was plotted against the percentage of acid added. Figures 3 and 4 show that the ammonia content increases with acid content and time. The smaller amounts of ammonia in those leathers aged at high relative humidities are in accord with results obtained by Innes. The figures also show that the presence of grease has a retarding effect on the formation of ammonia.

3. AMINO NITROGEN

The results for amino nitrogen are plotted against the pH rather than the percentage of acid, since hydrolysis is catalyzed by hydrogen ions. The amount of amino nitrogen formed in the leathers is small. The results shown in figure 5 compare well with those obtained by

the direct hydrolysis of hide substance by sulphuric acid solutions, figure 2. Only small amounts of amino nitrogen are formed above a

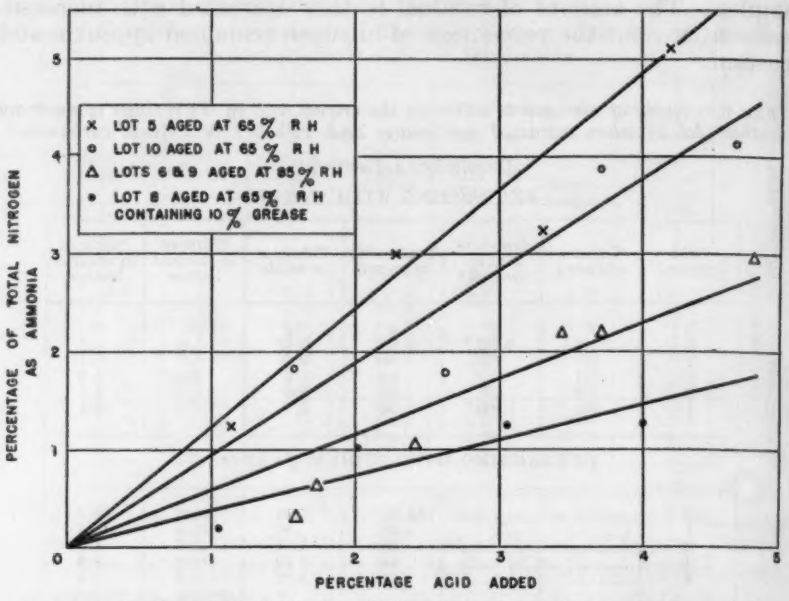
× LOT 5 AGED AT 65 % R H
○ LOT 10 AGED AT 65 % R H
△ LOTS 6 & 9 AGED AT 85 % R H
• LOT 8 AGED AT 65 % R H CONTAINING 10 % GREASE
PERCENTAGE OF TOTAL NITROGEN AS AMMONIA
PERCENTAGE ACID ADDED
0
1
2
3
4
5

FIGURE 3.—*Effect of relative humidity and grease on the ammonia content.*

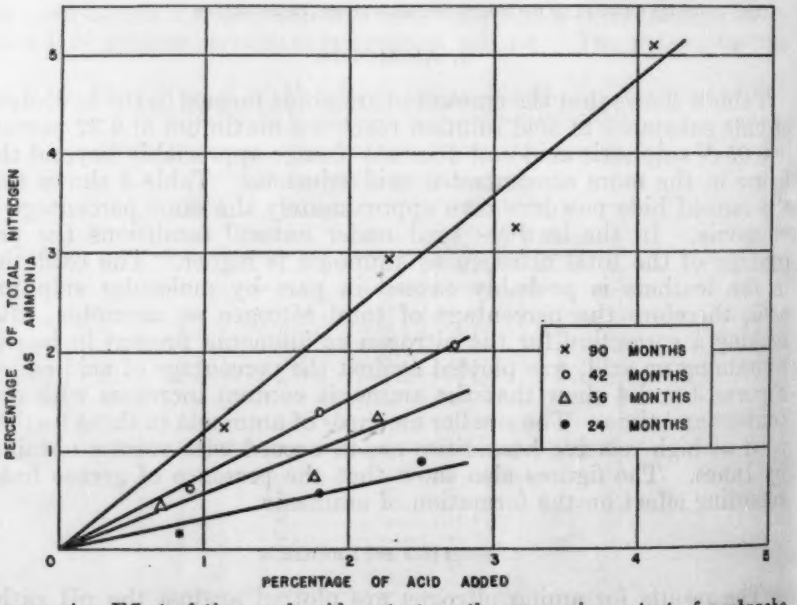

FIGURE 4.—*Effect of time and acid content on the ammonia content of quebracho leather.*

pH of 2, while below this pH the amount of amino nitrogen formed increased rapidly with decreasing pH. Figures 1 and 5 show that the formation of amino nitrogen is also a function of time.

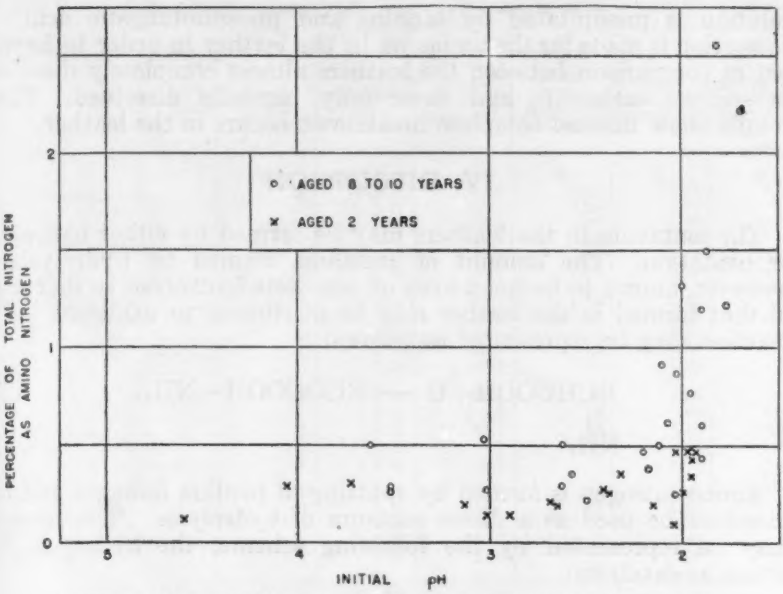

FIGURE 5.—*Effect of time and* pH *on the amino-nitrogen content.*

4. NITROGEN PRECIPITATED BY TANNINS AND BY PHOSPHOTUNGSTIC ACID

An examination of table 7 shows that over 90 percent of the total nitrogen extracted from the leather by a 0.1 *N* sodium carbonate

TABLE 7.—*Nitrogen compounds soluble in 0.1 N solution of sodium carbonate and precipitated by tannins and by phosphotungstic acid*

Lot [1]	Acid (approx.)	pH	Total nitrogen extracted	Total nitrogen precipitated	Total nitrogen extracted and precipitated	Total nitrogen extracted and precipitated, correcting for ammonia
	%		mg	mg	%	%
1	4	1.94	60.8	53.2	87.5	96.4
2	4	1.70	149.3	134.2	90.0	93.6
3	4	1.95	50.6	39.1	77.6	90.8
4	4	1.76	140.7	126.5	89.8	93.3
5	4	1.86	59.3	49.2	82.8	93.0
6	4	1.80	141.0	139.0	95.2	101.0
7 (10% grease)	4	1.92	149.1	134.8	90.4	91.8
7 (20% grease)	4	1.88	131.7	124.7	94.8	96.0
8 (10% grease)	4	2.03	121.6	119.9	98.5	101.5
8 (20% grease)	4	2.10	108.1	105.2	97.4	100.0
9	4	1.89	41.3	30.3	73.4	83.5
9 (85% RH) [2]	4	1.87	106.1	99.4	93.6	95.4
10	4	1.87	139.3	125.9	90.4	93.4
10 (85% RH)	4	1.82	141.8	129.4	91.2	93.5
21	3	1.94	102.2	92.2	90.2	91.7
21 (85% RH)	3	1.94	159.2	151.6	95.2	97.0
22	3	1.98	22.4	20.0	89.4	90.0
22 (85% RH)	3	1.98	52.0	46.3	89.1	94.6
23 (0% cod oil)	3	2.28	38.9	34.3	88.2	91.0
23 (10% cod oil)	3	2.35	34.7	30.5	87.9	91.1
25 (0% glucose)	3	2.16	82.6	77.3	93.6	95.4
25 (6% glucose)	3	2.30	48.7	43.9	90.2	94.6

[1] Unless otherwise stated the leathers were conditioned at 65 percent relative humidity for the first 2 years.
[2] RH=relative humidity.

solution is precipitated by tannins and phosphotungstic acid. A correction is made for the ammonia in the leather in order to have a better comparison between the leathers almost completely dissolved in sodium carbonate and those only partially dissolved. These results show that no complete breakdown occurs in the leather.

IV. DISCUSSION

The ammonia in the leathers may be formed by either hydrolysis or oxidation. The amount of ammonia formed by hydrolysis is, however, known to be small even on complete hydrolysis so that most of that formed in the leather may be attributed to oxidation. The reaction may be represented as follows:

$$\begin{array}{l} \mathrm{RCHCOOH} + \mathrm{O} \longrightarrow \mathrm{RCOCOOH} + \mathrm{NH_3}. \\ \quad\; | \\ \mathrm{NH_2} \end{array}$$

Amino nitrogen is formed by splitting of peptide linkages and can therefore be used as a direct measure of hydrolysis. The reaction may be represented by the following scheme, the hydrogen ions acting as catalysts:

$$\begin{array}{l} \mathrm{RCHCONHCH_2COOH} + \mathrm{H_2O} \xrightarrow{\mathrm{H}+} \mathrm{RCHCOOH} + \mathrm{NH_2CH_2COOH}. \\ \quad\; | \qquad\qquad\qquad\qquad\qquad\quad\; | \\ \mathrm{NH_2} \qquad\qquad\qquad\qquad\qquad\quad \mathrm{NH_2} \end{array}$$

Phosphotungstic acid precipitates the basic amino acids, peptones, and other incompletely hydrolyzed proteins. In this work, it may be used as a measure of the incompletely hydrolyzed proteins.

The results indicate that both oxidation and hydrolysis take place in the leather. It is, however, not necessarily true that both of these factors are the causes of physical deterioration. The formation of ammonia and amino nitrogen, which respectively indicate oxidation and hydrolysis, is shown to increase with time. The conditions under which these leathers were aged made both reactions take place slowly.

In table 8 the ammonia content is compared with the total nitrogen extracted and with the loss in tensile strength. The formation of ammonia shows no correlation to the loss in tensile strength, and hence it is probable that ammonia is not formed by the primary reactions which cause the physical deterioration of the leather. It is known that the guanidine nucleus of arginine which is free in the protein molecule is readily oxidized to form ammonia. Ammonia may also be formed from free amino nitrogen or amino nitrogen formed during hydrolysis.

TABLE 8.—*Soluble nitrogen compounds formed in leathers aged for different periods of time*

Lot [1]	Aging period	Original pH	Total nitrogen extracted	Total nitrogen as amino nitrogen	Total nitrogen as ammonia	Change in tensile strength [2]
	Years		%	%	%	%
8 (10% grease)	9	2.19	30.3	0.41	2.55	−16.5
3	10	2.17	17.3	.38	4.45	−31.8
1	10	2.12	18.2	.27	5.10	−20.5
7 (10% grease)	9	2.10	91.1	.92	2.23	−52.5
9	8	2.07	20.2	.62	5.82	−33.0
9 (85% RH) [3]	8	2.02	54.9	.87	2.35	−48.0
10 (85% RH)	8	2.00	85.3	1.33	2.69	−58.0
10	8	1.98	83.6	.65	4.90	−43.0
6	10	1.96	53.0	.77	2.35	−76.5
5	10	1.94	27.5	.48	4.12	−44.0
4	10	1.90	54.1	.64	4.98	−52.8
2	10	1.90	94.6	1.20	2.89	−63.4
29	2	2.40	5.5	.28	.93	−25.2
28	2	2.38	22.1	.28	1.15	−53.7
27	2	2.15	10.0	.21	1.52	−47.2
31	2	2.04	7.3	.11	1.31	−43.1
30	2	2.03	47.4	.47	1.43	−85.2
22	2	1.98	13.1	.26	1.38	−29.0
22 (85% RH)	2	1.98	30.5	.47	1.81	−62.0
21	2	1.94	57.8	.35	1.49	−61.2
21 (85% RH)	2	1.94	90.0	.45	2.09	−75.3

[1] Unless otherwise stated the leathers were conditioned at 65 percent relative humidity for the first 2 years.
[2] Determined after 2 years of aging. [3] RH=relative humidity.

There is, however, a relation between the amino nitrogen and the total soluble nitrogen. This is shown in figure 6, where the total

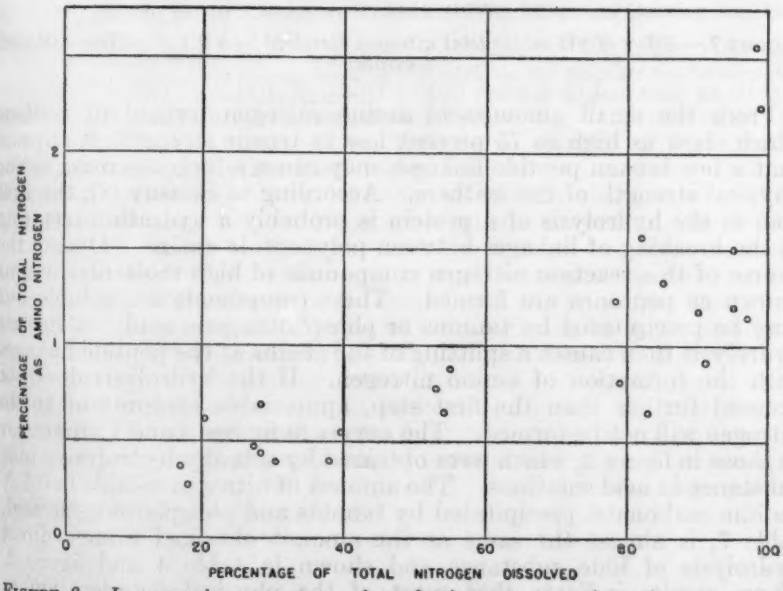

FIGURE 6.—*Increase in percentage of total nitrogen as amino nitrogen with the percentage of total nitrogen dissolved by a 0.1 N sodium carbonate solution.*

soluble nitrogen is plotted against the amino nitrogen. Previous work [9] has shown that a relationship exists between the total soluble nitrogen and the tensile strength and therefore there must also be a

relation between the tensile strength and the amino nitrogen. Comparing figure 5 with figure 7 shows that the amino nitrogen starts to increase, although to a smaller extent, at the same pH as that at which the amount of soluble nitrogen increases. This indicates that both may result from the same reaction.

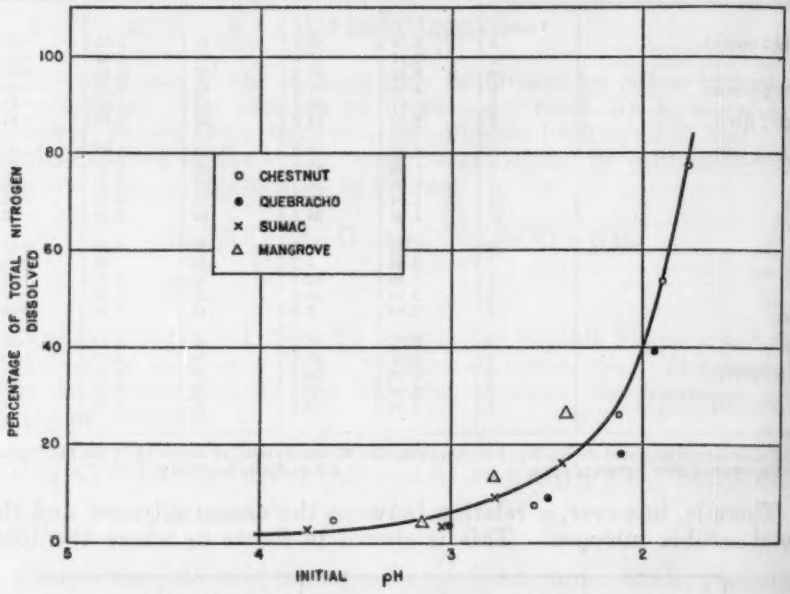

FIGURE 7.—*Effect of* pH *on the total nitrogen dissolved by a 0.1 N sodium carbonate solution.*

From the small amounts of amino nitrogen formed in leathers which show as high as 75 percent loss in tensile strength, it appears that a few broken peptide linkages may cause a large decrease in the physical strength of the leathers. According to Stiasny [8], the first step in the hydrolysis of a protein is probably a hydration resulting in the breaking of linkages between polypeptide chains. During the course of this reaction nitrogen compounds of high molecular weight known as peptones are formed. These compounds are soluble but may be precipitated by tannins or phosphotungstic acid. A further hydrolysis then causes a splitting of the chains at the peptide linkages with the formation of amino nitrogen. If the hydrolysis does not proceed further than the first step, appreciable amounts of amino nitrogen will not be formed. The curves in figures 5 and 7 are similar to those in figure 2, which were obtained by actually hydrolyzing hide substance in acid solutions. The amount of nitrogen soluble in 0.1 *N* sodium carbonate, precipitated by tannins and phosphotungstic acid, table 7, is almost the same as the amount obtained from a direct hydrolysis of hide substance and shown in table 4 and figure 2. These results indicate that most of the physical deterioration in leather is caused by hydrolysis.

V. SUMMARY

1. The deterioration of leather results in the formation of soluble decomposition products containing nitrogen.

2. An average of over 90 percent of the total nitrogen in the decomposition products is precipitated by phosphotungstic acid.

3. Among the decomposition products are ammonia and compounds containing amino nitrogen.

4. The amount of ammonia formed is a function of time and acid concentration, while the amount of amino nitrogen formed is a function of time and hydrogen ion concentration.

5. The data indicate that most of the physical deterioration is caused by hydrolysis.

VI. REFERENCES

[1] E. L. Wallace and J. R. Kanagy. *Deterioration of vegetable-tanned leathers containing sulphuric acid and glucose.* J. Research NBS **15,** 523 (1935) RP846.

[2] Veitch, Frey, and Leinbach. *Polluted atmosphere, a factor in the deterioration of bookbinding leather.* J. Am. Leather Chem. Assn. **21,** 156 (1926).

[3] R. Faraday Innes. *The deterioration of vegetable-tanned leather on storage.* J. Int. Soc. Leather Trades Chem. **17,** 725 (1933).

[4] R. Faraday Innes. *The deterioration of vegetable-tanned leather on storage.* J. Int. Soc. Leather Trades Chem. **15,** 480 (1931).

[5] R. Faraday Innes. *The deterioration of vegetable-tanned leather on storage.* J. Int. Soc. Leather Trades Chem. **14,** 624 (1930).

[6] R. W. Frey and C. W. Beebe. *The comparative permanence of chrome and vegetable leather as indicated by gas-chamber tests.* J. Am. Leather Chem. Assn. **29,** 489 (1934).

[7] Joseph R. Kanagy and Milton Harris. *Amino-nitrogen contents of wool and collagen.* J. Research NBS **14,** 563 (1935) RP787.

[8] J. Alexander, Colloid Chemistry **4,** p. 421. (The Chemical Catalog Co., Inc., 1932.)

[9] Everett L. Wallace, Joseph R. Kanagy, and Charles L. Critchfield. *Influence of some sulphur-containing tanning materials on the deterioration of vegetable-tanned leathers by sulphuric acid.* J. Am. Leather Chem. Assn. **30,** (1935), and J. Research NBS **15,** 369 (1935) RP835.

WASHINGTON, May 26, 1936.

U. S. Department of Commerce National Bureau of Standards

RESEARCH PAPER RP910

Part of Journal of Research of the National Bureau of Standards, Volume 17, August 1936

DISTRIBUTION OF COMPOUNDS IN PORTLAND CEMENT

By J. Arthur Swenson and E. P. Flint

ABSTRACT

Thirteen cements have been separated into size-fractions by means of air elutriation and chemical analyses have been made on all of the fractions and the whole cements. The compound compositions were calculated according to the method of Bogue and plotted by two different methods so as to show how the compounds are distributed with respect to size of particles. Heats of solution and hydration were determined for the fractions of five cements which were of very similar chemical composition and yet were known to differ considerably in certain physical properties. Studies of the observed heats of solution of the fractions of these cements as compared with the calculated theoretical heats of solution indicated discrepancies between the true compositions and the calculated compositions. The results of microscopic examination of etched sections of the cement clinkers gave further indication of the existence of such discrepancies.

CONTENTS

	Page
I. Introduction	261
II. Variation of chemical composition with particle size	262
1. Description of cements	262
2. Particle size and composition	262
III. Heats of hydration of size fractions	269
1. General details	269
2. Discussion of results	270
IV. Accuracy of calculated compound compositions as indicated by other methods	272
1. Studies of heats of solution	272
2. Microscopic analyses	274
V. Summary	275

I. INTRODUCTION

Investigations at the National Bureau of Standards and elsewhere during the past several years have emphasized the heterogeneous nature of portland cement by showing that its chemical constituents are distributed unequally among the differently sized particles making up the cement.[1] Recognition of the existence of these inequalities is important since they are sufficiently large in many cases to render futile any attempts at quantitative explanations of the behavior of the cement merely on the basis of the chemical analysis of the whole cement. The problem is further complicated by the fact that the

[1] Report of Conservation Bureau and Research Laboratory, Portland Cement Association, Spring meeting of 1932.
Rordam, Rock Products (July 30, 1932).
Carlson and Bates, Rock Products (Oct. 22, 1932).
Lerch and Bogue, J. Research NBS **12**, 645 (1934) RP684.
Swenson, Wagner, and Pigman, J. Research NBS **14**, 419 (1935) RP777.

true compound compositions may differ considerably from the calculated compositions under certain conditions of clinker cooling.[2] Data indicating the magnitude of both of these effects are presented in this paper.

II. VARIATION OF CHEMICAL COMPOSITION WITH PARTICLE SIZE

1. DESCRIPTION OF CEMENTS

Thirteen cements, representing products of six different manufacturers, were studied. Cements 1 to 4 in table 1 were produced at four different plants, 5 and 6 at one plant, and 7 to 13 at one plant. Cements 1, 2, 3, 4, 7, and 8 are of the low-heat-of-hardening type, 5, 6, and 9 are of the rather high-heat-of-hardening type, while 10, 11, 12, and 13 are moderately low-heat-of-hardening cements. Complete milling information is not available, but it is known that cements 5 and 6 were ground in Hardinge mills. It is also known that cements 10 and 11 were obtained from one finishing mill before and after, respectively, the addition of new balls, and that samples 12 and 13 were taken in the same way from a second mill. Cements 7 and 8, which are of the same type and brand, differ by about 1 year in date of manufacture.

2. PARTICLE SIZE AND COMPOSITION

Each of the cements was separated into five size-fractions [3] by means of air elutriation, using in the case of the two fine fractions for all cements except numbers 5 and 6, air having about 10-percent relative humidity. Chemical analyses were made on the whole cements and all of the fractions. The results of these analyses, together with the compound compositions as calculated according to the method of Bogue,[4] are presented in table 1. The percentages of the whole cements composed of material within the size ranges of each of the different fractions as determined by the Wagner turbidimeter [5] are also presented.

TABLE 1.—*Chemical compositions of whole cements and fractions and compound compositions calculated on ignition-loss basis*

Cement	Fraction size range	Percentage of whole	Oxide compositions								Calculated compound compositions				
			Loss on ignition	SiO_2	CaO	Fe_2O_3	Al_2O_3	MgO	SO_3	"Free" CaO	C_3S	C_2S	C_4AF	C_3A	$CaSO_4$
	Microns	%	%	%	%	%	%	%	%	%	%	%	%	%	%
1	Whole		1.0	26.4	63.2	1.9	3.3	2.6	1.7	0.4	27	55	5.8	5.5	2.9
	0–7	24	2.1	23.2	62.4	2.0	3.3	2.6	4.4	1.6	39	37	6.1	5.4	7.5
	7–22	21	.6	26.7	64.4	1.9	3.3	2.5	.8	.4	32	52	5.7	5.6	1.4
	22–40	22	.3	27.8	63.9	1.9	3.2	2.5	.4	.1	24	62	5.7	5.3	.7
	40–55	16	.2	28.3	63.5	2.0	3.5	2.5	.3	.1	16	69	6.1	5.9	.5
	>55	17	.3	28.5	63.1	2.1	3.4	2.5	.2	.0	14	71	6.3	5.5	.3
2	Whole		1.5	22.2	59.5	5.0	5.3	3.8	1.8	.5	25	45	15.3	5.5	3.1
	0–7	24	2.9	19.4	57.1	5.4	6.1	3.7	4.1	1.5	25	37	16.3	7.0	7.0
	7–22	26	1.2	23.5	61.0	4.5	4.7	3.7	1.1	.6	29	45	13.8	4.7	1.8
	22–40	17	.6	23.6	61.0	4.8	5.2	3.7	.5	.3	25	49	14.4	5.8	.9
	40–55	14	.5	23.4	60.6	5.1	5.5	3.9	.5	.1	24	49	15.4	6.1	.8
	>55	19	.5	23.5	59.9	5.2	5.6	3.9	.5	.3	20	53	15.9	5.8	.8

[2] Lea and Parker, Building Research (England) Technical Paper 16; also, Phil. Trans. Roy. Soc. 234, 1 (1934).

[3] Method of separating described in J. Research NBS 14, 419 (1935) RP777.

[4] Ind. Eng. Chem., Analytical Edition, 1, 192 (1929); also Portland Cement Association Fellowship Paper no. 21.

[5] Proc. Am. Soc. Testing Materials 33, II, 553 (1933).

TABLE 1.—*Chemical compositions of whole cements and fractions and compound compositions calculated on ignition-loss basis*—Continued

Cement	Fraction size range	Percentage of whole	Oxide compositions								Calculated compound compositions				
			Loss on ignition	SiO_2	CaO	Fe_2O_3	Al_2O_3	MgO	SO_3	"Free" CaO	C_3S	C_2S	C_4AF	C_3A	$CaSO_4$
	Microns	%	%	%	%	%	%	%	%	%	%	%	%	%	%
	Whole		1.0	23.4	61.5	5.5	5.4	0.9	1.8	0.8	22	50	16.6	5.1	3.0
	0–7	22	2.3	19.5	59.3	6.4	6.3	.9	4.6	1.3	28	35	19.4	5.8	7.9
	7–22	26	.8	24.4	62.5	5.1	4.8	.9	.8	.5	27	49	15.4	4.2	1.4
3	22–40	25	.4	25.2	62.4	4.9	4.7	.8	.4	.2	22	55	14.9	4.3	.7
	40–55	11	.4	25.3	62.2	5.3	5.0	.8	.3	.1	18	59	16.1	4.7	.5
	>55	16	.3	24.9	61.6	5.6	5.6	.8	.2	.1	15	60	17.1	5.3	.4
	Whole		1.2	23.0	59.4	5.5	5.4	3.6	1.7	.1	17	52	16.5	5.0	3.0
	0–7	22	2.3	19.7	57.1	6.4	6.0	4.1	4.1	.1	22	40	19.4	5.1	7.0
	7–22	31	.6	25.0	60.9	4.5	4.5	3.2	.8	.0	18	58	13.7	4.3	1.3
4	22–40	22	.4	24.8	60.6	4.9	5.1	3.3	.4	.0	16	59	15.0	5.3	.8
	40–55	12	.3	24.1	60.1	5.5	5.4	3.6	.4	.0	15	58	16.9	5.1	.6
	>55	13	.2	24.1	59.7	5.7	5.8	3.7	.3	.1	11	61	17.4	5.8	.6
	Whole		1.3	20.6	64.1	4.6	5.6	2.0	1.5	.7	55	17	13.9	7.2	2.5
	0–7	15	3.5	18.7	61.6	4.4	5.0	1.8	4.7	.8	55	12	13.4	5.8	8.0
	7–22	25	4.6	20.0	62.6	4.2	5.4	1.9	1.3	.4	57	14	12.8	7.2	2.2
5	22–40	23	1.5	21.0	64.9	4.6	6.0	2.0	.4	.3	55	18	13.9	8.2	.7
	40–55	13	.6	21.3	65.3	5.0	6.1	1.9	.2	.3	56	19	15.2	7.4	.3
	>55	24	.6	21.0	65.0	5.0	6.3	2.0	.2	.3	55	19	15.2	8.3	.3
	Whole		1.0	21.4	65.2	2.3	6.3	2.0	1.9	.7	52	22	7.1	12.8	3.2
	0–7	26	1.9	19.6	63.5	2.2	6.1	1.9	4.8	.5	52	17	6.9	12.3	8.1
	7–22	29	1.6	21.5	65.4	2.3	6.0	1.9	1.4	.3	54	21	6.9	11.9	2.4
6	22–40	23	.8	22.2	66.0	2.4	6.1	1.9	.5	.3	53	23	7.2	12.4	.8
	40–55	11	.3	22.4	66.1	2.5	6.4	2.0	.3	.3	51	26	7.6	13.0	.5
	>55	11	.3	22.4	66.0	2.5	6.6	1.9	.2	.5	47	29	7.8	13.4	.4
	Whole		1.0	21.9	59.3	5.7	5.3	4.7	1.6	.3	27	42	17.3	4.3	2.7
	0–7	26	2.1	18.8	57.2	6.4	6.0	5.0	3.5	.1	30	33	19.5	5.1	6.0
	7–22	24	.8	23.0	60.4	5.1	4.8	5.0	.7	.0	29	44	15.4	4.3	1.2
7	22–40	20	.5	24.1	60.8	4.9	4.6	4.3	.3	.0	25	51	14.7	4.0	.5
	40–55	12	.4	23.1	60.4	5.5	5.0	4.7	.2	.0	28	45	16.7	4.0	.3
	>55	18	.4	22.3	59.6	6.1	5.6	5.3	.2	.0	30	41	18.5	4.5	.3
	Whole		1.2	22.4	60.2	5.1	5.3	3.8	1.9	.2	27	44	15.5	5.3	3.2
	0–7	25	2.6	19.4	57.9	4.7	6.5	3.6	4.7	.7	22	39	14.2	9.4	8.1
	7–22	26	.9	23.1	61.7	4.6	4.4	3.7	1.3	.4	35	40	14.6	4.0	2.2
8	22–40	23	.5	24.6	62.2	4.5	4.2	3.3	.4	.1	30	48	13.7	3.6	.8
	40–55	11	.4	24.1	61.2	4.8	5.1	3.6	.3	.1	24	51	14.6	5.3	.5
	>55	15	.4	23.5	61.1	5.4	5.2	4.1	.3	.0	26	48	16.4	4.8	.5
	Whole		1.1	21.6	64.8	2.0	5.5	3.4	1.6	1.0	56	20	6.1	11.1	2.7
	0–7	28	2.9	19.4	62.8	2.0	5.6	3.1	4.0	2.8	56	14	6.1	11.4	6.8
	7–22	24	1.0	22.1	65.4	2.0	5.4	3.3	.8	.8	56	21	5.9	11.1	1.3
9	22–40	21	.6	22.7	65.6	1.9	5.5	3.4	.4	.0	54	25	5.8	11.4	.6
	40–55	10	.4	22.7	65.6	2.0	5.6	3.5	.2	.1	53	25	5.9	11.6	.4
	>55	17	.4	22.5	64.7	2.1	6.0	3.7	.2	.2	48	28	6.3	12.5	.4
	Whole		1.1	21.2	62.4	4.3	5.3	3.6	1.8	.1	46	26	13.0	6.9	3.1
	0–7	19	2.7	18.8	60.0	4.7	5.6	3.5	4.6	.6	43	22	14.3	7.0	7.8
	7–22	29	.9	21.7	63.3	4.0	5.0	3.6	1.4	.2	50	24	12.2	6.3	2.3
10	22–40	26	.5	22.6	64.0	3.9	5.1	3.5	.4	.1	48	29	11.8	6.9	.8
	40–55	13	.4	22.7	63.5	4.1	5.3	3.6	.2	.0	44	32	12.4	7.2	.3
	>55	13	.4	22.1	63.1	4.4	5.6	3.9	.2	.0	44	30	13.3	7.6	.3
	Whole		1.1	21.3	62.2	4.6	5.2	3.8	1.8	.4	45	27	14.2	5.8	3.1
	0–7	20	2.6	18.5	59.4	5.2	5.7	3.6	4.5	.7	43	21	15.8	6.4	7.6
	7–22	28	1.0	21.5	62.7	4.4	5.1	3.8	1.3	.2	52	23	13.4	5.1	2.2
11	22–40	23	.6	22.7	63.1	4.2	5.1	3.6	.4	.1	42	33	12.8	6.4	.7
	40–55	15	.5	22.4	62.9	4.5	5.4	3.8	.2	.2	43	32	13.7	6.6	.3
	>55	14	.4	22.1	62.6	4.9	5.3	4.0	.2	.1	43	31	14.8	5.8	.4
	Whole		1.1	21.2	62.7	4.1	5.5	3.6	1.9	.4	46	26	12.4	7.6	3.3
	0–7	21	2.6	18.6	60.0	4.5	5.7	3.5	4.7	.6	45	20	13.5	7.7	8.0
	7–22	27	1.0	21.5	63.5	3.9	5.1	3.6	1.5	.2	51	23	11.8	6.9	2.6
12	22–40	24	.6	22.6	64.2	3.7	5.3	3.4	.6	.1	46	30	11.3	7.7	.9
	40–55	12	.4	22.8	64.0	4.0	5.2	3.7	.2	.0	45	31	12.0	7.2	.4
	>55	16	.4	22.1	63.3	4.2	5.6	3.9	.3	.1	46	29	12.8	7.6	.5
	Whole		1.0	21.3	62.3	4.7	5.1	3.9	1.8	.4	45	27	14.0	5.8	3.1
	0–7	22	2.5	18.4	59.6	5.1	5.5	3.6	4.8	.5	45	19	15.5	5.9	8.2
	7–22	26	.9	21.7	62.8	4.4	4.7	3.8	1.4	.2	49	25	13.4	4.9	2.4
13	22–40	24	.5	22.8	63.6	4.2	4.8	3.6	.4	.1	46	30	12.8	5.5	.7
	40–55	12	.4	22.8	63.2	4.4	5.0	3.7	.2	.1	44	33	13.4	5.8	.3
	>55	16	.4	22.1	62.7	4.8	5.3	4.0	.2	.2	44	30	14.6	5.8	.3

Figures 1 to 4 are schematic diagrams which show pictorially the calculated compound compositions of the cements. There are also shown a series of curves giving the amount of each compound finer than any given size, expressed as the percentage of the whole cement.

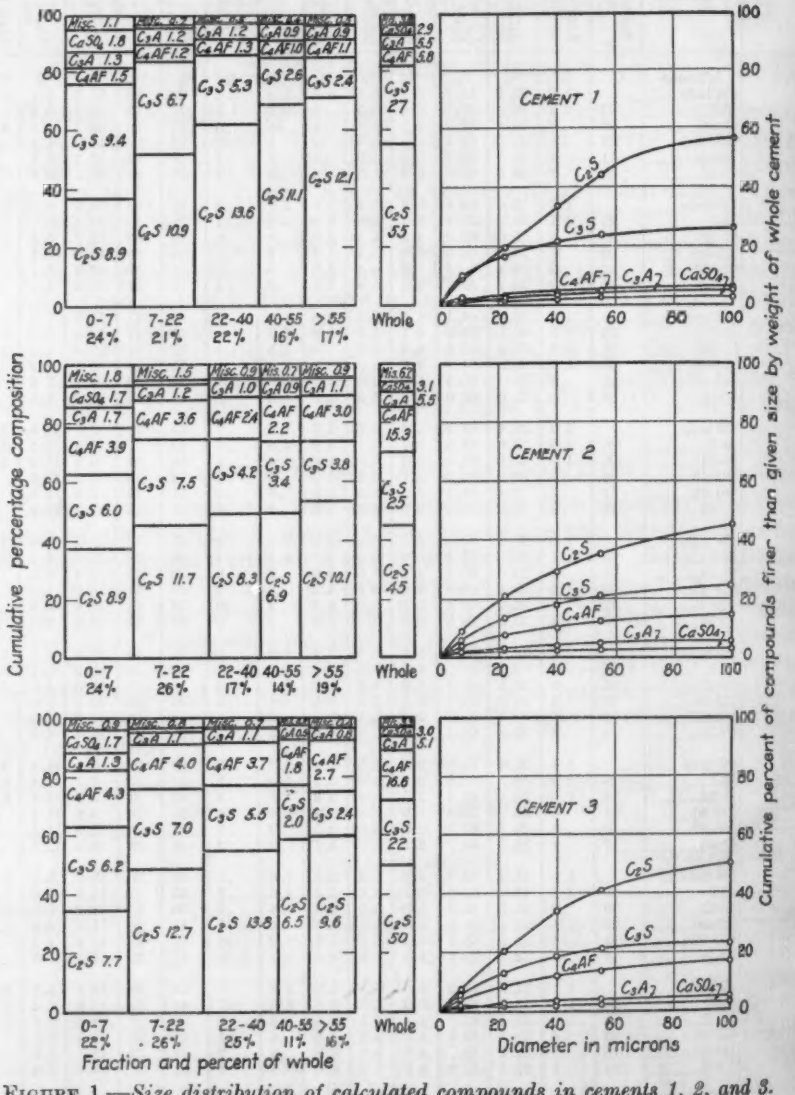

FIGURE 1.—*Size distribution of calculated compounds in cements 1, 2, and 3.*

The diagrams on the left can be looked upon as the cross sections of the cements with the particles segregated according to size and composition. The curves on the right show the amounts of each compound finer than any given size, expressed as percentages of the whole cement.

In the schematic diagrams the horizontal spacings are proportional to the percentages, as determined in the turbidimeter, of the whole cements composed of the several fractions, and the vertical spacings are proportional to the percentages of the various compounds con-

tained by the fractions. The diagram can accordingly be looked upon as a cross section of a cement with the particles segregated according to size and composition. Hence, the area of each small rectangle is in direct proportion to the amount of the particular compound represented which lies between the size limits of the particular fraction. These amounts, expressed as percentages of the whole cements, are printed in each of the rectangles. The graphs on the right are the progressive summations of these percentages plotted against an actual size horizontal scale running from 0 to 100 microns. In preparing these graphs it was assumed that all of the particles were finer than 100 microns, although this was not strictly true, so that the terminal point of each curve corresponds approximately to the percentage of the particular compound in the whole cement. The terminal points of these curves do not always correspond accurately with the analyses of the whole cements, since there is always a certain discrepancy between the granulometric composition as determined by the turbidimeter, and that as determined by air elutriation, because of the continual breaking up of the particles in the elutriation stacks.

Examination of table 1 and the diagrams shows that, in general, the different sizes of particles in a cement differ considerably in chemical composition. Of the four major constituents, the two silicate compounds are the ones which show the greatest variations. The tricalcium silicate (C_3S) tends to be more concentrated in the finer sizes, while the greatest percentages of dicalcium silicate (C_2S) are found in the coarser sizes. This trend is very pronounced in cements 1 to 4, inclusive. Cement 5, with a range of only 2 percent in C_3S for the different fractions, shows the least variation in this respect. However, the amount of C_2S increases considerably from the fine to the coarse material. Cement 6, although having the greatest percentage of C_3S in the 7–22 fraction, follows the general rule quite closely. Of the cements 7 to 13, inclusive, which were all produced by one manufacturer, only cement 9 follows the general rule exactly. The cements produced at this plant apparently tend to have the greatest percentages of C_2S and the least percentages of C_3S either in the 22–40 or the 40–55 micron fractions rather than in the largest sized fraction. However, they still show the same tendency as the other cements because the percentage of C_2S in the >55 fraction is in all cases considerably higher than that in the 0–7, and the greatest percentage of C_3S is found in either the 0–7 or the 7–22 micron fractions in all cements except no. 7, which has the same percentage of this compound in the >55 and 0–7 fractions.

The tetracalcium alumino-ferrite (C_4AF) and the tricalcium aluminate (C_3A) show less definite trends than the silicate compounds. The C_4AF does show a tendency to be of greatest concentration in either the 0–7 or the >55 fraction, and the least percentage is found in either the 7–22 or the 22–40 micron fractions. Similar irregular trends can be observed in the distribution of the C_3A. The tendency is for the least percentage of the C_3A to be in the 7–22 fraction.

The calcium sulfate is in all cases found largely in the two fine fractions. The percentage of $CaSO_4$ in the 0–7 fraction is usually of the order of twice the sum of the percentages of this compound in the other four fractions.

The finest fraction further differs from the others in that it usually has a much greater ignition loss. This is true for all the cements except 5 and 6, no. 5 showing a greater ignition loss in the 7–22 fraction than in the 0–7, and no. 6 having an ignition loss in the

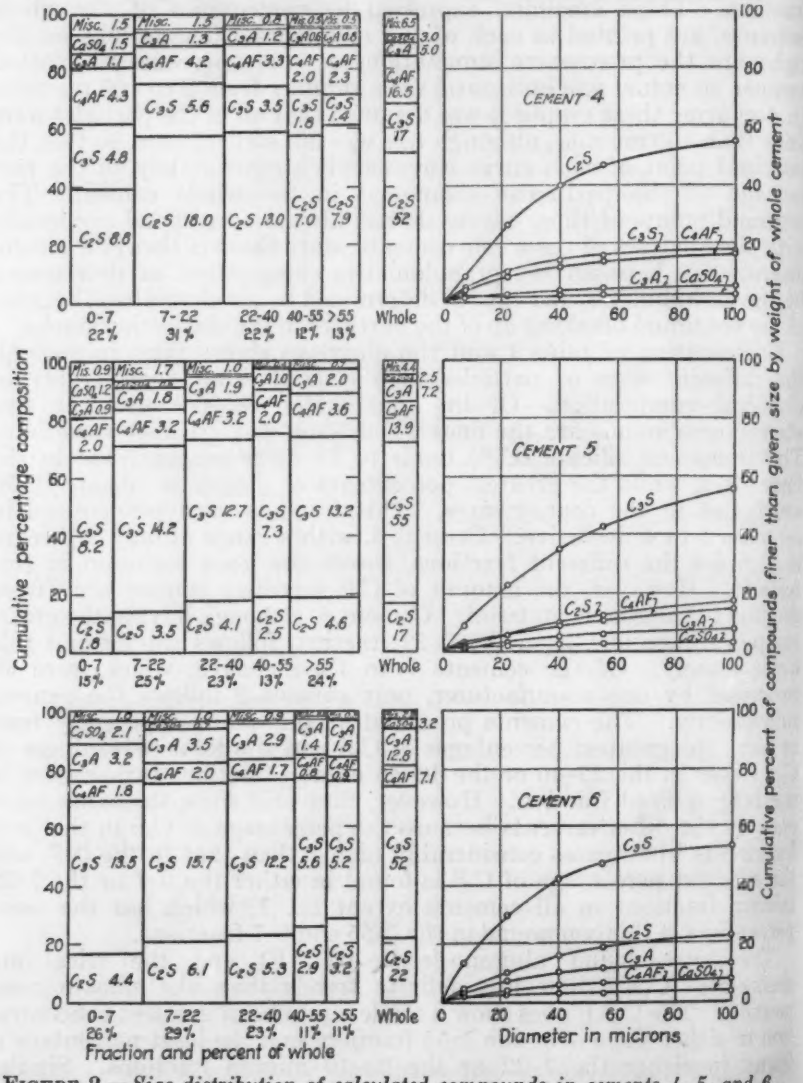

FIGURE 2.—*Size distribution of calculated compounds in cements 4, 5, and 6.*

The diagrams on the left can be looked upon as the cross sections of the cements with the particles segregated according to size and composition. The curves on the right show the amounts of each compound finer than any given size, expressed as percentages of the whole cement.

7–22 fraction almost as great as that in the 0–7. These two cements are exceptions because during their separation the system for drying the air in the elutriation stacks was not in operation. As a result, a considerable amount of hydration occurred during the separation. In separating the other cements the relative humidity of the circu-

lating air in the stacks was kept down to about 10 percent, so that very little hydration took place. This can be seen by comparing the ignition losses in the whole cements with those in the fractions. With the exception of cements 5 and 6, therefore, the ignition losses

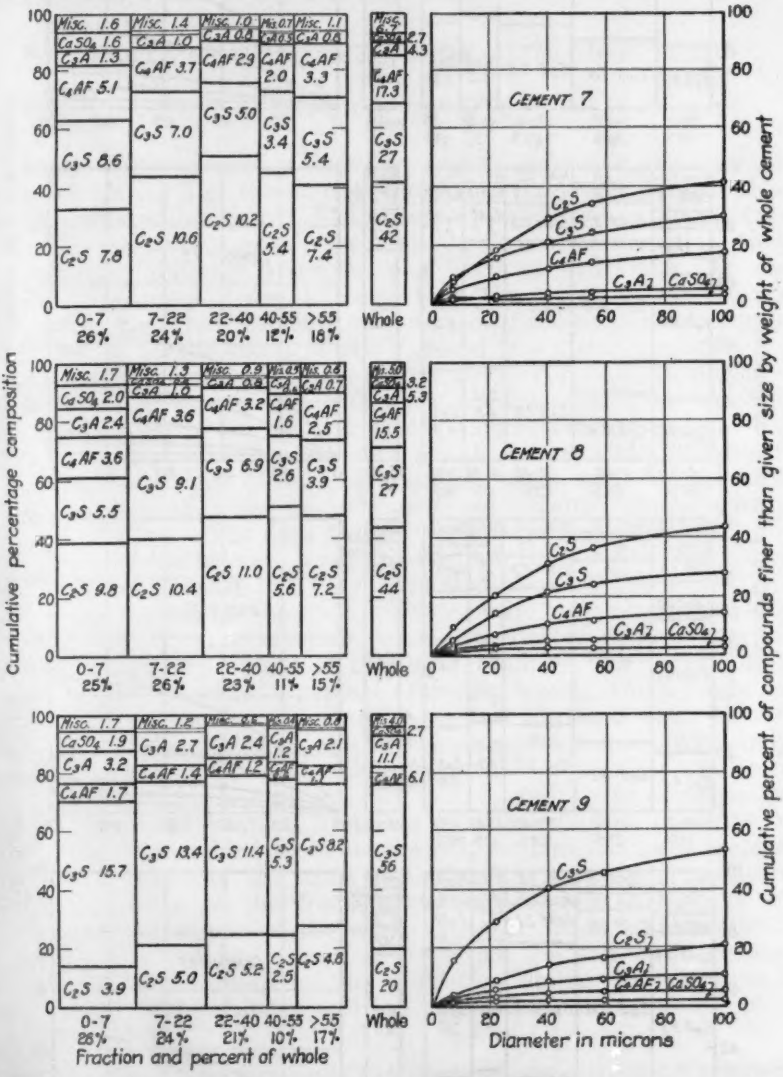

FIGURE 3.—*Size distribution of calculated compounds in cements 7, 8, and 9.*

The diagrams on the left can be looked upon as the cross sections of the cements with the particles segregated according to size and composition. The curves on the right show the amounts of each compound finer than any given size, expressed as percentages of the whole cement.

of the various fractions indicate the relative amounts of hydration of the various sizes in the whole cements. It is natural that the fine fraction should contain the most hydrated material since this fraction has a much greater surface area than any of the others exposed to hydration.

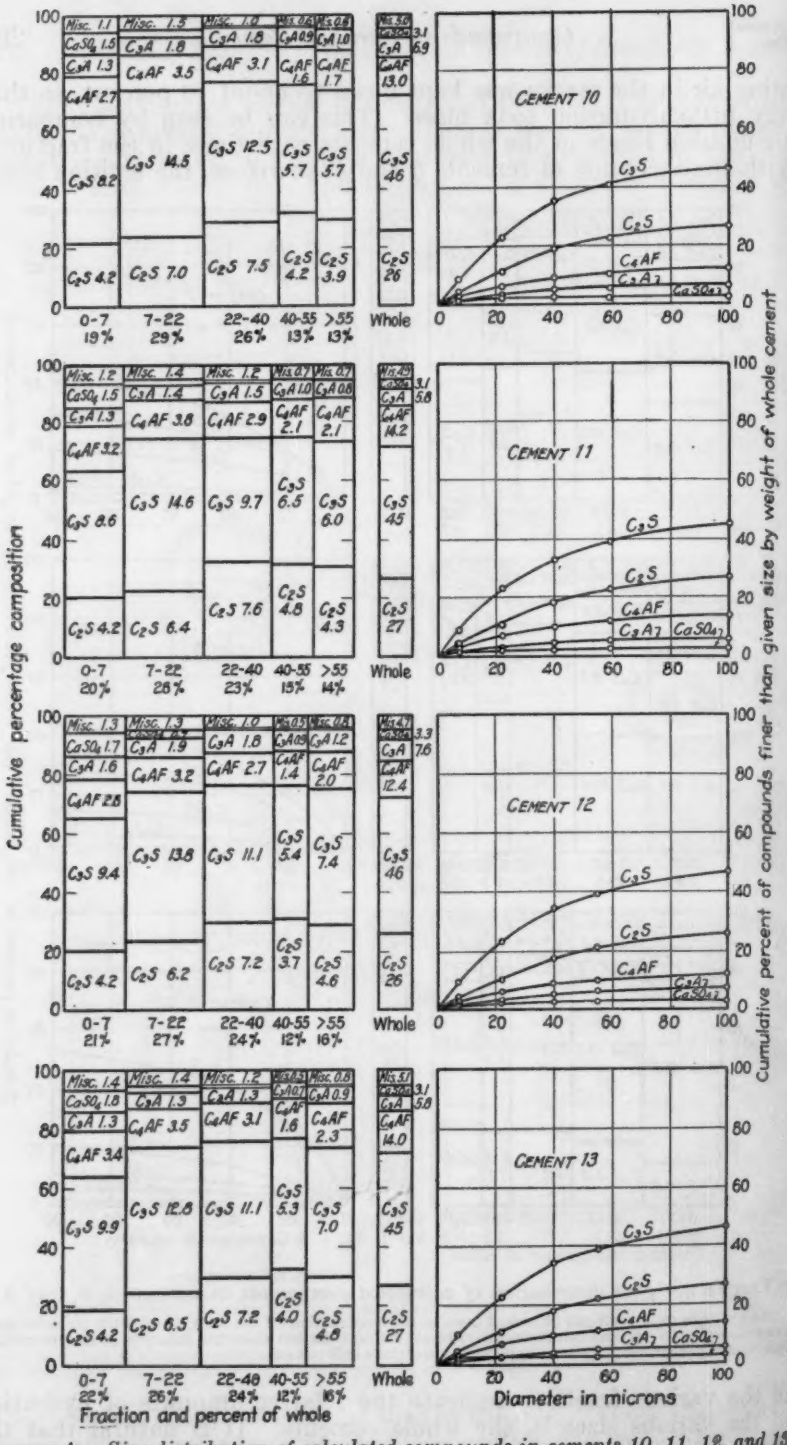

FIGURE 4.—*Size distribution of calculated compounds in cements 10, 11, 12, and 13.*

The diagrams on the left can be looked upon as the cross sections of the cements with the particles segregated according to size and composition. The curves on the right show the amounts of each compound finer than any given size, expressed as percentages of the whole cement.

The MgO content of the different fractions does not show very large variations for the majority of the cements. In five of the cements it remains practically constant. Cements 7 to 13 show slight variations in MgO with the greatest percentage in all seven cements being found in the >55 fraction.

III. HEATS OF HYDRATION OF SIZE FRACTIONS

1. GENERAL DETAILS

A considerable amount of data [6] on heat of hydration and strength was available for 5 of the 13 cements before the study of their size-fractions was undertaken. These data showed that although four of the five cements were of very similar chemical composition, they had markedly different strengths and heats of hydration. It was believed that some of the difficulty found in trying to explain the behaviors of the whole cements on the basis of their chemical compositions might be the result of the unequal size distributions of the chemical constituents, and, hence, that better correlations might be obtained if the properties of definite size-fractions were studied. The heats of hydration were therefore determined for most of the fractions of these same five cements, nos. 1, 2, 3, 4, and 7 in table 1.

The determinations of heat of hydration were made by the heat of solution method, using an isothermal calorimeter [7] at the ages of 3, 7, and 28 days. The data obtained are presented in table 2. No 3-day determinations were made for the two coarser fractions, since these fractions showed but very little hydration at this age. The heats of hydration of the >55 fraction were not determined for cements 1 and 7. The fractions were all hydrated with 45 percent of mixing water, by weight of the dry material. The 0–7 fraction was also hydrated with 60 percent of mixing water, which produced a paste of about the same consistency as that obtained when 45 percent of water was added to any of the other fractions. With only 45 percent of water the paste made from the 0–7 fraction was quite stiff. The 7–22 fraction of cements 1, 2, 3, and 4 was hydrated as obtained in the separation, and also after a sufficient quantity of gypsum had been added to make the SO_3 content the same as that of the 0–7 fraction of the same cement. The storage temperature for the hydration of the fractions was maintained at 70±3° F. The heats of hydration of the whole cements, when hydrated with 40 percent of water and stored at 70° F for the first 24 hours and 100° F for the remainder of the hydration period, for the ages 7 and 28 days, were available and are included in the table.

[6] Unpublished data obtained at this Bureau.
[7] Similar to the one used in testing the Boulder Dam cements and described in Bureau of Reclamation Specification 566.

TABLE 2.—*Heats of hydration at 70° F. of size-fractions obtained from five cements*

Fraction size range	Cement	Mixing water	Gypsum added	Computed heat for complete hydration	Heats of hydration for the ages			Percentages of available heat liberated at the ages		
					3 days	7 days	28 days	3 days	7 days	28 days
Microns		%	%	cal/g	cal/g	cal/g	cal/g	%	%	%
0-7	1	60	0	94	69	79	90	74	84	96
	2	60	0	90	71	74	80	79	82	89
	3	60	0	94	82	84	90	87	89	94
	4	60	0	87	68	70	85	78	91	98
	7	60	0	92	77	82	90	84	89	98
0-7	1	45	0	94	65	73	82	69	78	87
	2	45	0	90	64	70	73	71	78	81
	3	45	0	94	78	79	83	83	84	88
	4	45	0	87	68	73	80	78	84	92
	7	45	0	92	73	77	84	79	84	91
7-22	1	45	0	89	32	44	54	36	50	61
	2	45	0	88	32	44	57	36	50	65
	3	45	0	88	30	49	64	34	56	73
	4	45	0	81	24	41	58	35	51	72
	7	45	0	87	33	42	56	38	48	64
7-22	1	45	7.4	89	24	32	45	27	36	51
	2	45	6.3	89	28	34	43	31	38	48
	3	45	8.0	89	29	34	41	33	38	46
	4	45	7.0	82	25	31	39	28	35	44
22-40	1	45	0	86	17	24	40	20	28	46
	2	45	0	88	10	26	50	11	30	57
	3	45	0	85	15	28	57	18	33	67
	4	45	0	82	11	28	50	13	34	61
	7	45	0	85	------	25	44	------	29	52
40-55	1	45	0	81	------	16	35	------	20	43
	2	45	0	88	------	18	40	------	20	46
	3	45	0	84	------	20	44	------	24	52
	4	45	0	82	------	23	48	------	28	59
	7	45	0	87	------	17	36	------	20	41
>55	2	45	0	86	------	14	25	------	16	29
	3	45	0	84	------	17	37	------	20	44
	4	45	0	81	------	9	21	------	11	26
"Whole" [a]	1	40	0	86	------	50	63	------	58	73
	2	40	0	87	------	53	62	------	61	71
	3	40	0	87	------	60	68	------	69	78
	4	40	0	82	------	57	66	------	69	80
	7	40	0	87	------	60	69	------	69	79

[a] Hydrated at 70° F. for first 24 hours and 100° F. for remainder of period.

The heats available upon complete hydration of the fractions and also of the cements have been calculated from the compound compositions according to the method of Lerch and Bogue [8], using the values given by them for the heat liberated upon complete hydration of the individual compounds. The calculated heats of complete hydration and the experimentally determined heats of hydration, expressed as percentages of the total heat available, are included in table 2.

2. DISCUSSION OF RESULTS

The heat of hydration data for the fractions show that the amounts of heat liberated decrease regularly at all of the ages as the grain sizes of the fractions increase. This would be expected since the smaller surface areas present less opportunity for hydration. The

[8] BSJ. Research 12, 645(1934) RP684.

same trends were shown by the heats of hydration of the fractions studied by Lerch and Bogue.[9] The most striking feature about the data obtained in this study is the large unexplained decrease in the heat of hydration of the 7–22 fraction brought about by the addition of gypsum. The magnitude of this decrease at 7 and 28 days is considerably in excess of that which should have resulted if the same amount of some inert material had been added. Since the heat liberated upon the formation of the additional sulfo-aluminates in the material containing the added gypsum should very nearly have compensated for that of the cement displaced by the gypsum, only very small changes in the heat liberated might have been expected. This is shown by the near equality of the calculated heats available upon complete hydration for each of the cements with and without the gypsum.

An attempt to correlate some of the heats of hydration of the individual fractions with the compound compositions did not prove any more successful than the previous attempts at correlation of the properties of the whole cements with the compositions of the cements. Several equations were derived by the method of least squares giving the heats of hydration of one size-fraction for one age as linear functions of the four major compounds. However, none of these equations were found to yield very good correlations, and the constants derived did not appear to be such as to have any physical significance. For example, the equation derived for the 28-day heat of hydration of the 22–40 fraction was: Heat of hydration (cal/g)$=0.129\times\%$ of $C_3S+0.385\times\%$ of $C_2S+1.552\times\%$ of $C_4AF+0.811\times\%$ of C_3A. The heats of hydration as calculated from this equation were 40, 49, 51, 52, and 49, as compared with the experimentally determined values of 40, 50, 57, 50, and 44 calories per gram, respectively. With two out of the five cements showing differences between the observed and calculated values of five calories or more, this correlation could scarcely be considered good. Also, the coefficients for the different compounds are obviously not such as to indicate the relative amounts of heat evolved by these compounds. The C_3A should probably have a larger coefficient than the silicate compounds, since it hydrates more rapidly and with a greater evolution of heat, but the coefficient for the C_3S appears much too low in comparison and that of the C_4AF too high. The coefficient for the C_3S should at least be greater than that of the C_2S, since its heat of hydration is greater and since it is known to hydrate at a more rapid rate. The results of this study therefore indicated that the explanation of the poor correlation between the chemical compositions and the physical properties of these cements is not to be found entirely in the unequal size distributions of the chemical compounds

The only remaining possibility is that the clinkers from which these cements were made had fundamental differences aside from those shown by the chemical analyses or the calculated compound compositions. It is possible that some of the observed discrepancies were caused by differences in extent of crystallization brought about by differences in the cooling of the clinkers during manufacture. Such effects have recently been pointed out by Lea and Parker.[10]

[9] See footnote 8.
[10] Building Research (England) Technical Paper 16.

The method for calculating compound composition suggested by Bogue in 1929 [11] made use of the assumption of complete equilibrium crystallization of the compounds in the clinker except as corrected for uncombined lime and silica. It was recognized that such an assumption probably was not strictly correct and would be variable in different clinkers; but as no method was available for estimating the extent of crystallization of the erstwhile liquid, the assumption was justified as the only possible premise until such time as new information should provide opportunity for modification and higher precision.

IV. ACCURACY OF CALCULATED COMPOUND COMPOSITIONS AS INDICATED BY OTHER METHODS

1. STUDIES OF HEATS OF SOLUTION

In order to obtain some indication of the reliability of the calculated compound compositions of these five cements, a study was made of their heats of solution. The heat of solution of a cement should theoretically be equal to the sum of the heats of solution of the individual compounds in the relative proportions in which they occur. Furthermore, calorimetric measurements may be made with relative precision. The heats of solution of cements, as well as those for the pure compounds, can be determined within a probable error of about 0.3 cal/g for a single observation with the apparatus used. Therefore, if the true compound composition of a cement were known, it should be readily possible to obtain agreement within 1 cal/g between the observed and calculated heats of solution.

The heats of solution of the pure compounds in the acid mixture used (648.5 g of 2.5 $\pm$ .002 N nitric acid, 11.5 g of 48-percent hydrofluoric acid) are given in table 3. The observed and calculated heats of solution for the whole cements and the fractions are presented in table 4. No allowance was made for the presence of the calcium sulfate in making the calculations because of the uncertainty as to the form in which this compound occurred. It was also known that this compound has a very low heat of solution and could have only a negligible effect, except possibly in the case of the 0–7 fraction.

TABLE 3.—*Heats of solution of pure compounds*

Compound	Heat of solution
	cal/g
C_3S	631
C_2S	562
C_4AF	582
C_3A	797
MgO	875

[11] Ind. Eng. Chem., Analytical Edition, 1, 192(1929); also Portland Cement Association Fellowship Paper 21.

TABLE 4.—*Observed and calculated heats of solution of whole cements and size-fractions*

Cement	Value	Heats of solution (cal/g) and their differences for fractions					
		"Whole"	0–7 μ	7–22 μ	22–40 μ	40–55 μ	>55 μ
1	Observed	585	555	598	598	595	----
	Calculated	580	555	594	597	593	----
	Difference	+5	0	+4	+1	+2	----
2	Observed	587	547	595	604	606	601
	Calculated	577	549	586	596	599	597
	Difference	+10	−2	+9	+8	+7	+4
3	Observed	582	548	592	592	592	596
	Calculated	565	540	577	576	583	581
	Difference	+17	+8	+15	+16	+9	+15
4	Observed	583	551	593	598	601	596
	Calculated	567	553	582	591	591	592
	Difference	+16	−2	+11	+7	+10	+4
7	Observed	594	561	605	604	604	----
	Calculated	582	573	598	599	600	----
	Difference	+12	−12	+7	+5	+4	----

It is believed that most of the differences between the observed and calculated heats of solution shown in table 4 are sufficiently pronounced to indicate a real significance. Although there is a considerable variation between the differences for the various fractions of any one cement, when the different cements are compared it is seen that they show rather distinct individual trends. The agreement between the observed and calculated values for cement 1 would indicate that the true compound composition was very nearly given by the Bogue method of calculation. In the case of cement 2, where the differences are nearly the same for the whole cement and two of the fractions, a systematic deviation of the true composition from the calculated composition is indicated. Cement 3, which shows the greatest deviations between the observed and calculated values, would seem to be of a composition considerably different from that obtained by the calculation. In the same way, the larger observed than calculated values of cements 4 and 7, for all but the 0–7 fraction, suggest proportionate disagreements between the true and calculated compositions.

The results for the 0–7 fraction do not follow the trends for the other fractions and the whole cements. For three of the cements the calculated value is greater than the observed. The relatively low observed heat of solution as compared with that calculated for this fraction is probably the result of partial hydration, and since the extent of this hydration is unknown, much significance cannot be attached to the heat of solution data for this fraction as an indication of the chemical composition.

According to the theory of Lea and Parker,[12] the true compositions of cements 2, 3, 4, and 7 should be those given by the Bogue calculation unless glass had been formed in the clinker. These cements all have alumina-iron oxide ratios which fall within the range given by these investigators for independent crystallization, wherein the Bogue values should hold without correction, and in the case of cement 1 this ratio is just slightly over the 1.7 limiting maximum. According

[12] Building Research (England) Technical Paper 16.

to this theory, therefore, it would seem that the deviations of the true compound compositions from the calculated compositions, indicated for some of the cements by this heat of solution study, would have to be explained on the basis that glass had been formed during the cooling of the clinker.

2. MICROSCOPIC ANALYSES

In order to determine if these clinkers did contain glass and, if so, to what extent, microscopic examinations [13] were made of polished etched sections prepared from samples of clinker. Quantitative estimates were made of four constituents identified as C_3S, C_2S, C_4AF, and glass. The C_3A was not identified. The minor compounds were ignored and the clinkers considered to be made up exclusively of the four constituents. The results, reduced to the weight basis, are given in table 5. The calculated probable error of the values for the silicate compounds is approximately 1.5 and that of the other two constituents about 0.8.

TABLE 5.—*Quantitative microscopic analysis of cement clinkers*

Cement	Number of sections examined	Average compound composition			
		C_3S	C_2S	C_4AF	Glass
		Percent	*Percent*	*Percent*	*Percent*
1	7	34	54	10	2
2	7	33	46	15	6
3	7	29	48	18	5
4	3	29	47	23	1
7	11	36	39	22	3

In table 6 are given, for comparison, the compound compositions of the cements calculated by the Bogue method and the microscopic analyses reduced to the cement basis by allowing for the presence of the minor constituents of the cements. The results obtained by the microscopic method indicate that the C_3S content is higher and the C_2S content lower than the calculated values in all cases. For three of the five cements, the C_4AF content is considerably higher by the microscopic method than as calculated.

TABLE 6.—*Microscopic analysis of clinkers reduced to cement basis, and calculated compositions of cements*

Cement	Compound composition							
	C_3S		C_2S		C_4AF		Glass C_3A [1]	
	Microscopic	Calculated	Microscopic	Calculated	Microscopic	Calculated	Microscopic	Calculated
1	32	27	50	55	9.3	5.8	1.9	5.5
2	30	25	42	45	13.8	15.3	5.5	5.1
3	28	22	46	50	17.1	16.6	4.8	5.0
4	27	17	43	52	21.2	16.5	0.9	4.3
7	33	27	36	42	20.2	17.3	2.7	

[1] C_3A not noted petrographically.

[13] This work was carried out by Dr. H. Insley of this Bureau. A more detailed account of the work, together with data obtained on other clinkers, will be contained in a future report.

In order to obtain a further comparison between the two methods, the heats of solution were calculated from the microscopic data as reduced to the cement basis. The heat of solution of the glass was not known, but was assumed to be the same as that of the C_3A. Since the glass content was not large, this approximation should not introduce serious error. The values obtained, together with the observed heats of solution of the cements, are presented in table 7.

TABLE 7.—*Comparison of observed heats of solution with heats of solution calculated from microscopic analyses*

Cement	Heats of solution		
	Observed	Calculated	Difference
	cal/g	cal/g	cal/g
1	585	575	10
2	587	583	4
3	582	581	1
4	583	574	9
7	594	591	3

In four out of the five cases better agreement is found between the experimentally determined heats of solution and those calculated from the microscopic data than was obtained between the observed heats of solution and those calculated from the Bogue compositions. The results would indicate that the true compositions of the cements were more nearly equal to those determined microscopically than to those calculated by the Bogue method. However, too much weight should not be given to this comparison, since the heats of solution were not determined for the clinkers, and the cements for which they were determined may have been made from clinkers of slightly different composition.

In considering all of the data which would indicate the accuracy of the calculated compositions, it should be borne in mind that four of the five cements were of very similar oxide compositions. These data, therefore, do not necessarily indicate that the Bogue method of calculation is invalid for other cements. Rather, it confirms the opinions held by Bogue, Lerch, Lea and Parker, Bates, Woods, and other investigators that equilibrium crystallization may not in all clinkers be complete, but that an incomplete crystallization, with resultant changes in the compound composition, may have a significant effect upon the properties of the cement.

V. SUMMARY

Thirteen cements were separated into the five nominally sized fractions 0–7, 7–22, 22–40, 40–55, and $>$ 55 microns, and chemical analyses were made on the fractions and on the whole cements. The compound compositions were calculated according to the method of Bogue. Heats of hydration were determined for the fractions of five of the cements at the ages 3, 7, and 28 days. The compound compositions of the clinkers of these five cements were estimated from sections with a microscope.

On the basis of the calculated compound compositions the greatest percentages of tricalcium silicate appeared in the finer particles,

while the dicalcium silicate tended to be more concentrated in the coarser particles. The tricalcium aluminate and the tetracalcium alumino-ferrite were about equally distributed between the fine and coarse particles.

No satisfactory correlations were found between the calculated compositions and the heats of hydration.

The addition of about 7 percent of gypsum to the 7–22 micron fraction caused a greater reduction in the heat of hydration than would have been brought about by the addition of a like quantity of some inert material.

The observed heats of solution of five of the cements and those calculated from the Bogue compound compositions, using the heats of solution of the pure compounds, showed quite large differences for some of the cements, thus possibly indicating disagreement between the actual compound composition and that calculated by the Bogue method.

Quantitative estimates obtained with a microscope indicated that the tricalcium silicate was higher and the dicalcium silicate lower than the quantities indicated by the calculation from the oxide compositions. The tricalcium aluminate was not identified petrographically, although glass was found to be present.

The heats of solution of the cements calculated from the compound compositions as estimated microscopically were closer to the observed values than those calculated from the compound compositions computed by the method of Bogue.

Acknowledgment is made to P. H. Bates for originally suggesting this study and for suggestions offered during its progress. In determining the heats of hydration the authors were assisted by F. B. Hornibrook.

WASHINGTON, June 12, 1936.

U. S. DEPARTMENT OF COMMERCE NATIONAL BUREAU OF STANDARDS

RESEARCH PAPER RP911

Part of Journal of Research of the National Bureau of Standards, Volume 17, August 1936

THE SYSTEM K_2O-PbO-SiO_2

R. F. Geller and E. N. Bunting

ABSTRACT

The system was investigated by means of well known methods involving quenching, petrographic examination, and heating curves. Five ternary compounds were identified by optical properties and the chemical composition of four of these established. A number of melts were studied also as glasses to obtain data of interest to manufacturers of glasses, glazes, and enamels.

CONTENTS

	Page
I. Introduction	277
II. Preparatory work	278
1. Preparation and preservation of mixtures	278
2. Chemical analyses	279
III. Experimental procedure	279
1. Thermal studies	279
2. Microscopic examinations	280
3. Linear thermal-expansion determinations	280
IV. Results	280
1. Ternary compounds	282
2. Fields of stability	284
(a) Quintuple points	285
(b) Boundary curves	285
3. Binary systems within the diagram	286
4. Compositions as glasses	287
V. Discussion	287
VI. Summary	288

I. INTRODUCTION

The simple oxides involved in this system are constituents of many ceramic glazes, glasses, and enamels. Consequently, the study of the glass and crystalline phases is an essential step in obtaining information upon which to base studies of the more complex systems encountered in ceramic practice. There remains the possibility, also, that ceramic products of both higher quality and of relatively simple composition may result from a thorough investigation of the basic ternary systems. Of these basic systems, the ones involving PbO as one component offer a virgin field for study. This report, the first on phase equilibria of the oxides K_2O, PbO, and SiO_2, is also, so far as the authors are aware, the first on any ternary system in which PbO is a component. However, some work has been done on glasses composed primarily of potassium oxide, lead oxide, and silica. A recent article [1] offers some new data of limited significance

[1] R. Rieke and H. Mields. Ber. deut. keram. Ges. 16, 331 (1935).

(because of impurities in the melts) and contains references to earlier pertinent reports.

Although there are other oxides of lead, only the monoxide is stable above approximately 450° C.[2]

Phase equilibria have been established for the systems $K_2O.SiO_2$–SiO_2[3] and PbO–SiO_2.[4]

The present investigation was limited to studies of compositions in which the molecular ratio of K_2O to SiO_2 is unity, or less than unity, partly because of the extremely unstable nature of melts of higher K_2O:SiO_2 ratio, partly because of the physical impossibility (with available equipment) of obtaining or maintaining these melts free of CO_2 present as K_2CO_3, and partly because of excessive attack on the platinum crucibles and thermocouples. These facts were ascertained by preliminary tests, as was also the fact that K_2CO_3 and PbO were mutually insoluble in the solid and liquid states at atmospheric pressure, and that no binary compounds of K_2O and PbO were formed.

II. PREPARATORY WORK

1. PREPARATION AND PRESERVATION OF MIXTURES

The "end members" were sublimed litharge (PbO) containing 0.02 percent of total detected impurities; quartz crystal (SiO_2), which contained 0.02 percent of nonvolatile residue on evaporation with hydrofluoric and sulphuric acids; and potassium carbonate (K_2CO_3 as the source of K_2O) of which two 1-kg batches were used. The first batch, obtained in 1932, contained less than 0.037 percent of impurities and the second, obtained in 1935, contained less than 0.045 percent of impurities.[5]

All fusions were made in platinum, using electrically heated furnaces. The well mixed ingredients were allowed to react overnight at 700 to 800° C in order to drive off most of the CO_2 and were then taken to the minimum temperature required for fusion. By repeated grinding and remelting, instead of prolonged heating, the volatilized K_2O did not exceed 1 percent and was usually within 0.2 percent. No difficulty was experienced in obtaining melts within 0.2 percent of the desired PbO content, except with those melts approaching the potassium metasilicate in composition from which as much as 1 to 2 percent might be volatilized.

Seventy-four melts were analyzed chemically and portions used in various combinations to obtain additional preparations. A total of 165 melts was prepared (fig. 1).

Many compositions were so hygroscopic that they absorbed moisture except when kept over P_2O_5. Consequently, for convenience, all mixtures both as glass and in the crystallized form were kept over this material.

---

[2] J. W. Mellor, A Comprehensive Treatise on Inorganic and Theoretical Chemistry (Longmans, Green & Co., New York, N. Y.) vol. 7, p. 672. Mellor states that PbO apparently goes to Pb_3O_4 when heated which, on higher heating, again goes to PbO, the temperature range of maximum Pb_3O_4 being about 425 to 450° C.

[3] F. C. Kracek, N. L. Bowen, and G. W. Morey, J. Phys. Chem. 33 1857 (1929).

[4] R. F. Geller, A. S. Creamer, and E. N. Bunting, J. Research NBS. 12, 237 (1934) RP705.

[5] Analyses were made by the Chemistry Division of the National Bureau of Standards. The litharge was analyzed for Cu (0.002%), Bi (0.018%), Fe (less than 0.001%), and for Zn, Ni, and Mn which were not detected. The potassium carbonate was analyzed for insoluble matter, silica and ammonium hydroxide precipitate, Ca and Mg, sulphates and chlorates, N, As, Fe, H_2S metals, phosphate, and Na. The principal impurity (loss on ignition not being considered as such) was Na, which was reported as "<0.02 percent" in each batch. In the first batch other impurities were present in quantities of 0.003 percent or less; the second contained "<0.02 percent of insoluble matter, <0.015 percent of Ca and Mg, and <0.005 percent of phosphate."

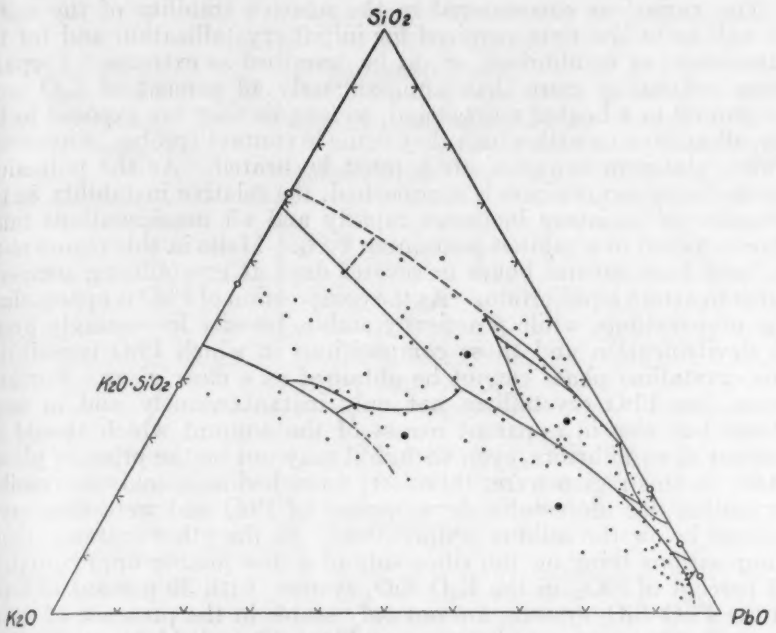

FIGURE 1.—*Points plotted in this figure show the compositions of the melts investigated.*

2. CHEMICAL ANALYSES

The PbO content was determined electrolytically and also as sulphate. The sample was treated with dilute nitric and hydrofluoric acids, dissolved in dilute nitric acid, the lead deposited on platinum gauze as PbO_2, dried at 110° C, and (by using the determined factor of 0.931) calculated to PbO. This deposit, after having been dissolved in dilute nitric acid and alcohol added to the solution, was converted with sulphuric acid to $PbSO_4$ and weighed as such. With few exceptions results by these two methods agreed within 0.1 percent. The electrolyte was evaporated to dryness, treated with hydrochloric acid, the KCl transferred to a small platinum dish and weighed. It was established by analysis that the SiO_2 content could be determined satisfactorily by difference.

All the chemical analyses of melts were made by A. S. Creamer. This involved modification of test methods as well as routine determinations.

III. EXPERIMENTAL PROCEDURE

1. THERMAL STUDIES

Thermal studies were made by the quenching method supplemented, in the case of a relatively small number of compositions, with heating curves obtained by the differential thermocouple method. Both of these methods are well established [6] and need no further description. Pt to Pt–Rh thermocouples were used for all temperature measurements and were calibrated by observing the inversion temperature of K_2SO_4 (583 ± 1° C), or the temperature of melting of K_2SO_4 (1069.1° C), or of KCl (770.3° C).

[6] F. C. Kracek, N. L. Bowen, G. W. Morey J. Phys. Chem. 33, 1857 (1929).

The variations encountered in the relative stability of the melts, as well as in the time required for initial crystallization and for the attainment of equilibrium, might be described as extreme. Preparations containing more than approximately 40 percent of K_2O must be ground in a heated mortar and, so long as they are exposed to the air, all apparatus with which they come in contact (probes, microscope slides, platinum capsules, etc.), must be heated. As the potassium metasilicate composition is approached, the relative instability in the presence of moisture increases rapidly and all manipulations must be conducted in a cabinet containing P_2O_5. Melts in this region must be held from several hours to several days at crystallizing temperatures to attain equilibrium. As the composition of PbO is approached, the preparations, while practically stable, become increasingly prone to devitrification and those compositions in which PbO constitutes one crystalline phase cannot be obtained as a clear glass. Furthermore, the PbO crystallizes not only instantaneously and in large plates but also in apparent excess of the amount which should be present at equilibrium, even though it may not be the primary phase. Melts in this region were, therefore, quenched as quickly as possible to inhibit this metastable development of PbO and were then crystallized below the solidus temperature. As the other extreme, those compositions lying on the silica side of a line joining approximately 70 percent of SiO_2, in the K_2O–SiO_2 system, with 30 percent of SiO_2, in the PbO–SiO_2 system, are not only stable in the presence of water vapor but require months to crystallize. One, held 6 months near the solidus temperature, had not crystallized sufficiently to establish the primary phase. Consequently the details of procedure were modified as the peculiarities of the preparations demanded.

2. MICROSCOPIC EXAMINATIONS

The petrographic microscope was used to determine the phases present in quenched samples. Identification of the crystalline phases was limited practically to the establishment of optical character and indices of refraction. Solid media, ranging in index of refraction from 1.74 to 2.58, were available from a previous investigation.[7] Samples in solid media were examined by means of white light passed through a no. 25 Wratten filter, which type of illumination had been used in determining the indices of the media.

3. LINEAR THERMAL-EXPANSION DETERMINATIONS

Determinations of linear thermal expansion were made by the interferometer method, using electrically heated furnaces, a temperature rise of from 2.0 to 2.5° C per minute, and chromel-alumel thermocouples for temperature measurements.

IV. RESULTS

The results of the equilibrium studies are summarized in table 1 and plotted in figures 2, 3, and 4.

[7] R. F. Geller, A. S. Creamer, and E. N. Bunting, J. Research NBS 13, 237 (1934) RP705.

TABLE 1.—*Invariant points*

[Compositions and melting temperatures]

Compounds	Composition, by weight						Temperature [a]
	$K_2O.SiO_2$	PbO	SiO_2	K_2O	PbO	SiO_2	
	%	%	%	%	%	%	°C
BINARY COMPOUNDS [b]							
$K_2O.SiO_2$	100.0			61.1		38.9	976
$K_2O.2SiO_2$	72.0		28.0	44.0		56.0	1,036
$K_2O.4SiO_2$	46.2		53.8	28.2		71.8	765
PbO.SiO_2		78.8	21.2		78.8	21.2	764
2PbO.SiO_2		88.1	11.9		88.1	11.9	743
4PbO.SiO_2 [c]		93.7	6.3		93.7	6.3	725
TERNARY COMPOUNDS							
$K_2O.2PbO.2SiO_2$	23.4	67.5	9.1	14.3	67.5	18.2	918
$K_2O.4PbO.8SiO_2$	10.5	60.8	28.7	6.4	60.8	32.8	779
$K_2O.PbO.4SiO_2$	27.7	40.0	32.3	16.9	40.0	43.1	757
$2K_2O.PbO.3SiO_2$ [c]	52.1	37.7	10.2	31.8	37.7	30.5	735 ± 5
BINARY EUTECTICS [b]							
$K_2O.SiO_2$–$K_2O.2SiO_2$	89.2		10.8	54.5		45.5	775
$K_2O.2SiO_2$–$K_2O.4SiO_2$	50.7		49.3	31.0		69.0	752
$K_2O.4SiO_2$–SiO_2	45.8		54.2	28.0		72.0	764
SiO_2–PbO.SiO_2		70.4	29.6		70.4	29.6	732
PbO.SiO_2–2PbO.SiO_2		84.6	15.4		84.6	15.4	716
2PbO.SiO_2–4PbO.SiO_2		91.8	8.2		91.8	8.2	714
PbO–4PbO.SiO_2 [c]		93.3	6.7		93.3	6.7	725
BINARY EUTECTICS WITHIN THE TERNARY SYSTEM							
$K_2O.2SiO_2$–$K_2O.2PbO.2SiO_2$	44.5	38.0	17.5	27.2	38.0	34.8	806
$K_2O.2SiO_2$–$K_2O.PbO.4SiO_2$	37.0	31.8	31.2	22.6	31.8	45.6	740
$K_2O.4SiO_2$–$K_2O.PbO.4SiO_2$	38.5	16.5	45.0	23.5	16.5	60.0	715 ± 5
SiO_2–$K_2O.PbO.4SiO_2$	20.6	30.4	49.0	12.6	30.4	57.0	718
$K_2O.4PbO.8SiO_2$–$K_2O.PbO$ $4SiO_2$	18.8	50.7	30.5	11.5	50.7	37.8	719
$K_2O.2PbO.2SiO_2$–$K_2O.PbO.4SiO_2$	26.2	49.3	24.5	16.0	49.3	34.7	716
$K_2O.2PbO.2SiO_2$–$K_2O.4PbO.8SiO_2$	15.1	63.2	21.7	9.2	63.2	27.6	683
PbO.SiO_2–$K_2O.4PbO.8SiO_2$	2.9	73.7	24.4	1.8	73.7	24.5	737
2PbO.SiO_2–$K_2O.2PbO.2SiO_2$	3.3	85.2	11.5	2.0	85.2	12.8	704
PbO–$K_2O.2PbO.2SiO_2$	3.3	95.5	1.2	2.0	95.5	2.5	840
QUINTUPLE POINTS							
Points in figure 3:							
1 [d]	75	15	10	46	15	39	
2	65	26	9	40	26	34	
3	61	27	12	37	27	36	725 (?)
4 [d]	43	16	41	26	16	58	705 ± 10
5	29	19	52	18	19	63	
6 [d e]	16	39	45	10	39	51	
7 [e]	16	43	41	10	43	47	700 ± 5
8 [e]	5.2	60.0	34.8	3.2	60.0	36.8	742
9 [d]	.8	71.0	28.2	.5	71.0	28.5	730
10	4.9	78.0	17.1	3.0	78.0	19.0	676
11 [d]	2.5	91.7	5.8	1.5	91.7	6.8	705
12 [d]	2.9	88.0	9.1	1.8	88.0	10.2	693
13 [d]	8.2	74.5	17.3	5.0	74.5	20.5	637
14 [d]	18.0	59.5	22.5	11.0	59.5	29.5	682
15 [d]	32.7	41.7	25.6	20.0	41.7	38.3	708

[a] Accurate within ± 3° C, unless otherwise stated. This does not apply to values taken from reports cited in footnote [b].

[b] Data for the system K_2O–SiO_2 are taken from F. C. Kracek, N. L. Bowen, and G. W. Morey, J. Phys. Chem. **33**, 1857 (1929). Data for the system PbO–SiO_2 are taken from R. F. Geller, A. S. Creamer, and E. N. Bunting, J. Research NBS **13**, 237 (1934) RP705.

[c] Melts incongruently.

[d] Eutectic.

[e] The composition of the primary phase within the area of which these points form the apices has not been established.

The extremely unstable nature of compositions along the join $PbO–K_2O.SiO_2$, and the rapidity with which they attack thermocouples and platinum containers, make the values obtained of little significance. Heating curves for 4 compositions, varying in PbO from 74 to 92 percent, show a break between 740 and 750° C and also at about 800° C. The ternary compound $K_2O.2PbO.2SiO_2$ is the primary phase in the composition containing 59 percent of PbO, which shows that the system is not binary, and the liquidus (by the quench method) is approximately 860° C. In the composition containing 42 percent of PbO the same ternary compound is the primary

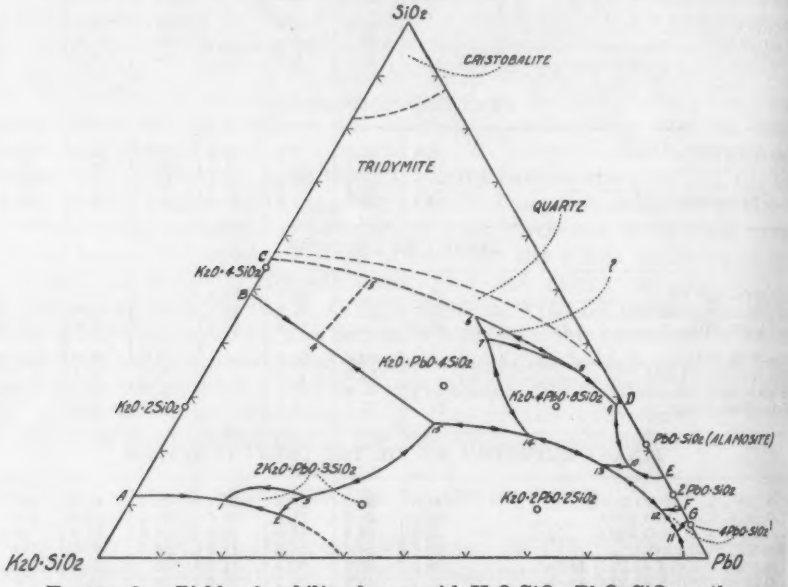

FIGURE 2.—*Fields of stability drawn with* $K_2O.SiO_2$–PbO–SiO_2 *as the components.*

phase, the liquidus (by the quench method) is about 835° C, and heating curves have a well defined break at 780° C (which may be the melting temperature at the intersection with the $K_2O.SiO_2$–$K_2O.2PbO.2SiO_2$ boundary curve.) When the composition containing 42 percent of PbO is completely crystallized, or when held for a short time (30 min) at 810° C, the crystalline phase resembling the 1:2:2 compound in optical character, cleavage, and general appearance, has indices of refraction of ϵ 1.62, ω 1.72. However, when held for 48 hr at 810° C this crystalline phase, the only one present in addition to glass and constituting 5 to 10 percent of the total, has the correct indices of refraction for $K_2O.2PbO.2SiO_2$. The change in indices indicates solid solution, possibly with $K_2O.SiO_2$.

1. TERNARY COMPOUNDS

The chemical composition, melting temperature, and optical properties of four ternary compounds were established, and the existence of a fifth is indicated by optical properties.

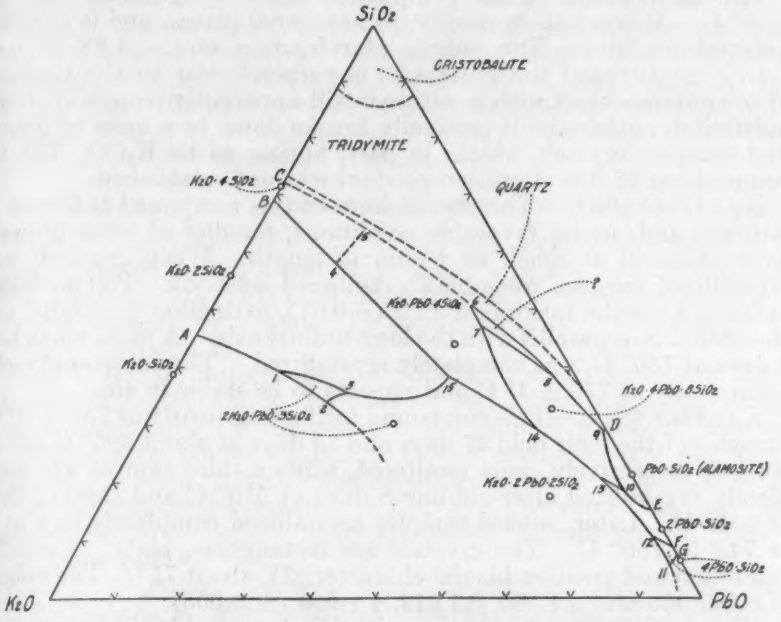

FIGURE 3.—*Fields of stability for the system* K_2O–PbO–SiO_2.

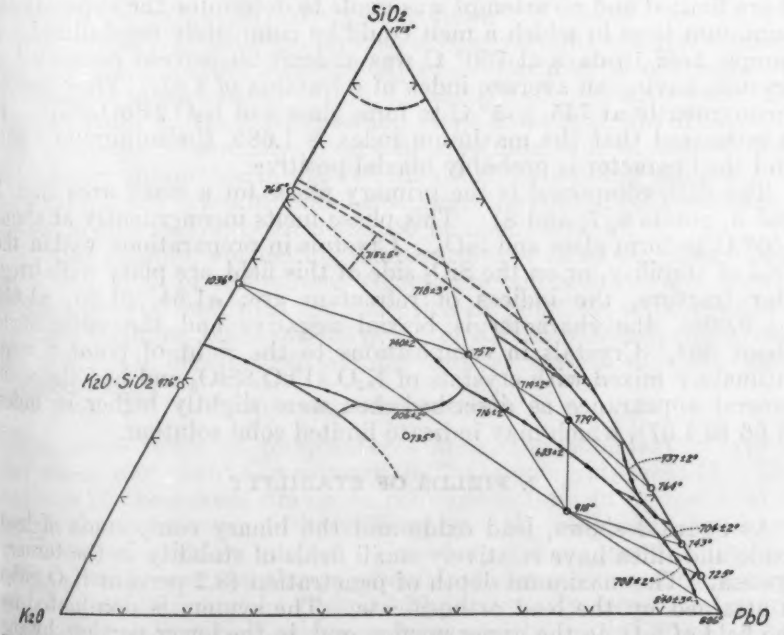

FIGURE 4.—*Tie-lines within the ternary system along which phase equilibria were investigated.*

$K_2O.2PbO.2SiO_2$.—This compound melts congruently at 918 ± 3° C. It crystallizes readily, as hexagonal plates, and is optically uniaxial negative. The indices of refraction are: ω 1.93 ± 0.01, ϵ 1.72 ± 0.01 and the optic axis is perpendicular to the cleavage. When not in contact with moisture it will apparently remain unaltered indefinitely, otherwise it gradually breaks down to a mass of minute and complex crystals which, in part, appear to be K_2CO_3, but the composition of this alteration product was not established.

$K_2O.4PbO.8SiO_2$.—The crystal form of this compound is fibrous or lath-like and, under favorable conditions, bundles of these growths were obtained as much as 1 mm in length. When crushed, well crystallized samples resemble short-fibered asbestos. The minimum index is 1.69, the maximum 1.79 (±0.01), extinction is parallel and the optic axis is parallel with the longitudinal axis. A melt, when held 2 days at 750° C, was completely crystallized. The compound melts congruently at 779 ± 3° C and appears to be stable in air.

$K_2O.PbO.4SiO_2$.—This compound melts congruently at 757 ± 3° C. Samples of the melt held 27 days and 33 days at about 690° C and at 600° C, respectively, were unaltered, while a third sample was completely crystallized after holding 8 days at 510° C and then 10 days at 605° C. Later, seeded samples crystallized completely in 3 days at 745 to 750° C. The crystals are rectangular, platy, of parallel extinction and positive biaxial character; 2V about 75°. The indices of refraction are: α 1.590, β 1.612, γ 1.650 (± 0.005).

$2K_2O.PbO.3SiO_2$.—This composition is so unstable that more than momentary exposure to ordinary air, except in heated containers, will destroy it for purposes of optical examination. Data concerning it are limited and no attempt was made to determine the approximate minimum time in which a melt could be completely crystallized. A sample held 10 days at 700° C was at least 90 percent converted to crystals having an average index of refraction of 1.67. They melted incongruently at 735 ± 5° C to form glass and $K_2O.2PbO.2SiO_2$. It is estimated that the maximum index is 1.685, the minimum 1.665, and the character is probably biaxial positive.

The fifth compound is the primary phase for a small area (figs. 2 and 3, points 6, 7, and 8). This phase melts incongruently at about 750° C to form glass and SiO_2. Crystals in preparations within the field of stability, or on the SiO_2 side of this field, are platy with irregular fracture, the indices of refraction are: α1.64, β1.65, γ1.655 (± 0.005), the character is biaxial negative and the optic angle about 80°. Crystals in compositions to the right of point 8 were intimately mixed with crystals of $K_2O.4PbO.8SiO_2$ and had the same general appearance as described, but were slightly higher in index (1.66 to 1.67), which may indicate limited solid solution.

2. FIELDS OF STABILITY

As figure 3 shows, lead oxide and the binary compounds of lead oxide and silica have relatively small fields of stability in the ternary system. The maximum depth of penetration (8.2 percent $K_2O.SiO_2$) is attained by the lead orthosilicate. The system is dominated by the field of SiO_2 in the upper portion and, in the lower portion, by the fields of $K_2O.2SiO_2$ and $K_2O.2PbO.2SiO_2$. In the former field it is possible that an area adjoining the composition of the potassium

disilicate should be assigned to the "$K_2O.2SiO_2$ mix crystals" noted by Kracek, Bowen, and Morey.[8] A thorough investigation of this possibility was not made, but compositions on the tie-lines joining the disilicate with $K_2O.PbO.4SiO_2$ and with $K_2O.2PbO.2SiO_2$, and containing as little as 5 percent of PbO, apparently contained only crystals of $K_2O.2SiO_2$ and glass when held at temperatures which were expected to develop the mixed crystals.

(a) QUINTUPLE POINTS

Fourteen quintuple invariant points were located and another is indicated (point 5, figs. 2 and 3); of these, nine are ternary eutectics (table 1 and fig. 2). It is interesting to note the small range of temperatures covered by the melting points, from 637° C for point 13 to 742° C for point 8.

Point 1, ternary eutectic for the potassium metasilicate and disilicate and $2K_2O.PbO.3SiO_2$, and points 2 and 3 form the apices of the area in which the 2:1:3 compound is the primary phase. The compositions of these points, as given in table 1, are believed to be correct within ±1 percent, but the melting-temperature data were unsatisfactory because of the presence of K_2CO_3. The values indicate that the composition at point 1 melts above 700° C, and that at point 3 melts below 735° C.

Point 4, ternary eutectic for $K_2O.2SiO_2$, $K_2O.4SiO_2$, and $K_2O.PbO.4SiO_2$, is not definitely located because of insufficient data to locate either point 5 or the connecting boundary. In fact, no crystallization of $K_2O.4SiO_2$ as the primary phase was obtained in any composition. Kracek, Bowen, and Morey obtained this compound by hydrothermal crystallization.[9]

Points 6 and 7, although in an area of compositions which crystallize very slowly and usually incompletely even after months of treatment, are believed to be located within 0.5 percent of their true positions. Data for point 8, which composition melts at 742° C, are of satisfactory precision, practically complete crystallization of neighboring melts being obtainable in about 3 months. A melting temperature for point 6 is not given in table 1 but, from the contour of the liquidus surface in this region, is estimated to be about 690° C.

As table 1 shows, the melting temperatures of all of the other points are within 3° C of the correct values, the compositions are correct to ±0.1 percent and, with the exception of point 10, all are ternary eutectics. No. 10, the invariant point for $K_2O.4PbO.8SiO_2$, $PbO.SiO_2$, and $2PbO.SiO_2$, lies just outside the ternary system of these three compositions.

(b) BOUNDARY CURVES

The entire range of temperatures along the boundary curves is only about 200° (840° C maximum, 637° C minimum; table 1). The locations of the curves drawn as continuous lines in figures 1 to 4, inclusive, are believed to be sufficiently well established by determinations of primary phases. However, the isotherms (liquidus temperatures) were not always established, for reasons already elaborated upon, but may be deduced approximately from the general trends of the adjoining liquidus surfaces and by means of van Alkemade's theorem.[10]

[8] F. C. Kracek, N. L. Bowen, and G. W. Morey. J. Phys. Chem. **33**, 1857 (1929).
[9] See footnote 8.
[10] Bancroft, The Phase Rule, p. 149. Published by J. Phys. Chem. (1897).

For example, the data indicate that the melting temperature at point 1 is above 700° C, and it must also be below 735° C. The melting temperature at point 2 must be above that of point 1, may be above or below that of point 3, but probably does not differ much from the latter, and the very limited data obtainable indicate 720° C as the melting temperature. The curves from point 3 to point 1, and from point 2 to point 1, slope downward; but between points 2 and 3 there must be a maximum at the intersection of the curve with the tie-line, extended, from $K_2O.2PbO.2SiO_2$ to $2K_2O.PbO.3SiO_2$.

The curves from points 6 to 7 to 8, on the other hand, exemplify how their determined slopes may assist in establishing the identity of the phase which is primary within the area they circumscribe. In this case there is a maximum (750° C) along curve 6–8, and a maximum (743° C) along curve 7–8; both maxima are on or very near the intersection of these curves with the tie-line from the 1:4:8 compound to SiO_2. The composition 5 percent of K_2O, 47.3 percent of PbO, and 47.7 percent of SiO_2 (molecular ratio 1:4:15 or a base-acid ratio of 1:3) lies on this tie-line, slightly above the 6–8 curve. The suggestion is offered that this is the ternary compound described in section IV–2. A melt of this composition, held 2½ months at 700° C, was one-third crystals having the properties of the suggested 1:4:15 compound and the balance was glass. A specimen then held at 740° C for 4 hours was unchanged, but when held at 750° C for 4½ hours, contained less than 1 percent of these crystals in glass. A specimen held at 760° C for 2 hours before quenching contained only glass. Tridymite was identified in specimens held overnight above 940° C and below the liquidus (1,025 ± 10° C).

3. BINARY SYSTEMS WITHIN THE DIAGRAM

Phase relations in eight binary systems within the ternary system were established (fig. 4). Five of the eight involve $K_2O.2PbO.2SiO_2$ as one component, the other three connect the compounds $K_2O.2SiO_2$ with $K_2O.PbO.4SiO_2$; $K_2O.PbO.4SiO_2$ with $K_2O.4PbO.8SiO_2$; and $K_2O.4PbO.8SiO_2$ with $PbO.SiO_2$. They are all simple systems.

No compositions on the $K_2O.4SiO_2$ side of the $K_2O.4SiO_2$–$K_2O.PbO.4SiO_2$ eutectic were even partially crystallized after holding 3 months at 650 to 680° C. Location of a eutectic was approximated by extrapolation of the $K_2O.PbO.4SiO_2$ liquidus. The same method was used in approximating the composition of a SiO_2–$K_2O.PbO.4SiO_2$ eutectic. A composition on the SiO_2 side of the estimated eutectic showed no crystallization after holding 6 months at 700° C, while a composition on the other side was almost completely crystallized after 2 months at 600° C. It follows, therefore, that the existence of true binary systems between these compounds, although probable, was not established.

Binary systems do not exist between $K_2O.4PbO.8SiO_2$ and either SiO_2 or $2PbO.SiO_2$, or between $4PbO.SiO_2$ and $K_2O.2PbO.2SiO_2$. As figure 4 shows, each tie-line crosses a field in which a third compound is the primary phase. The break in the $4PbO.SiO_2$ liquidus, at the intersection of the PbO–$4PbO.SiO_2$ boundary curve with the $4PbO.SiO_2$–$K_2O.2PbO.2SiO_2$ tie line, occurs at a temperature of about 721° C and the composition must be very close to 0.5 percent of K_2O; 92.8 percent of PbO; and 6.7 percent of SiO_2.

4. COMPOSITIONS AS GLASSES

The values for index of refraction and also, in nine cases, for the linear thermal expansion and for the softening temperature (by the interferometer method) are summarized in figure 5. It is evident that a relatively small portion of the compositions produce glasses resistant to weathering. Although immiscibility is indicated in the lower portion of the diagram, the immiscibility is probably due wholly or in part to the presence of K_2CO_3. The limiting compositions were not determined, but it is known that the area does not cross the PbO–$K_2O.SiO_2$ tie-line. The liquids separate into two sharply defined layers which crystallize very rapidly upon solidification. Each layer of two melts was examined petrographically and also analyzed chemically. It was evident that the top layer in each case was composed primarily of K_2CO_3, the bottom layer primarily of PbO.

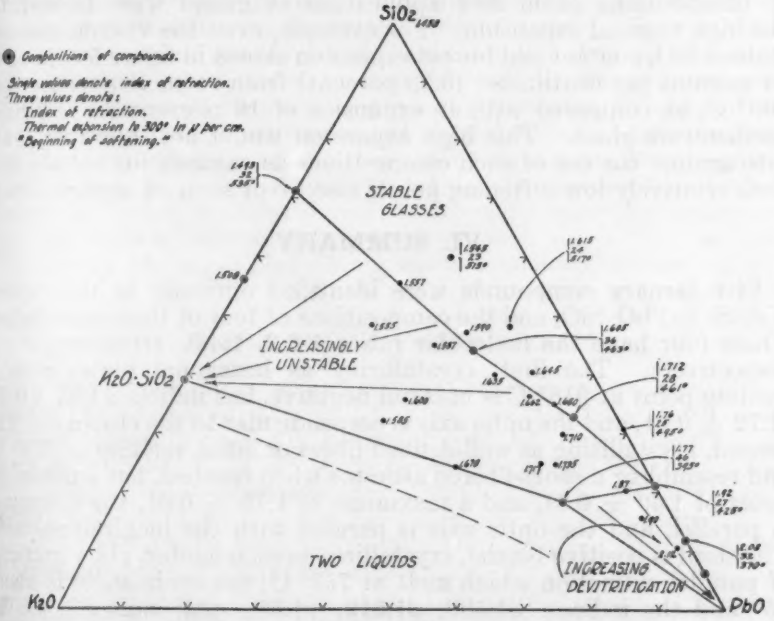

FIGURE 5.—*Summary of data obtained on melts as glasses.*

V. DISCUSSION

Since this report is the first dealing with a ternary system involving lead oxide, no comparisons can be made with systems of silica, lead oxide, and oxides of other elements, such as sodium and lithium, which systems might show trends similar to the one investigated.[11]

[11] The following tests were made to obtain an indication of the probable behavior of a similar system substituting Na_2O for K_2O:

A melt of molecular composition $Na_2O.PbO.4SiO_2$ held at 500° C for 6 days contained about 10 percent of crystals in a glass of index of refraction 1.65. The crystals appeared as prisms radiating from a common center, or as rectangular plates, and of very low birefringence and average index 1.50.

A melt of molecular composition $Na_2O.4PbO.8SiO_2$ held at 500° C for 8 days contained less than 2 percent of glass (index 1.69) and two crystalline phases in about equal amounts. Phase A was prismatic, almost fibrous, with parallel extinction, very low birefringence, and average index 1.71. Phase B was platy and the indices of refraction ranged from 1.72 to 1.75.

A melt of molecular composition $Na_2O.2PbO.2SiO_2$ held at 500° C for 8 days had attacked the platinum capsule and was dark brown in color. Minute crystals of irregular fracture and indices ranging from 1.79 to 1.92 were identified.

The stable compounds crystallize from glasses which are so viscous, and crystal growth is relatively so slow, that their development as "stones" in glass under manufacturing conditions is very unlikely. The system itself will be important to those investigators studying similar, as well as more complex, systems encountered in glaze and glass technology. The difficulties to be encountered, should the need for completion of the present system arise, are indicated, and it is probable that similar difficulties would confront the student of, for example, the system Na_2O–PbO–SiO_2.

A narrow band of compositions along the silica side of the boundary separating the fields of stable and unstable glasses (fig. 5) have potential value as glasses. Those higher in SiO_2 would be so viscous that fusing them to a homogeneous glass, without excessive loss of K_2O and PbO by volatilization, would be impracticable; or, if this were accomplished, they would still be unworkable. The same band of compositions could find application as glazes were it not for the high thermal expansion. For example, even the viscous glass of highest SiO_2 content and lowest expansion shown in figure 5 expanded 23 microns per centimeter (0.23 percent) from room temperature to 300° C, as compared with an expansion of 16 microns for a typical earthenware glaze. This high expansion would not, however, militate against the use of such compositions as enamels for metals, and their relatively low softening points also favor such an application.

VI. SUMMARY

Five ternary compounds were identified optically in the system $K_2O.SiO_2$–PbO–SiO_2 and the compositions of four of these established. These four have the molecular ratios 1:2:2, 1:4:8, 1:1:4, and 2:1:3, respectively. The first, crystallizing as hexagonal plates with a melting point at 918° C is uniaxial negative, has indices ω1.93 ± 0.01, ϵ1.72 ± 0.01, and the optic axis is perpendicular to the cleavage. The second, crystallizing as well-defined fibers or laths, melting at 779° C, and resembling a short-fibered asbestos when crushed, has a minimum index of 1.69 ± 0.01, and a maximum of 1.79 ± 0.01, the extinction is parallel, and the optic axis is parallel with the longitudinal axis. The third is positive biaxial, crystallizes as rectangular, platy granules of parallel extinction which melt at 757° C; the optic angle is about 75° and the indices: α1.590, β1.612, γ1.65. (All indices ± 0.005.) The fourth is platy with an average index of approximately 1.67, melts incongruently at 735° C, and is very unstable. The crystalline phase of undetermined composition apparently melts incongruently at about 750° C to form glass and SiO_2. The crystals are platy, the indices α1.64, β1.65, γ1.655 (± 0.005), 2V about 80°, character biaxial negative.

Glasses in that portion of the ternary diagram lying on the silica side of the tie-lines connecting the compound compositions $K_2O.4SiO_2$, $K_2O.PbO.4SiO_2$, $K_2O.4PbO.8SiO_2$, and $PbO.SiO_2$ are stable in air. Compositions in this area and near these tie-lines fuse to a homogeneous glass with sufficient ease to be of possible commercial application. However, the temperatures required to produce a glass, and the viscosity of the product, rise very rapidly with increase in silica. It is believed that the band or area of commercially usable composi-

tions would be narrow. Compositions on the K_2O side of the tie-lines mentioned are either unstable in air or, in that area bounded by the tie-lines from $PbO.SiO_2$ and from PbO to $K_2O.2PbO.2SiO_2$, prone to devitrification. Also, many compositions below a line connecting PbO with the $K_2O.SiO_2$ composition separate into two immiscible liquids.

The usefulness or lack of usefulness of a composition as a glass will generally determine also its potential value as a glaze for porcelain or earthenware. In addition, a glaze must have the proper thermal dilatation to "fit" the ware upon which it forms a coating. Unfortunately, all the glasses examined, and which otherwise held promise of usefulness as glazes, on heating or cooling undergo volume changes so great as to preclude their use on clay ware as now manufactured, with the exception of certain "high silica" and "high talc" wall tile.

WASHINGTON, JUNE 3, 1936.

U. S. DEPARTMENT OF COMMERCE NATIONAL BUREAU OF STANDARDS

RESEARCH PAPER RP912

Part of Journal of Research of the National Bureau of Standards, Volume 17, August 1936

LOAD DISTRIBUTION AND STRENGTH OF ELEVATOR CABLE EQUALIZERS

By Ambrose H. Stang and Leroy R. Sweetman

ABSTRACT

Tests to determine the equalizing ability and strength of four makes of elevator cable equalizers were made under conditions similar to but more severe than those encountered during ordinary use.

The cables were represented by jointed steel rods, hinged to allow freedom of motion in all directions. The middle rod of each assembly was equipped with 2-inch Tuckerman optical strain gages and calibrated as a dynamometer.

The distribution of load among the six shackles was determined for various amounts of movement of the shackles singly and in pairs. The limits of travel of the shackles were determined in each case.

CONTENTS

	Page
I. Introduction	291
II. Elevator cable equalizers	292
III. Method of test	293
1. Testing machine	293
2. Load distribution	293
(a) Loading fixtures	293
(b) Designation of shackles	293
(c) Load-measuring apparatus	293
(d) Testing procedure	294
(e) Program	294
(f) Accuracy	295
3. Strength	295
IV. Results of the tests, with discussion	295
1. Load distribution	295
2. Effective travel	320
3. Strength	320
V. Summary	320

I. INTRODUCTION

Most elevator cars are supported by more than one wire rope and the safety of passengers depends to a large extent on the strength of the ropes. These supporting ropes are designed to carry a car with a liberal margin of safety, provided the load is equally distributed among the ropes. Although the ropes are of equal length when installed and the load on each rope is adjusted by means of threaded shackles to be as nearly uniform as possible when new cables are put in service, these loads do not remain uniform except in a very few instances. All wire ropes stretch appreciably under load, and, in addition, there is a gradual lengthening of the ropes under load,

which may continue for months or even years. For ropes of the usual construction, this stretch amounts to about 1 percent of the length of the rope under loadings usually used in elevator practice. However, the stretch of two identical lengths of wire rope under the same loading will seldom be the same. This may be due to variations in the wires of which the strands are made, to variations in the tightness of the lay, to variations in the core, or to other causes. In the case of elevator ropes, the distance between the crosshead of the car and the cable anchorage on the counterweight remains substantially the same, with the result that the tendency of the ropes to stretch different amounts results in unequal forces on the ropes. The rope carrying the greatest load will deteriorate more rapidly than the others and also cause greater wear on its groove in the sheave. Wear of a groove decreases the effective diameter, resulting in slipping of the rope in that groove. This causes increased wear of both the rope and the groove, particularly of the sheaves which have V grooves, and this rope will need to be replaced when the other ropes may still have sufficient strength to carry their share of the total load. This unequal distribution of load among the wire ropes is obviously uneconomical and may become dangerous.

Devices designated as elevator cable equalizers have been designed to compensate for the unequal changes in length of the ropes and to equalize the loads on the ropes. The tests described in this paper were made to determine to what degree the loads are equalized and to determine the strength of the equalizers.

Two types of equalizers are manufactured in this country. For the first type, the equalizer is attached to the car only and tends to equalize the loads in the portion of the ropes between the car and the driving sheave. For the second type, the equalizer consists of two separate portions, one attached to the car and the other to the counterweight.

The tests reported in this paper deal only with elevator cable equalizers of the first type. For equalizers of the second type the distribution of the load on the cables under service conditions could not be determined satisfactorily by these methods; therefore equalizers of this type were not included in the program. The results give the load distribution for that portion of the cables between the car and the driving sheave. The load distribution for the portion of the cables between the driving sheave and the counterweight was not determined and cannot be estimated from the results of these tests.

II. ELEVATOR CABLE EQUALIZERS

Tests of four elevator cable equalizers were made. For convenience in this report they are designated as equalizers A, B, C, and D. Equalizer A was a multiple-lever type; equalizer B, a rack and pinion type; equalizer C, a multiple-lever type with roller bearings; and equalizer D a type having fixed sheaves and floating sheaves supported by a wire rope. Photographs of these equalizers are shown in figures 1, 2, 3, and 4, respectively.

Each equalizer was designed for six wire ropes, $\frac{5}{8}$-in. diameter, traction steel.

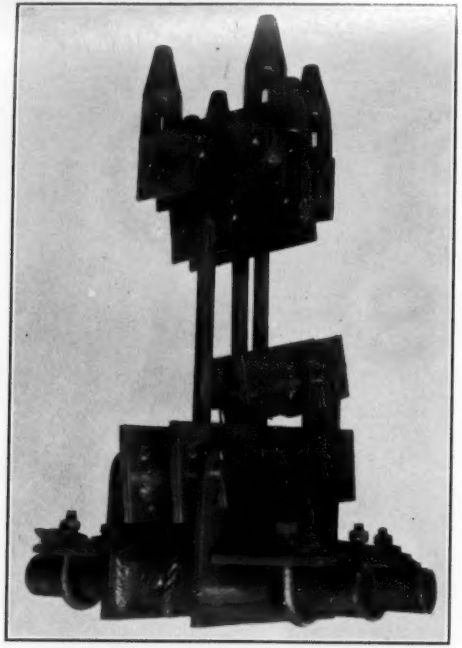

FIGURE 1.—*Elevator cable equalizer* A.

The failure of this equalizer during the strength test was due to the bending of the link indicated at F in figure 7.

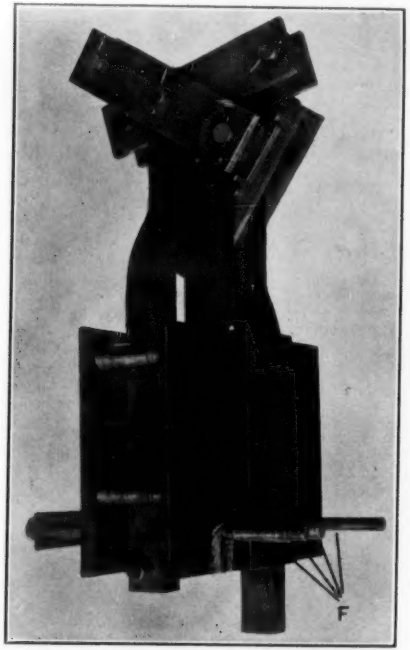

FIGURE 2.—*Elevator cable equalizer* B.

The failure of this equalizer during the strength test was due to the bending of the pins and bolts at F.

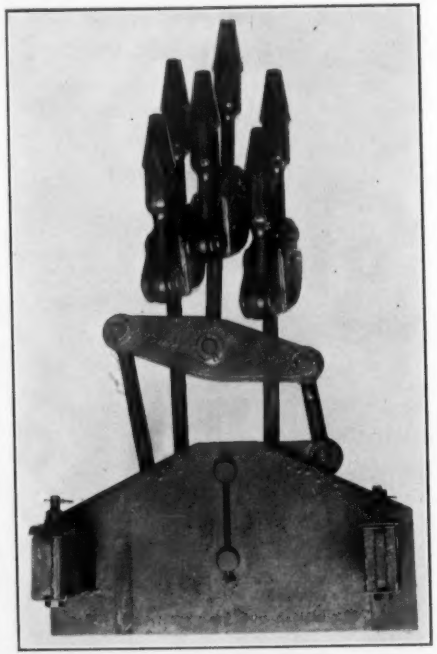

FIGURE 3.—*Elevator cable equalizer* C.

The failure of this equalizer during the strength test was due to tensile failure in the link indicated at F in figure 23.

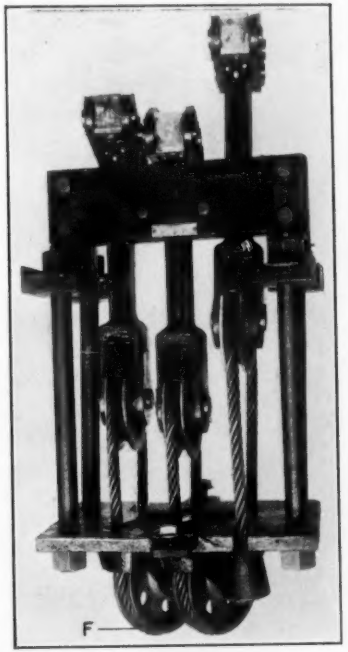

FIGURE 4.—*Elevator cable equalizer* D.

The failure of this equalizer during the strength test was due to the failure of the wire rope at F.

The distance between shackle centers on the singletrees was as follows:

Equalizer A	7 inches.
Equalizer B	9 inches.
Equalizer C	6 inches.
Equalizer D	6 inches.

III. METHOD OF TEST

1. TESTING MACHINE

The tests of the equalizers were made in a vertical, screw power, beam-and-poise type of testing machine having a capacity of 600,000 lb. using a poise which corresponded to a capacity of 300,000 lb.

2. LOAD DISTRIBUTION

(a) LOADING FIXTURES

The arrangement for determining the load distribution is shown in figure 5.

When installed on a car the equalizer is attached to the top of the car frame and the cables attached to the shackles extend upward to the sheave.

For convenience in making these tests this arrangement was reversed. Equalizer E was supported by two I-beams I, representing the car frame, which, in turn, were bolted to the fixed platen of the testing machine. Tension rod R was attached to each shackle. These rods passed down through a steel plate attached to the movable platen of the testing machine. The load was transmitted from each rod to this plate by a nut on the threaded lower end of the rod. Self-aligning ball thrust bearings were placed between the plate and the nuts of four of the rods.

(b) DESIGNATION OF SHACKLES

For convenience in this report, numbers were used as designations for the shackles and rods as shown diagrammatically in figures 7 to 30. The pairs of shackles 1 and 4, 2, and 5, and 3 and 6 were connected by a singletree.

(c) LOAD-MEASURING APPARATUS

The load on each shackle was measured with a special tension dynamometer. These dynamometers were steel drill rods, 0.5 in. in diameter and about 30 in. long, to which were attached at midlength two Tuckerman optical strain gages having a 2-in. gage length and placed diametrically opposite on the rod. Dynamometer rods R and gages G are shown in figure 5 below link-joints L, which are near the lower ends of shackles S. The dynamometers had been calibrated in a testing machine previous to use in this test. It was found that the strain in the drill rods, which produced a change of 1.0 division in the reading of the gages, corresponded to a load of 117 lb. Readings were estimated to 0.1 division or 11.7 lb.

(d) TESTING PROCEDURE

The procedure used in making the load-distribution determinations was as follows:

With no load on the equalizer, all of the shackle fulcrum pins were brought to the same horizontal plane by rotating the nuts below the plate. A load was then applied to the equalizer, gage readings were taken, and the load reduced to zero. Gage readings were again taken. The load on each shackle was calculated from the difference between the gage readings on the rod attached to the shackle.

These loads were obviously for a movement of zero inches of the shackles.

The load was again applied, and the nut at the bottom of one of the rods was rotated until this shackle had been lowered a predetermined distance, 0.2 in. The load on the equalizer had meantime been kept constant. Gage readings were taken, the load removed, and gage readings again taken. The load on each shackle was again calculated from the difference between the gage readings on the rod attached to the shackle. These loads were for a 0.2 in. movement of the shackle. This procedure was repeated with the same load for several positions of the shackle until the limit of travel of the shackle was reached. Shackle movements were made while the equalizer was under load.

When tested in this way there was little vibration of the shackles and the bearings in the equalizer. The differences in the loads on the shackles was therefore in all probability greater than would exist in an elevator installation where the relatively long ropes are attached to the shackles and the movement of the car causes considerable vibration.[1] It is believed, therefore, that the differences found in these tests were the maximum which would exist under the given conditions, and that under service conditions the differences might be somewhat less than these values. The test conditions were, however, the same for all the equalizers.

(e) PROGRAM

Load-distribution determinations were made by moving shackle 2, shackle 3, shackles 2 and 5 together, and shackles 3 and 6 together. It was not considered necessary to make tests to determine the load distribution for movements of shackle 1 or of shackles 1 and 4 together, since for each of the equalizers, shackles 1 and 4 were symmetrical with regard to their connections to the other parts of the equalizer, with shackles 3 and 6. The load distributions may be expected to be the same for both pairs of shackles.

For the tests to determine the load distribution when shackles 2 and 5 were moved together, the procedure was to move shackle 2 from, for example, the 1-inch position to the 2-inch position and then induce the same movement in shackle 5. Similarly, when shackles 3 and 6 were moved together, the movement of shackle 3 was completed and then that of shackle 6.

The four sets of load-distribution determinations were made with the following loads on the equalizers: for equalizer A, at 6,000, 12,000, and 18,000 lb; these loads corresponded to an average load

[1] G. P. Boomsliter, Acceleration Stresses in Hoisting Ropes. Research Bulletin 2, Engineering Experiment Station, University of West Virginia, Morgantown, W. Va.

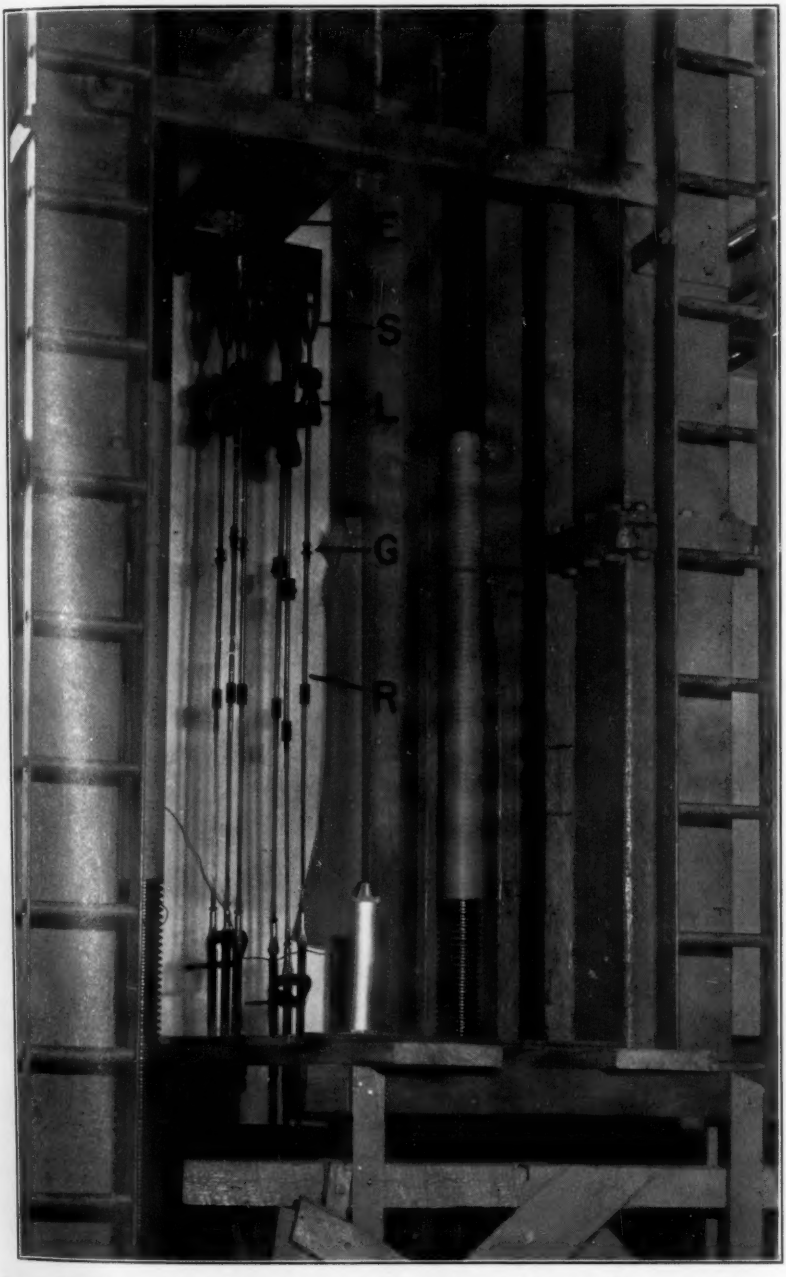

FIGURE 5.—*Elevator cable equalizer* A *in the testing machine for the load-distribution test.*

Note the Tuckerman optical strain gages on the dynamometer rods and the autocollimator on the platform.

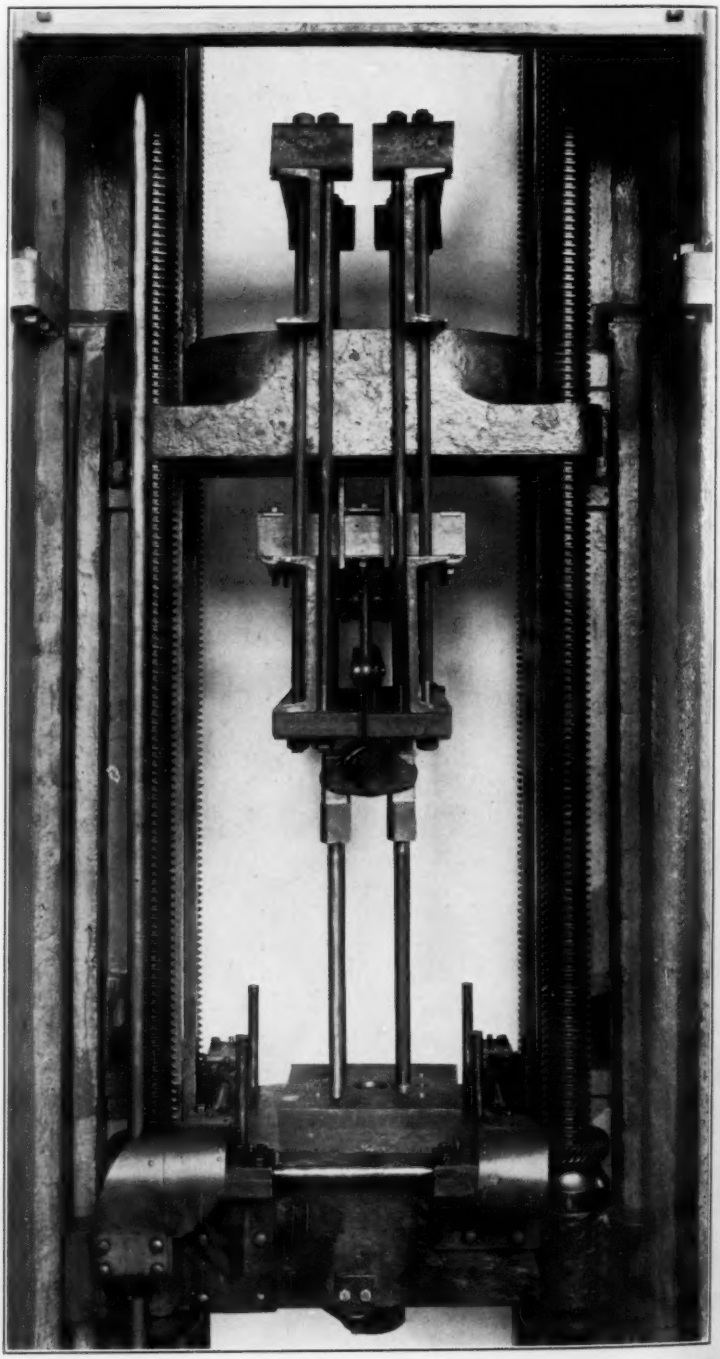

FIGURE 6.—*Elevator cable equalizer* C *in the testing machine for the strength test.*

on each shackle of 1,000, 2,000, or 3,000 lb. For equalizers B, C, and D, at 12,000 lb corresponding to an average load on each shackle of 2,000 lb.

(f) ACCURACY

When the total load on the equalizer was 6,000 lb, the sum of the loads on the six shackles as determined by the gage readings of the dynamometer rods did not differ by as much as 3 percent from the load indicated by the testing machine. When the total load on the equalizer was either 12,000 or 18,000 lb, the sum of the loads on the shackles did not differ by more than 1 percent from the load indicated by the testing machine.

3. STRENGTH

After the tests to determine the ability of the device to equalize the loads on the different shackles were completed, the strength of the equalizers was determined. For this test the shackles were removed and fixtures, as shown in figure 6, were attached to the shackle fulcrum pins and to the movable platen of the testing machine.

IV. RESULTS OF THE TESTS, WITH DISCUSSION

1. LOAD DISTRIBUTION

The results of the load-distribution tests are given in figures 7 to 30, inclusive. A diagrammatic sketch of the mechanism of the equalizers is given on each figure. The shackle or shackles moved are indicated by arrowheads.

The different loads of 6,000, 12,000, and 18,000 lb used for the tests of equalizer A did not appear to change the character of the load-distribution curves for this equalizer. For this reason, tests of the other equalizers were made only for a 12,000-lb load.

Although there are some exceptions to each of the following statements, the results of the tests, as indicated by the load-distribution curves, may be summarized as follows:

The shackle which was moved while under load took more than its share of the load, beginning with a very small movement. In general, the load on the shackle increased slowly with increase in movement and then more rapidly as the limit of travel of the shackle was approached.

If the movement was confined to a single shackle, the other shackle on the same singletree at first took more than its share of the load but generally not as much as the shackle which was moved. As the limit of travel of the moved shackle was approached, the other shackle of the pair took less and less load, apparently transferring its share of the load to the moved shackle. The load on the other four shackles was approximately constant.

If two of the shackles were moved, the shackle moved last sustained a greater load than the shackle first moved and both took more than the average load.

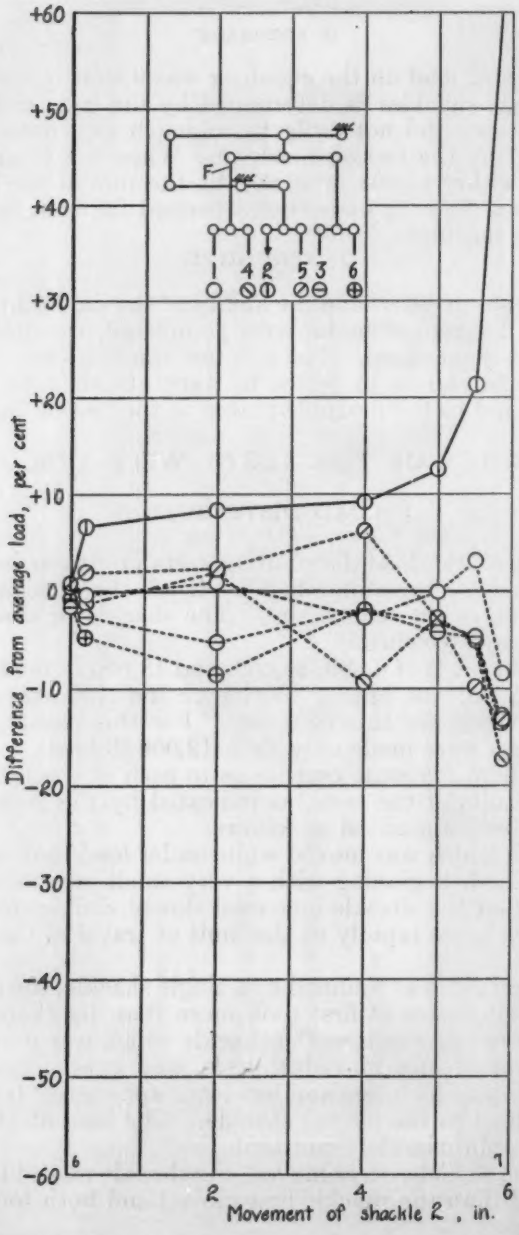

FIGURE 7.—*Load distribution for elevator cable equalizer* A *as shackle 2 was moved.*

Total load 6,000 lb. Link F failed during the strength test.

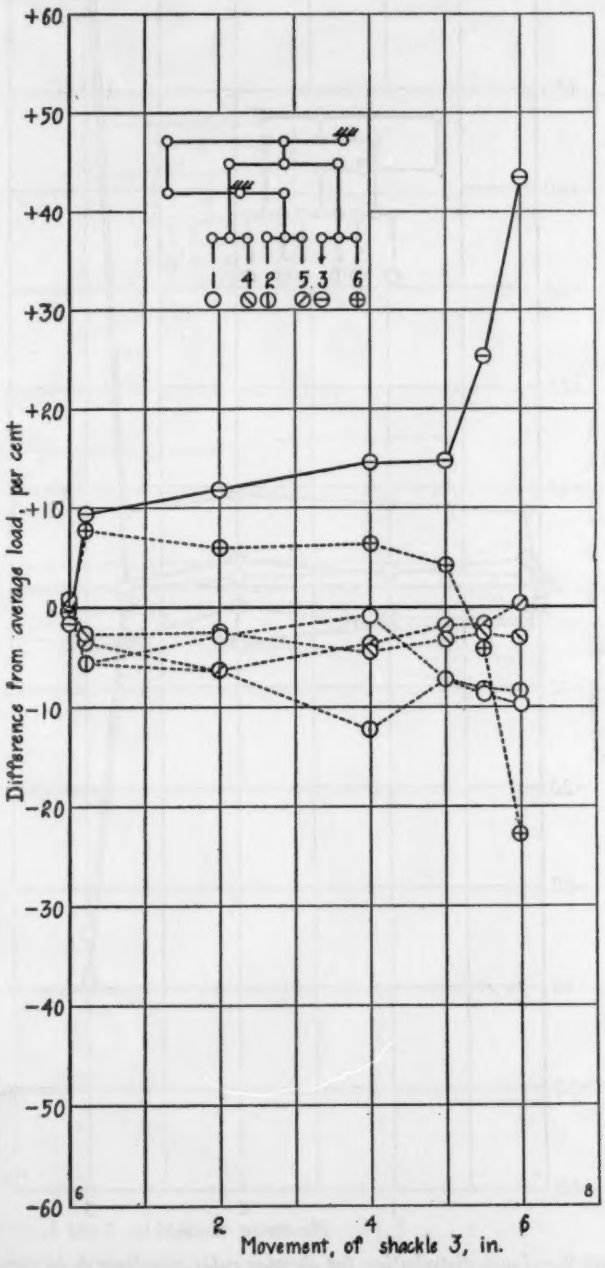

FIGURE 8.—*Load distribution for elevator cable equalizer* A *as shackle 3 was moved.*

Total load 6,000 lb.

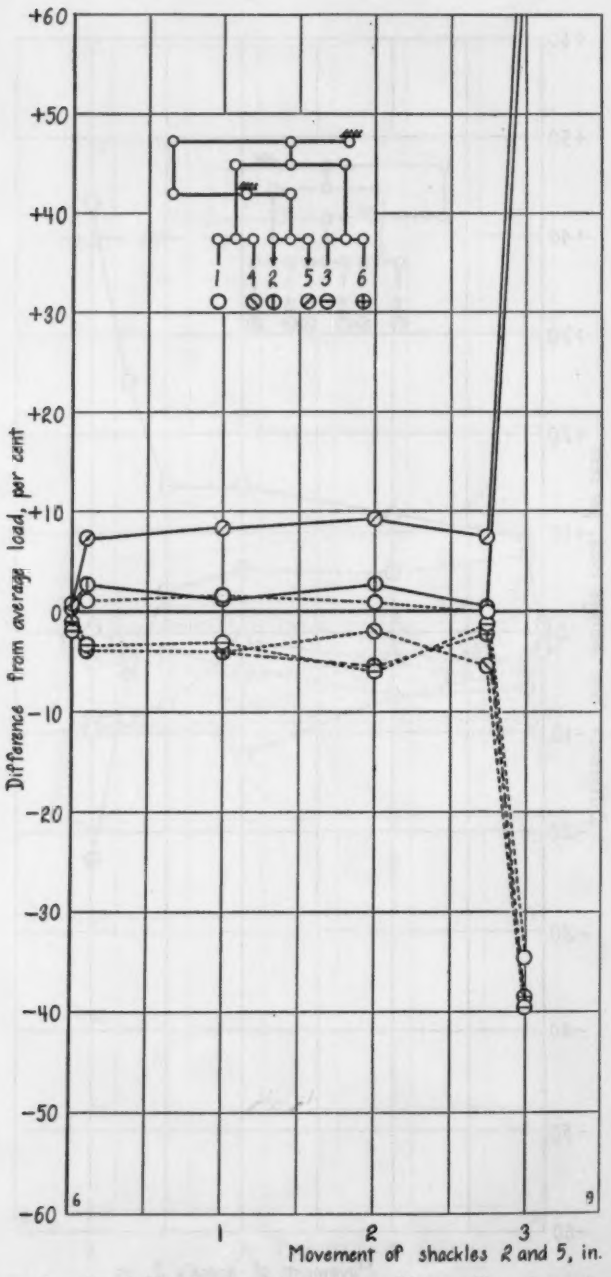

FIGURE 9.—*Load distribution for elevator cable equalizer A as shackles 2 and 5 were moved.*

Load 6,000 lb.

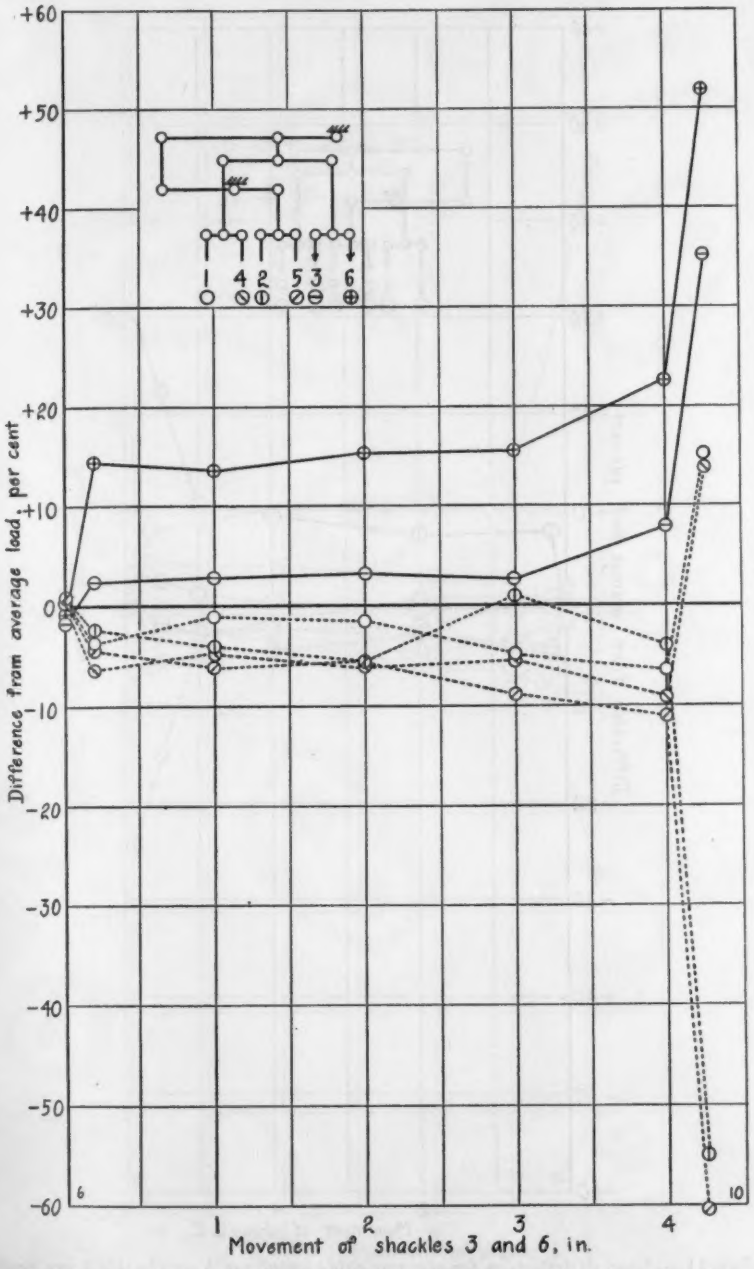

FIGURE 10.—*Load distribution for cable elevator equalizer* A *as shackles 3 and 6 were moved.*

Load 6,000 lb.

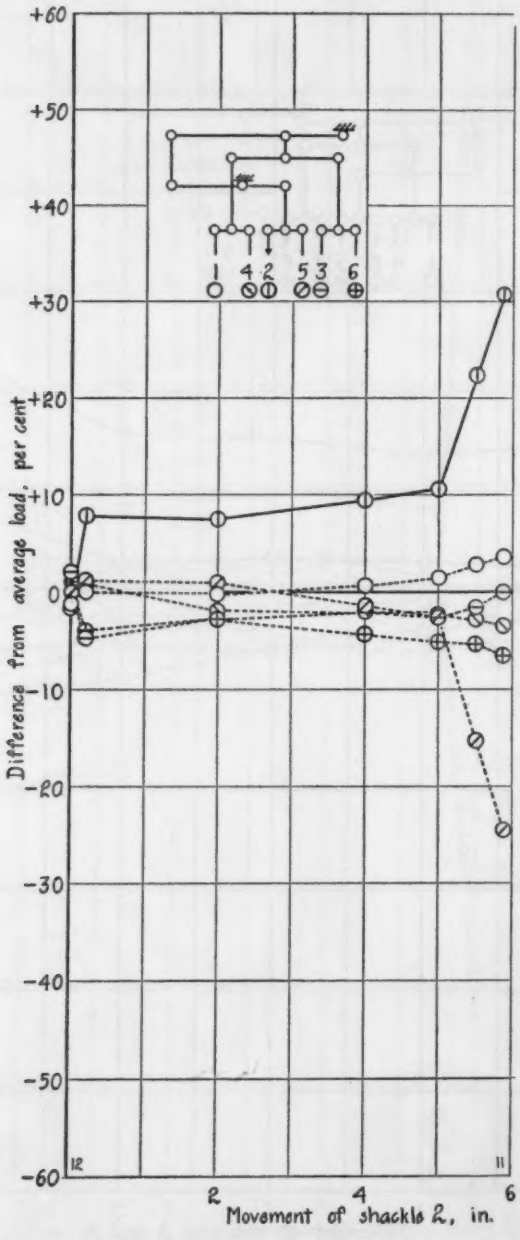

FIGURE 11.—*Load distribution for elevator cable equalizer* A *as shackle 2 was moved.*

Total load 12,000 lb.

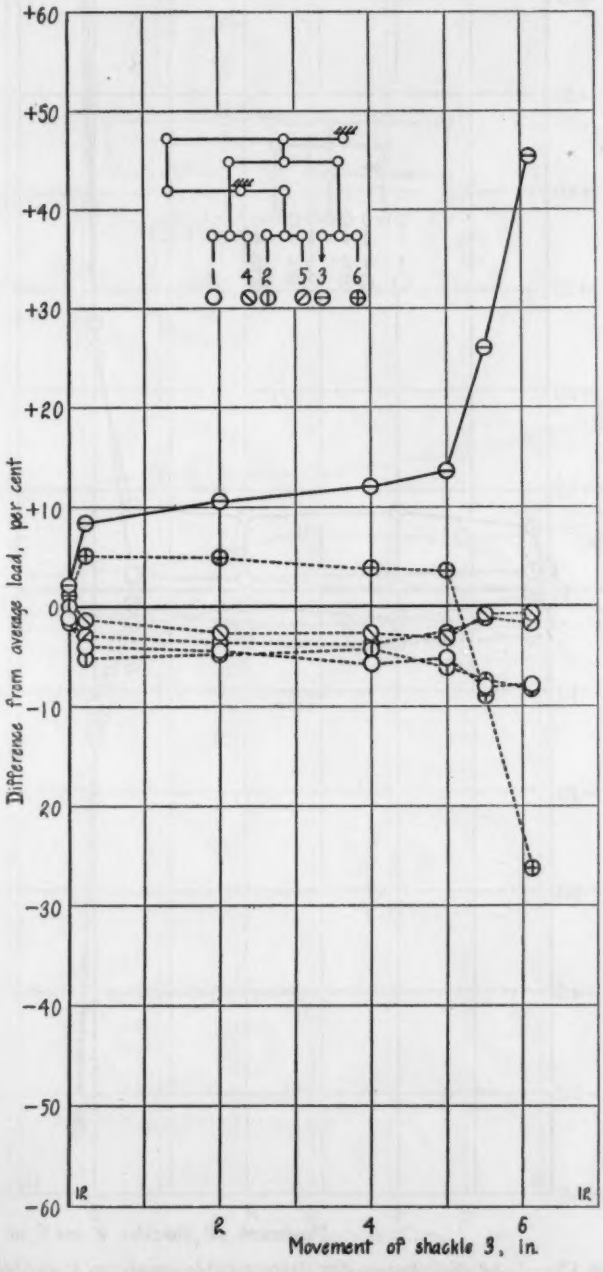

FIGURE 12.—*Load distribution for elevator cable equalizer* A *as shackle 3 was moved.*

Total load 12,000 lb.

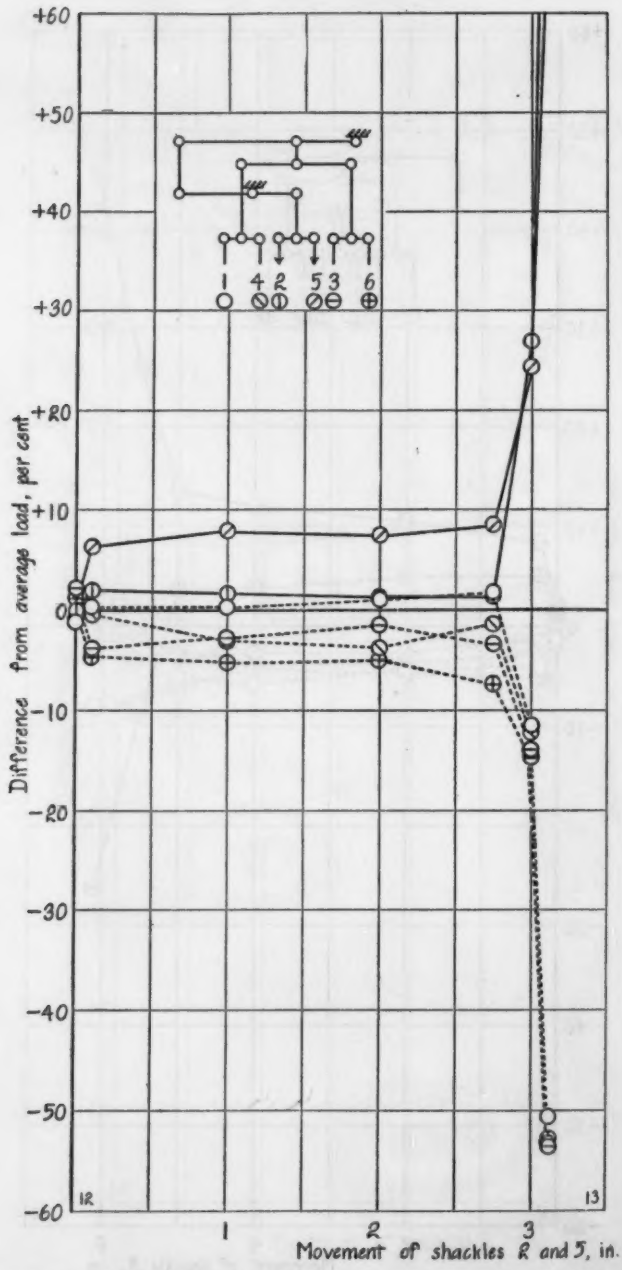

FIGURE 13.—*Load distribution for elevator cable equalizer A as shackles 2 and 5 were moved.*

Total load 12,000 lb.

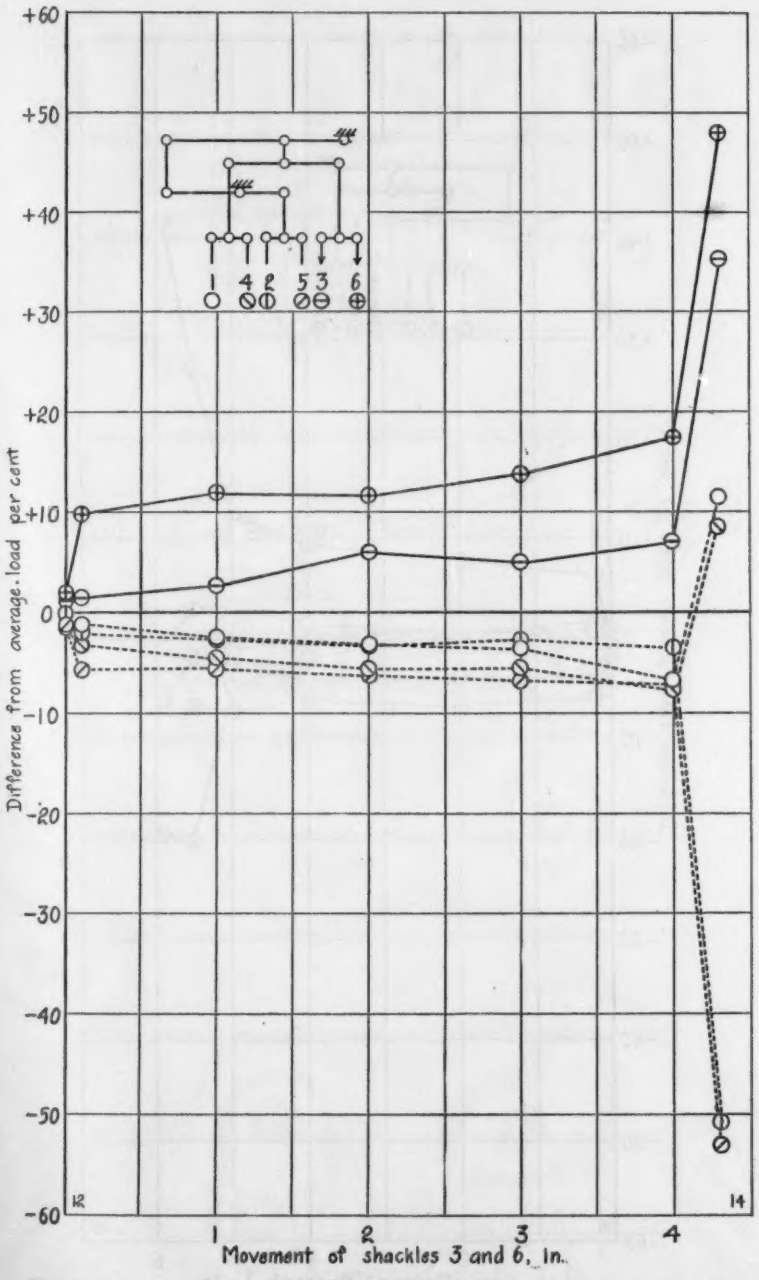

FIGURE 14.—*Load distribution for elevator cable equalizer* A *as shackles 3 and 6 were moved.*

Total load 12,000 lb.

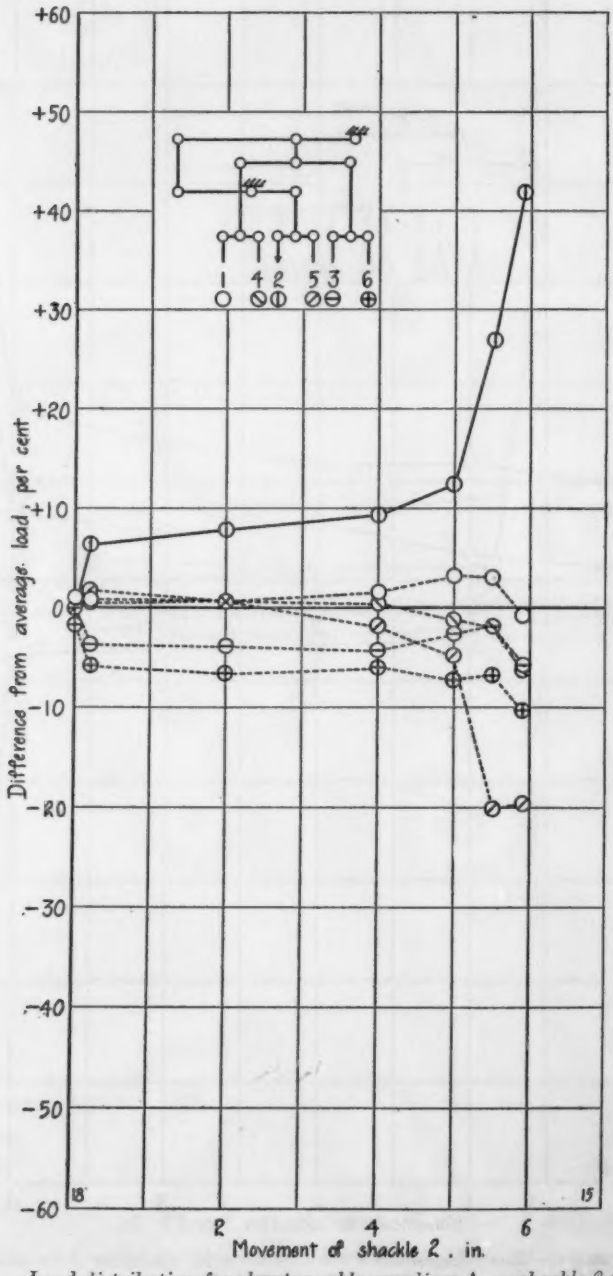

FIGURE 15.—*Load distribution for elevator cable equalizer A as shackle 2 was moved.*

Total load 18,000 lb.

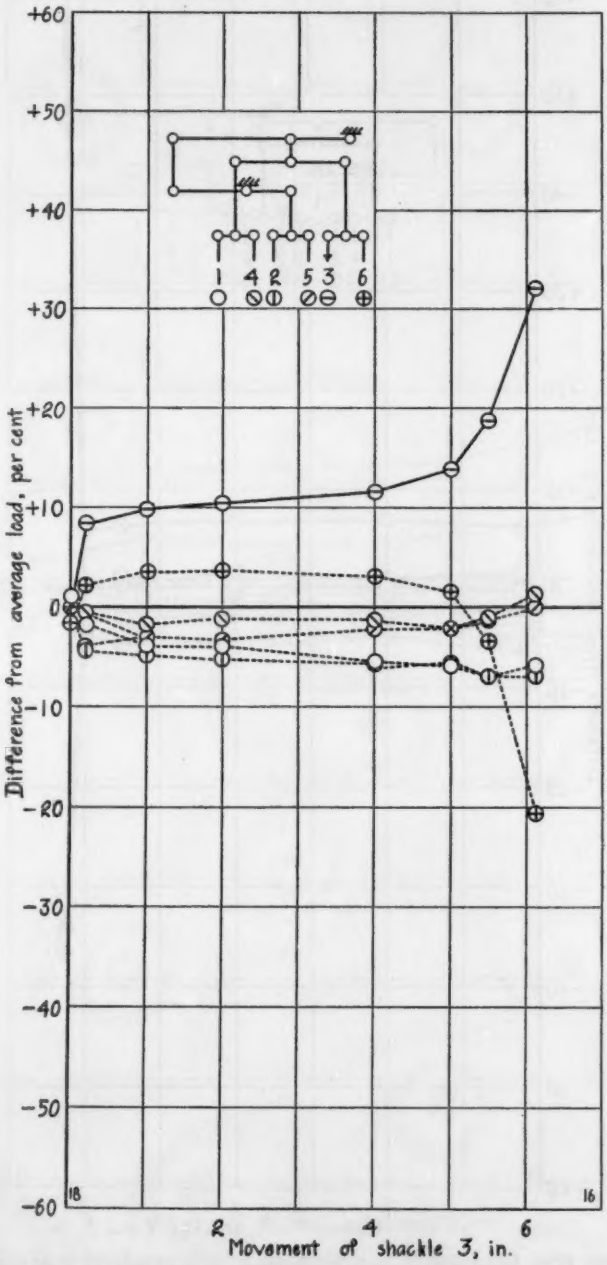

FIGURE 16.—*Load distribution for elevator cable equalizer* A *as shackle 3 was moved.*

Total load 18,000 lb.

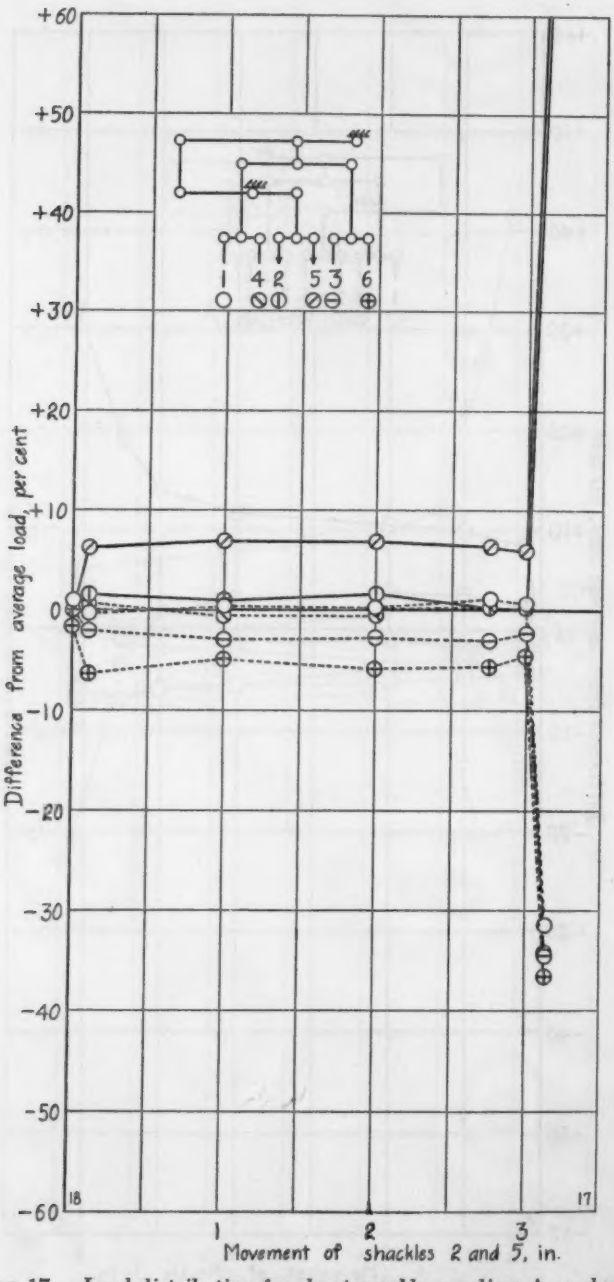

FIGURE 17.—*Load distribution for elevator cable equalizer A as shackles 2 and 5 were moved.*

Total load 18,000 lb.

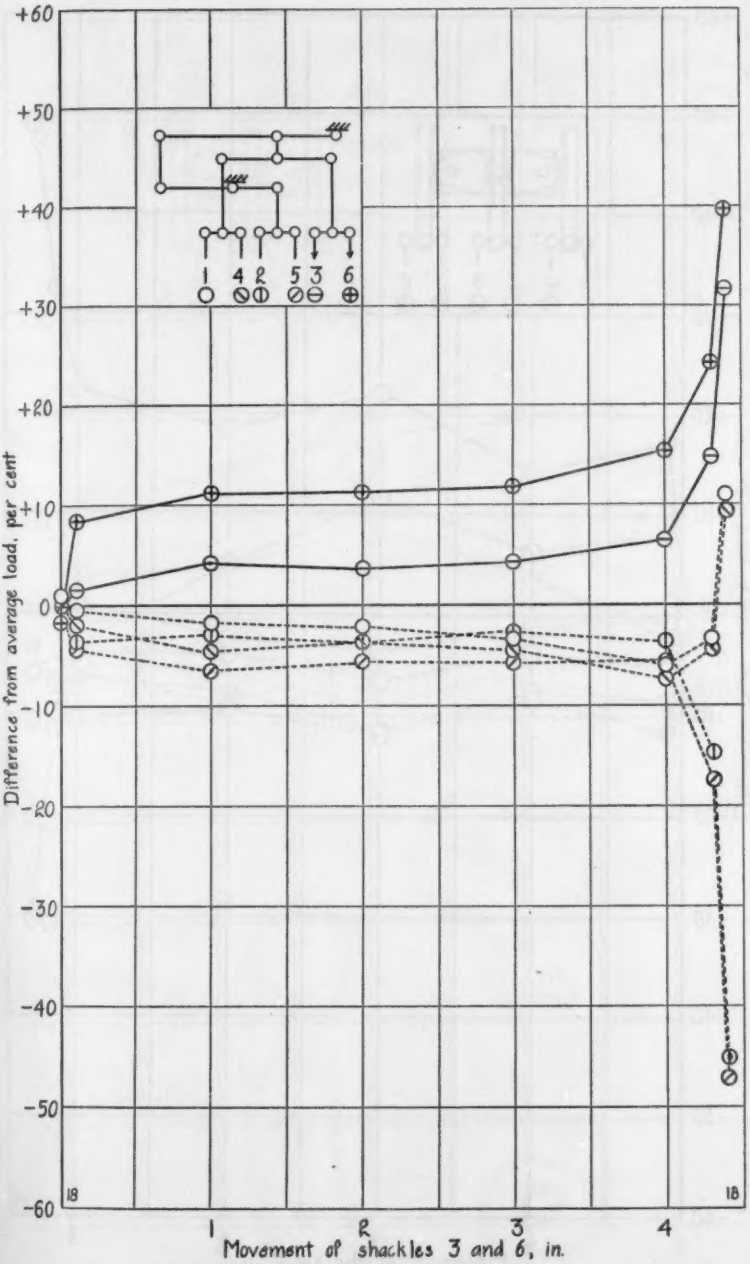

FIGURE 18.—*Load distribution for elevator cable equalizer A as shackles 3 and 6 were moved.*

Total load 18,000 lb.

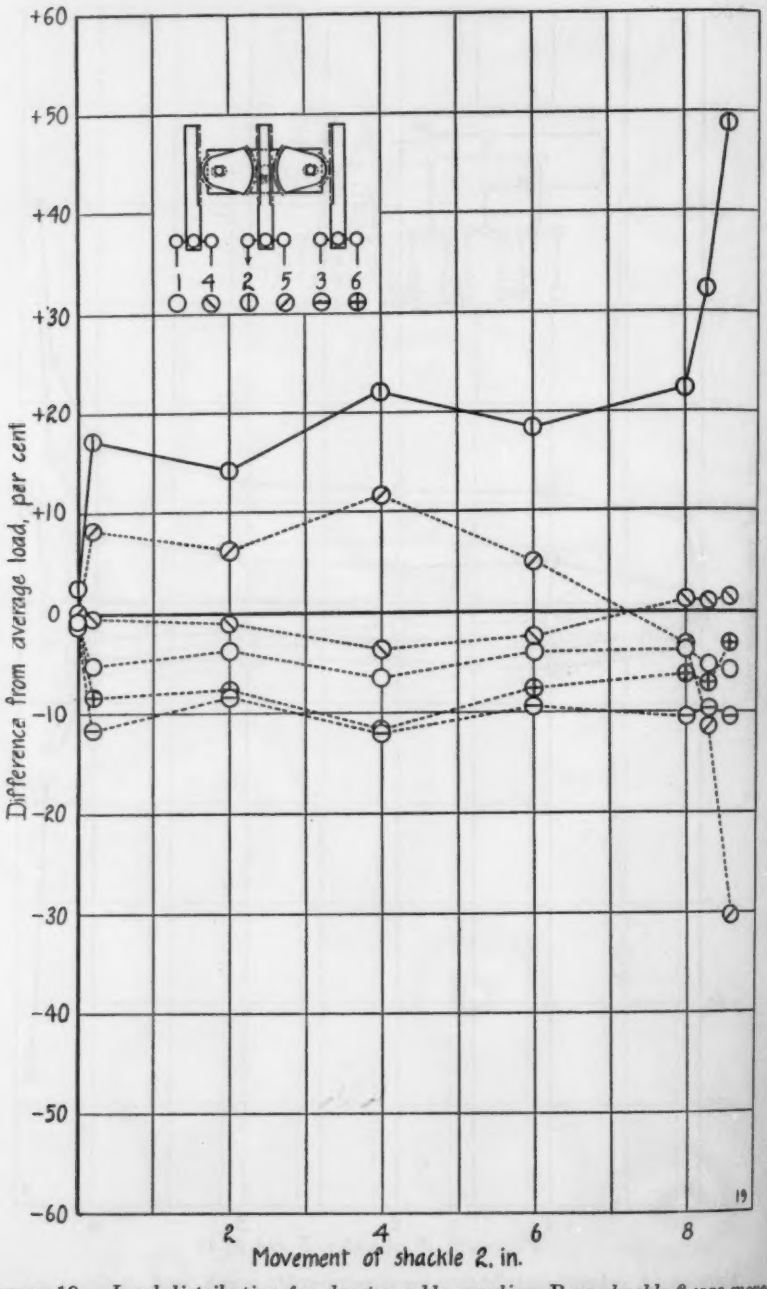

FIGURE 19.—*Load distribution for elevator cable equalizer* B *as shackle 2 was moved.*

Total load 12,000 lb.

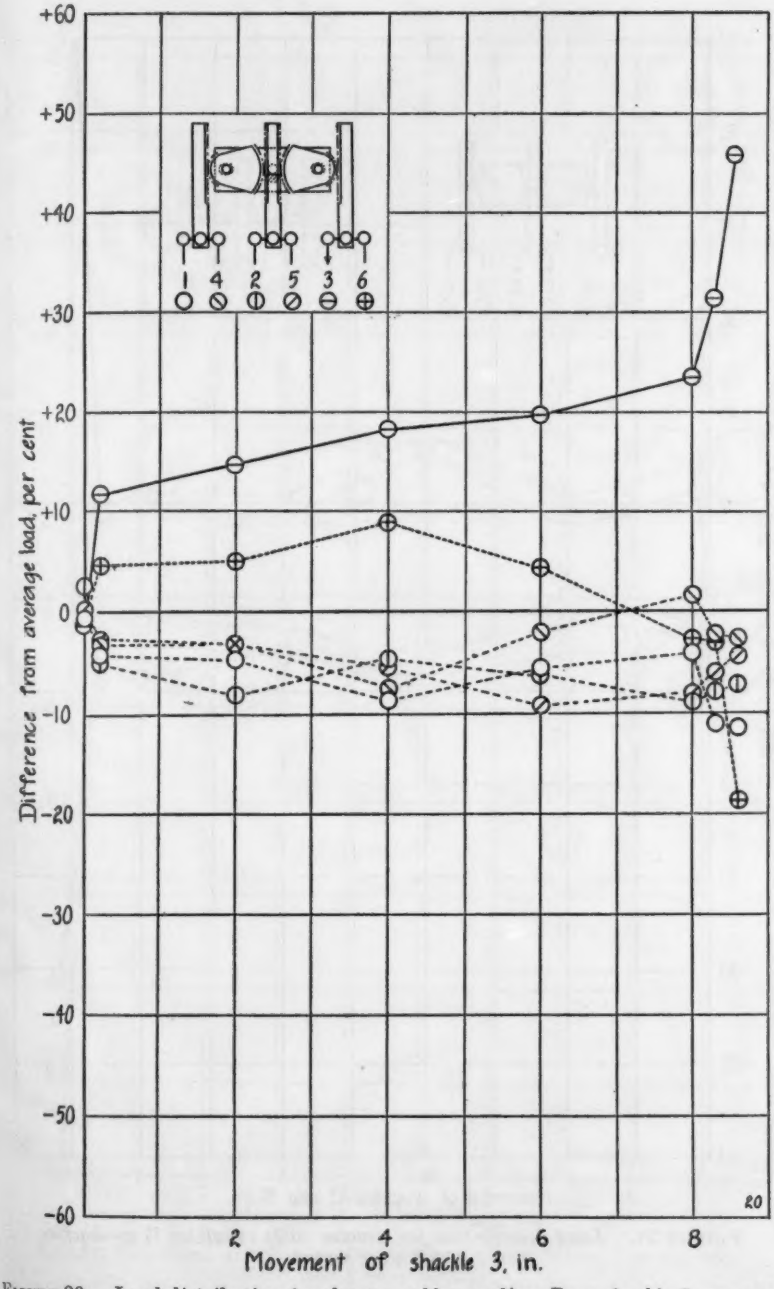

FIGURE 20.—*Load distribution for elevator cable equalizer* B *as shackle 3 was moved.*

Total load 12,000 lb.

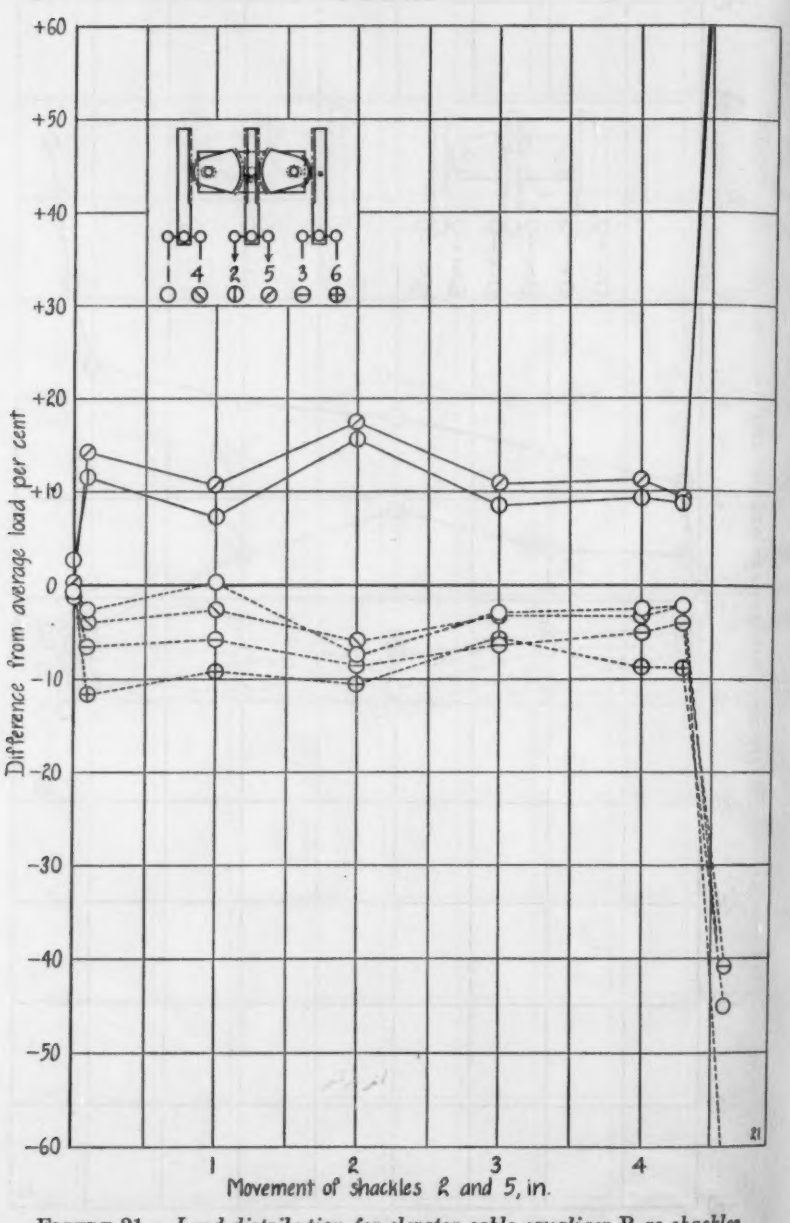

FIGURE 21.—*Load distribution for elevator cable equalizer* B *as shackles 2 and 5 were moved.*

Total load 12,000 lb.

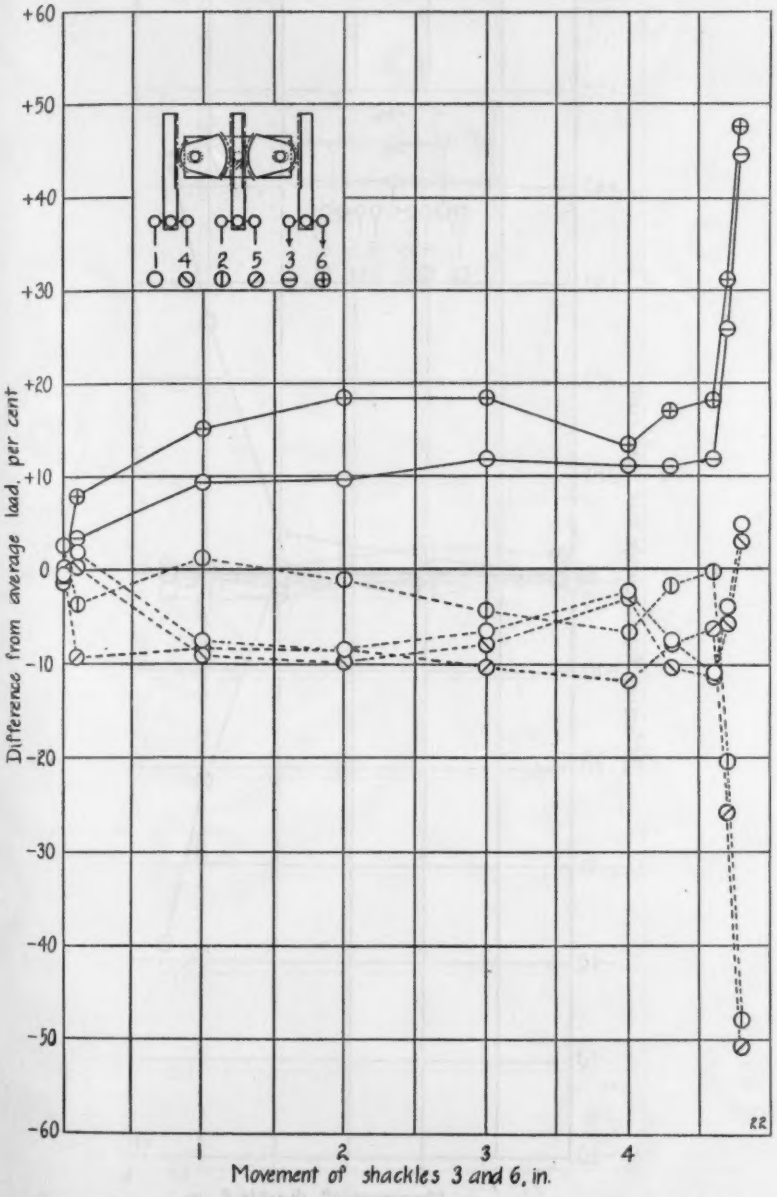

FIGURE 22.—*Load distribution for elevator cable equalizer* B *as shackles 3 and 6 were moved.*

Total load 12,000 lb.

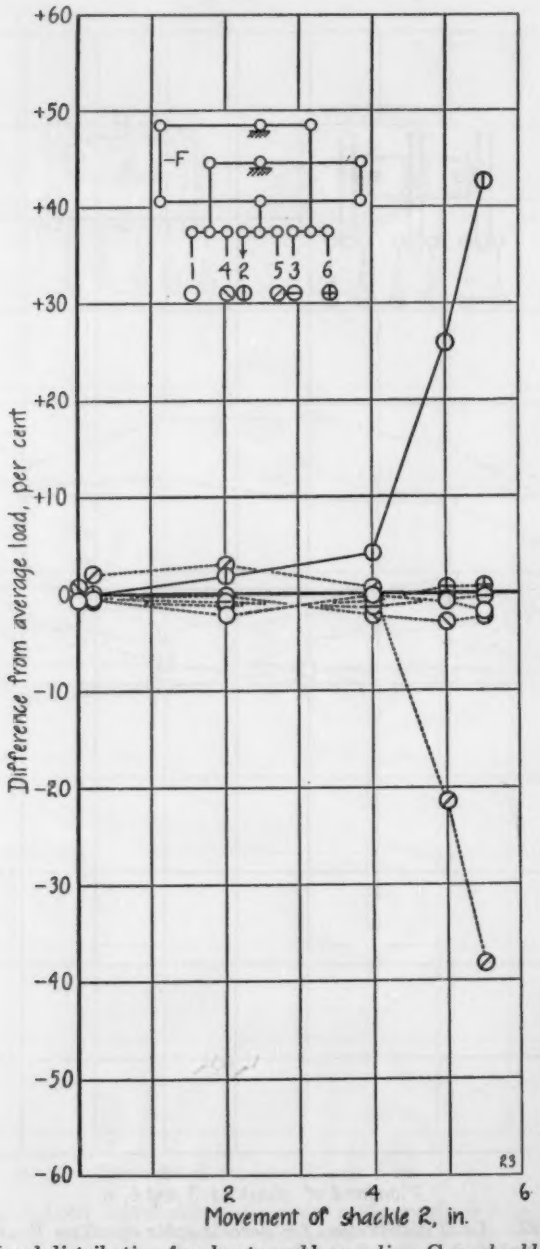

FIGURE 23.—*Load distribution for elevator cable equalizer* C *as shackle 2 was moved.*

Total load 12,000 lb. Link F broke during the strength test.

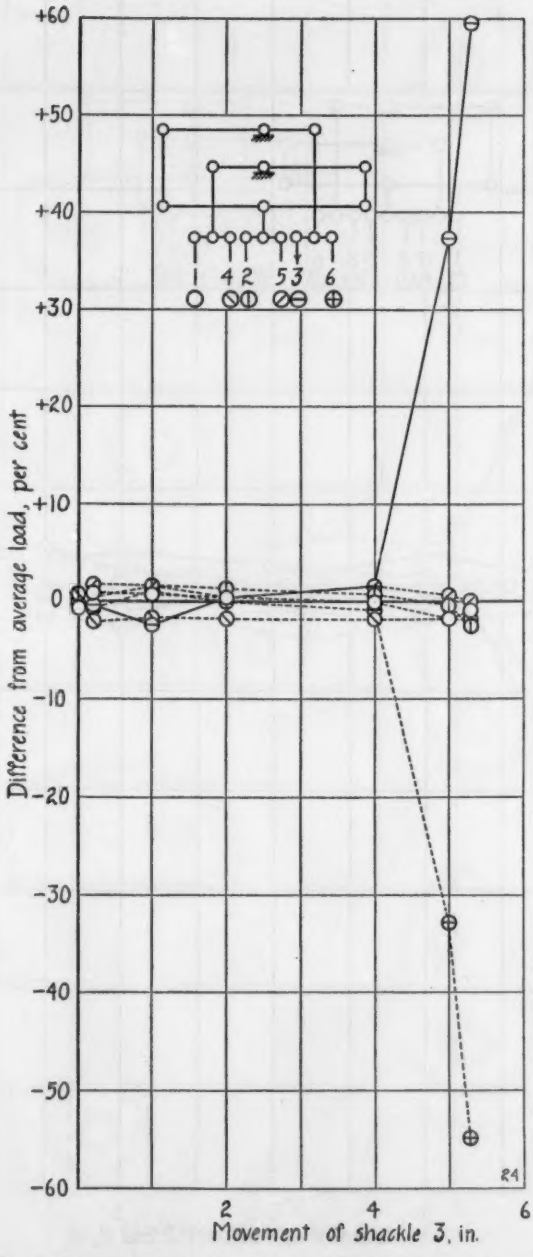

FIGURE 24.—*Load distribution for elevator cable equalizer* C *as shackle 3 was moved.*

Total load 12,000 lb.

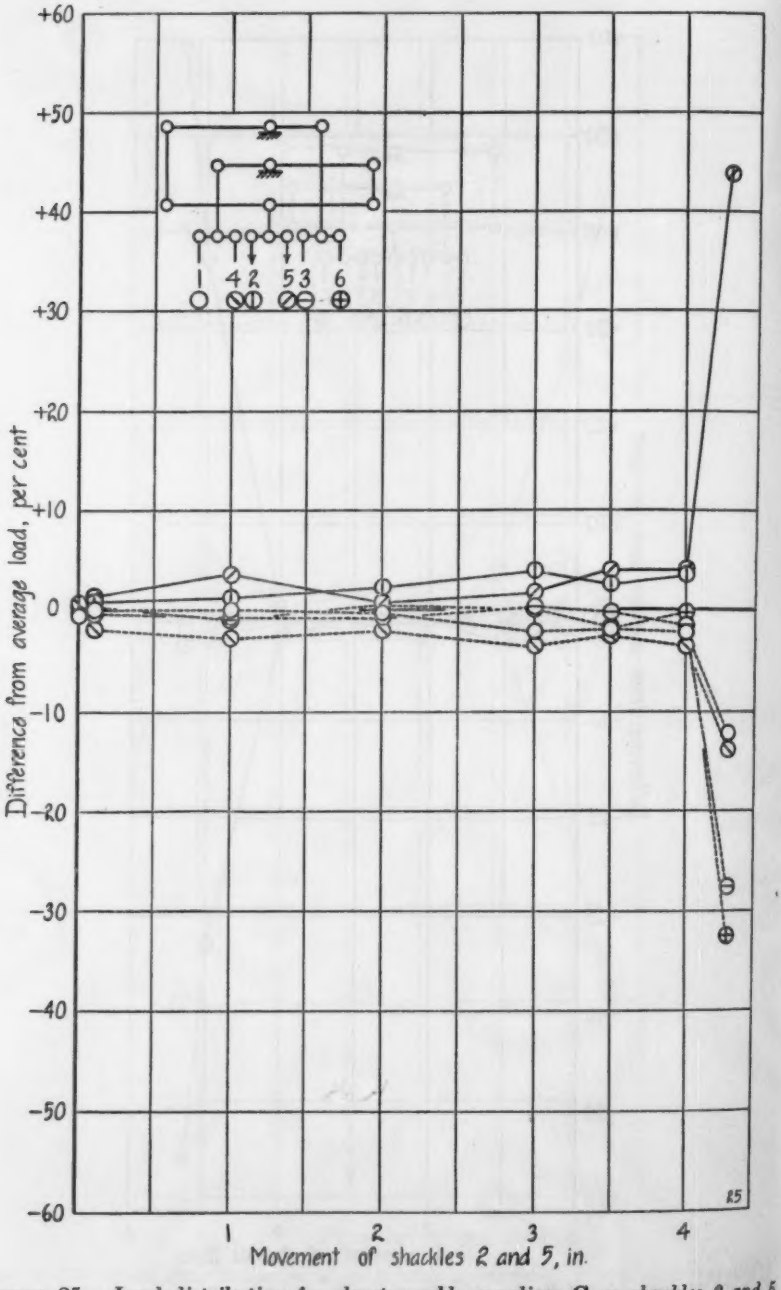

FIGURE 25.—*Load distribution for elevator cable equalizer* C *as shackles 2 and 5 were moved.*

Total load 12,000 lb.

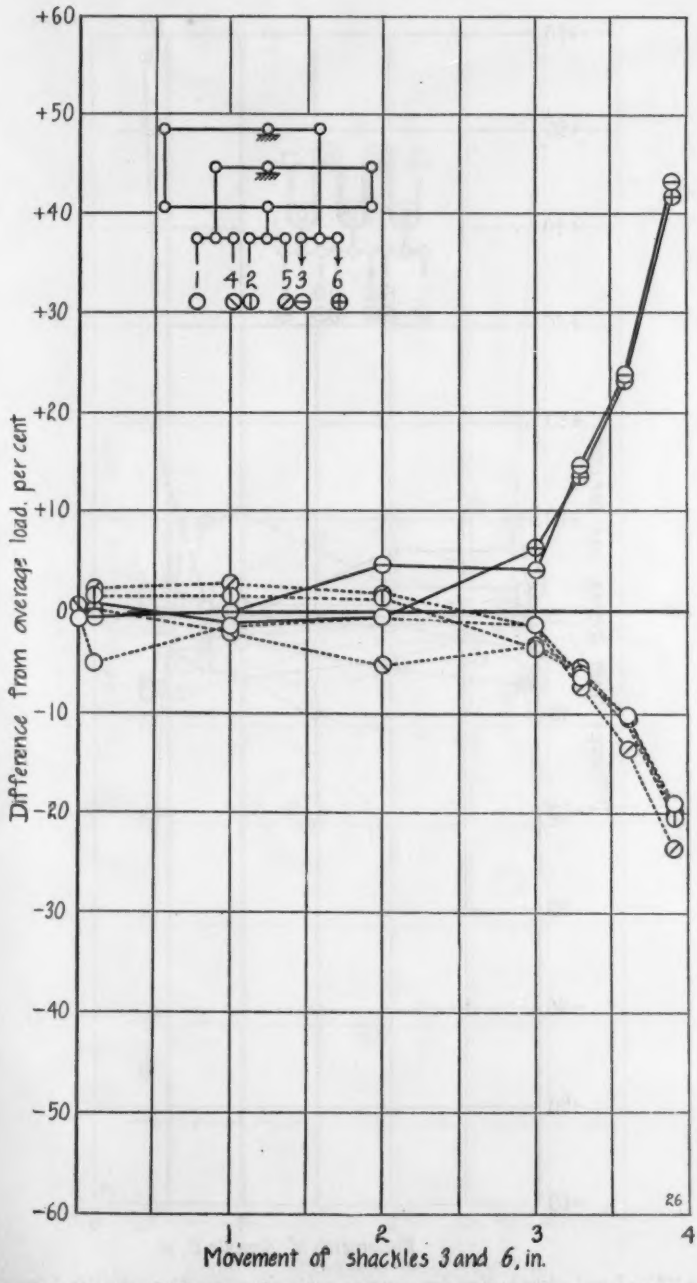

FIGURE 26.—*Load distribution for elevator cable equalizer* C *as shackles 3 and 6 were moved.*

Total load 12,000 lb.

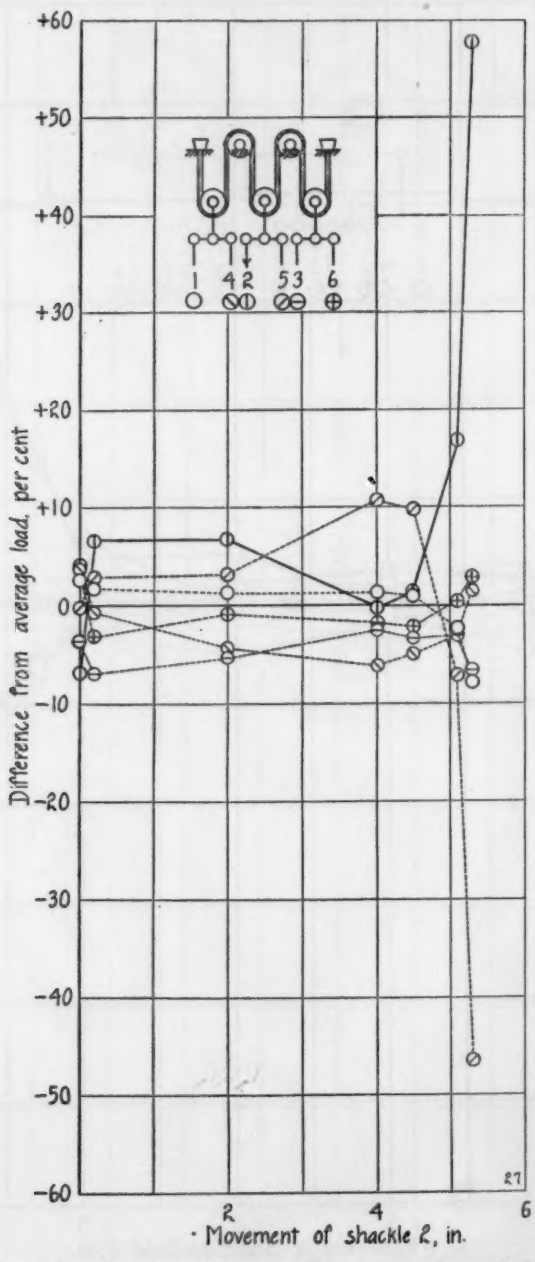

FIGURE 27.—*Load distribution for elevator cable equalizer* D *as shackle 2 was moved.*

Total load 12,000 lb.

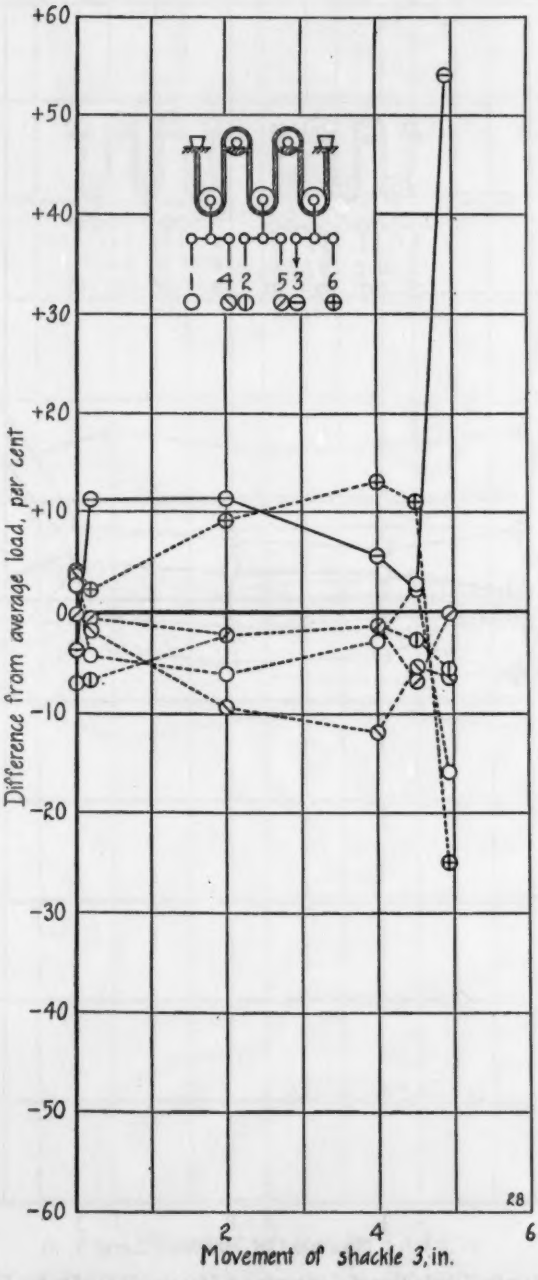

FIGURE 28.—*Load distribution for elevator cable equalizer* D *as shackle* 3 *was moved.*

Total load 12,000 lb.

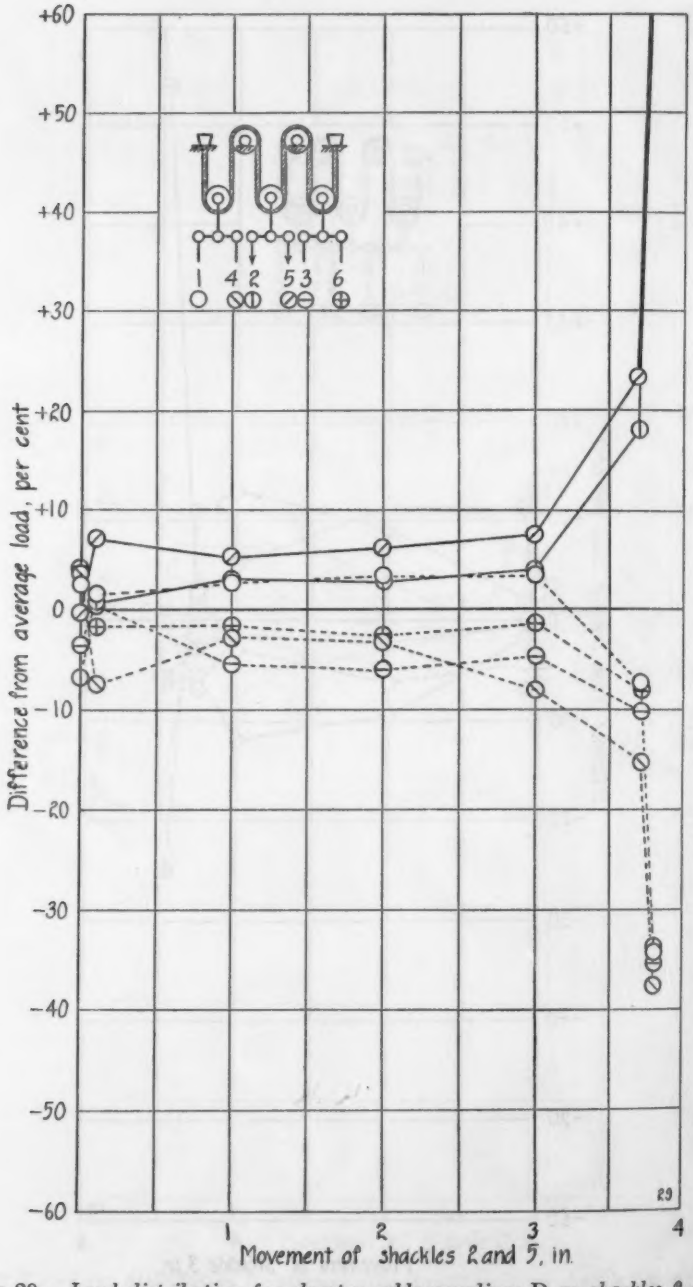

FIGURE 29.—*Load distribution for elevator cable equalizer* D *as shackles 2 and 5 were moved.*

Total load 12,000 lb.

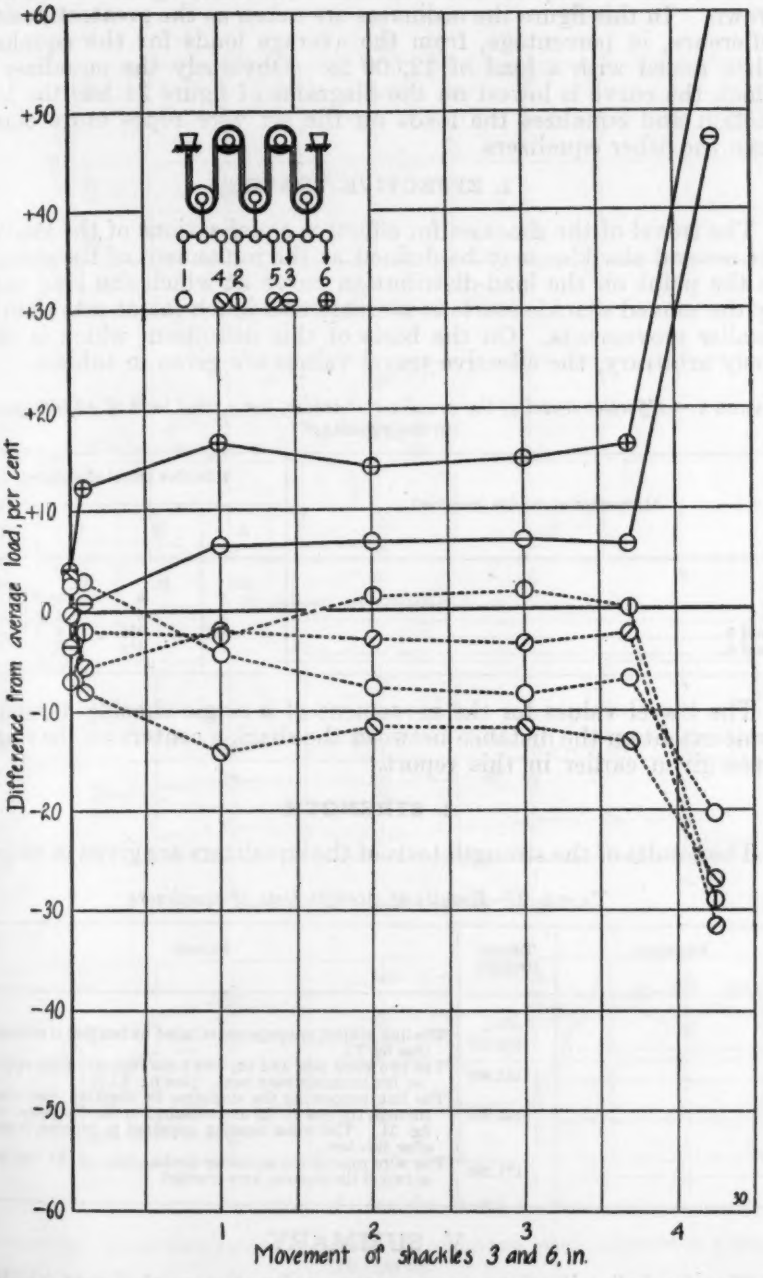

FIGURE 30.—*Load distribution for elevator cable equalizer* D *as shackles 3 and 6 were moved.*

Total load 12,000 lb.

To obtain a comparison of the four equalizers, figure 31 has been drawn. In this figure the ordinates are taken as the greatest positive difference, in percentage, from the average loads for the equalizers when tested with a load of 12,000 lb. Obviously the equalizer for which the curve is lowest on the diagrams of figure 31 has the least friction and equalizes the loads on the six wire ropes more closely than the other equalizers.

2. EFFECTIVE TRAVEL

The travel of the shackles for effective equalizations of the loads on the several shackles may be defined as the movement of the shackles to the point on the load-distribution curve at which the load taken by the moved shackle starts to increase at a much faster rate than for smaller movements. On the basis of this definition, which is obviously arbitrary, the effective travel values are given in table 1.

TABLE 1.—*Effective travel of the equalizer shackles, for a total load of 12,000 pounds on the equalizer*

Movement of shackle (number)	Effective travel of equalizer:			
	A	B	C	D
	in.	in.	in.	in.
2	5	8	4¼	5
3	5	8	4½	4½
2 and 5	2¾	4¼	4	3½
3 and 6	4	4½	3	3¾

The travel values for the movement of a single shackle depend to some extent on the distance between the shackle centers on the singletrees given earlier in this report.

3. STRENGTH

The results of the strength tests of the equalizers are given in table 2.

TABLE 2.—*Results of strength tests of equalizers*

Equalizer	Tensile strength	Failure
	lb.	
A	119,150	The link subject to compression failed by bending at midlength. (See fig. 7.)
B	137,800	The two shear pins and the two bolts supporting the equalizer on the channels were bent. (See fig. 2.)
C	133,950	The link supporting the singletree for shackles 1 and 4 broke through the eye at the end attached to the doubletree. (See fig. 23.) The roller bearing appeared to function properly after this test.
D	177,200	The wire rope of the equalizer broke. (See fig. 4.) The hubs of two of the sheaves were cracked.

V. SUMMARY

The load-distribution curves, especially those of figure 31, the effective travel values of table 1, and the breaking-strength values of table 2 afford bases for comparisons of the four equalizers.

Equalizer C, for shackle movements within the travel limits given in table 1, equalized the loads on the shackles more closely than the

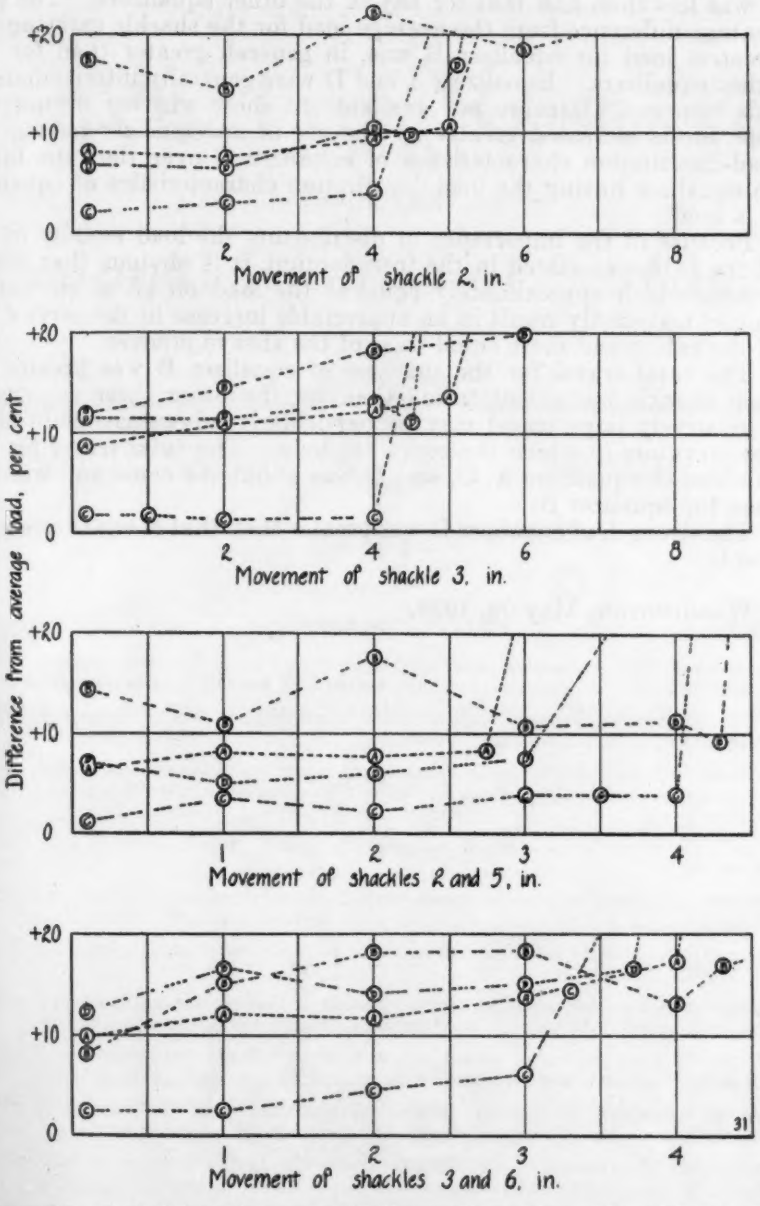

FIGURE 31.—*Load-distribution curves for the equalizers when subjected to a load of 12,000 lb.*

The letters in the circles are the equalizer designations.

other equalizers. In most cases, the percentage difference from the average load for the shackle carrying the greatest load for equalizer C was less than half that for any of the other equalizers. The percentage difference from the average load for the shackle carrying the greatest load for equalizer B was, in general, greater than for the other equalizers. Equalizers A and D were generally intermediate in this respect. Data are not available to show whether or not the rope life is increased greatly by the use of an equalizer having the load-distribution characteristics of equalizer C over the rope life if an equalizer having the load-distribution characteristics of equalizer B is used.

Because of the importance of distributing the load equally on all of the cables as stated in the introduction, it is obvious that mechanisms which approximately equalize the load on all of the cables should necessarily result in an appreciable increase in the service life of the cables and more equal wear of the sheave grooves.

The total travel for the shackles of equalizer B was greater for each shackle movement tested than for the other three equalizers. A relatively large travel may be particularly advantageous in high-rise elevators in which the ropes are long. The total travel for the shackles of equalizers A, C, and D was about the same and was less than for equalizer B.

The strength of equalizer D was greater than that of equalizers A, B, and C.

WASHINGTON, May 26, 1936.